Brittany Elizabeth Retallack, BSc

# Standardized procedures for geno- and phenotyping of *Haematococcus pluvialis* strains

**MASTER'S THESIS**

to achieve the university degree of

Diplom-Ingenieurin

Master's degree programme:

Biotechnology

submitted to

**Graz University of Technology**

**Supervisor**

Univ.-Prof. Dipl.-Biol. Dr.rer.nat. Gabriele Berg

Institute of Environmental Biotechnology

Graz, September 2020

## AFFIDAVIT

I declare that I have authored this thesis independently, that I have not used other than the declared sources/resources, and that I have explicitly indicated all material which has been quoted either literally or by content from the sources used. The text document uploaded to TUGRAZonline is identical to the present master's thesis.

Date, Signature

# I. Acknowledgements

First and foremost, I would like to recognize my supervisor Univ.-Prof. Dipl.-Biol. Dr. rer. nat. Gabriele Berg for the opportunity to complete my master thesis at the Institute of Environmental Biotechnology. Her support and expertise have accompanied my enrichment of knowledge and passion for scientific advancements.

I would like to also pay my respects to my co-supervisors Lisa Krug and Tomislav Cernava for their guidance and encouragement throughout my project. There doors were always open for any questions or troubles during my whole Master Thesis.

I am very appreciative for my colleagues at the Institute of Environmental Biotechnology for the contributions to the enhancement of my learning, wonderful discussions, and the genuine ambition for the discovery of profound scientific insights.

I also would like to thank BioLife Science GmbH (BDI) for the opportunity to collaborate and gain practical experience working in the field of algal biotechnology.

Thank you.

# II. Abstract

*Haematococcus pluvialis* is a green unicellular microalgae widely recognized as currently being the best-known natural source of the ketocarotenoid astaxanthin, a powerful antioxidant. Strains of *H. pluvialis* often differ in various important characteristics such as cell size, stress tolerance, growth rate, biomass abundances, and astaxanthin accumulation. Therefore, the main objective of this study was to evaluate 17 strains from the BDI strain collection considered for astaxanthin production and to create a Standard Operational Protocol (SOP) for their characterization. Integrative characterization of various strains of *H. pluvialis* targeted sanger sequencing of the phylogenetic marker genes 18S rRNA and ITS revealed a sequence identity between 96.02 - 100 % within the combined 2,475-bp region. Complementary analyses included the construction of a phylogenetic tree as well as PCR-based assessments of microbial fingerprints. Implementation of BOX-PCR and enterobacterial repetitive intergenic consensus PCR (ERIC-PCR) allowed for the most efficient method for distinguishing *H. pluvialis* strains. Additional phenotype characteristics of the industrial algae strains were obtained with cultivation experiments and different supplements. The metabolic growth capabilities of autotrophic and heterotrophic growth indicated the most variation when 0.8 g/L sodium acetate was added to the commonly used Bold Basal Media (BBM), especially during heterotrophic growth. However, autotrophic growth in BBM media alone and BBM supplemented with 0.8 g/L glucose showed significant variation only for 11.8% of the implemented strains. Growth curves over a 15 - day period in aerated 1 L closed bioreactors and the corresponding biomass (dry weight) values were not efficient at distinguishing any of the strains. Analysis of volatile secondary metabolites via headspace GC-MS analysis revealed methyl furan, tetrahydrofuran and dimethyl disulfide present in various samples. These compounds were so far not detected in freshwater algae, but are commonly found in bacteria and thus may be the result of contamination as axenic algal cultures still remain a significant challenge of the industry. The results of this thesis provide new insights into the intra-species diversity and predict the best growing strains that should be used for industrial algal cultivation.

# III. Kurzfassung

*Haematococcus pluvialis* ist eine grüne, einzellige Mikroalge, die biotechnologisch als bestbekannter Produzent von Keto-Caretinoidem Astaxanthin gilt, welches als starkes Antioxidant angesehen wird. *H. pluvialis*-Produktionsstämme können sich bezüglich ihrer Zellgröße, Stressempfindlichkeit, Wachstumsrate, Biomassezunahme und vor allem der Astaxanthin-Akkumulation deutlich voneinander unterscheiden. Daher war das Hauptziel dieser Arbeit eine detaillierte Charakterisierung von 17 Stämmen aus der Stammsammlung eines Industriepartners (BDI-BioLife Science GmbH) durchzuführen. Zusätzlich sollte ein Standard Operational Protocol (SOP) erstellt werden, um Einordnungen neuer Astaxanthin-Produktionsstämme in Zukunft zu erleichtern. Zu Beginn der Studie wurden *H. pluvialis*-Stämme mittels Sanger-Sequenzierung des phylogenetischen Markergens 18S rRNA und der ITS-Region klassifiziert. Hier wurde eine Sequenzidentität zwischen 96,02 und 100% der kombinierten Genabschnitte mit einer Gesamtlänge von 2,475 bp festgestellt. In nachfolgenden Analysen wurden ein phylogenetischer Stammbaum aller Isolate rekonstruiert sowie PCR-Analysen von weiteren mikrobiellen Genabschnitten durchgeführt um Verwandtschaftsverhältnisse abzuleiten. Die mittels BOX-PCR und ERIC-PCR gewonnen Daten wurden. unterschiedlichen Phänotypen der Industriealgenstämme zugeordnet. Zusätzlich wurde das autotrophe und heterotrophe Wachstums untersucht. Unterschiede wurden bei Zugabe von 0,8 g/L Natriumacetat zum Bold Basal Medium (BBM) fesgestellt, speziell unter heterotrophen Wachstumsbedingungen. Das autotrophe Wachstum in BBM-Medien mit und ohne Zugabe von 0,8 g/L Glukose hat bei 11,76% der implementierten Stämme eine Auswirkung auf die Biomassebildung gezeigt. Über einen Zeitraum von 15 Tagen in belüfteten 1L Bioreaktoren konnten keine signifikanten Unterscheide bestätigt werden. Abschließende Analysen flüchtiger Sekundärmetaboliten mittels Headspace-GC-MS-Analyse zeigten, dass Methylfuran, Tetrahydrofuran und Dimethyldisulfid von unterschiedlichen Algenstämmen gebildet wurden. Diese Verbindungen wurden bis jetzt nicht in Süßwasseralgen nachgewiesen, kommen aber als Bakterienmetaboliten in Frage und könnten einen Hinweis dazu liefern, dass die Kulturen nicht axenisch waren. Die Ergebnisse dieser Arbeit verdeutlichen die Artenvielfalt von Mikroalgen und das Potential aus dieser Vielfalt leistungsstarke Produktionsstämme zu selektieren

# Content

# 1. Introduction

## 1.1 Algal biotechnology

Both microalgae and macroalgae encompass a vast spectrum of diversity on a phylogenetic, physiological, morphological and biochemical level. This is exploited in their occurrence in numerous habitats worldwide. With such diversity yields the opportunity for a range of algal biotech applications for sources of lipids, carbohydrates, proteins and pigments. Currently the species: *Haematococcus, Chlorella* and *Dunaliella* are the main microalgae used for commercial production. However, also additional algal species are already applied in various industries such as feed, food, pharmaceutical, nutraceutical, biofertilizers, natural pigments for dyes, etc. Microalgae have the potential for sustainable biofuel production due high amounts of lipids and oils and can be coupled with fuel gas $CO_2$ migration, wastewater treatment and high value products such as astaxanthin. Thus, at least a partial solution to current energy and climate change issues (Salih et al., 2012). Algal cultivation is thus a possible long-term sustainable source for a variety of products and have untapped economic potential due to several positive attributes such as the ability to grow on unarable land, significantly higher $CO_2$ fixation capabilities compared to terrestrial plants, they can consume harmful pollutants and can be applied in a variety of cultivation systems. Furthermore, only sunlight, water, nutrients, $CO_2$, and land are the major requirements for growing algae. With new developments in cultivation, harvesting, downstream processing, as well as insights with molecular biology tools such as 'omics' techniques, a potential advancement in the field of agal biotechnology seems promising.

## 1.2 Occurrence and characteristics of *Haematococcus pluvialis*

The freshwater unicellular green microalgae *H. pluvialis* was first described by (Flotow, 1844). *H. pluvialis* synonymous to *Haematococcus lacustris* has been found distributed across diverse environmental and climate conditions. Such habitats include a freshwater basin in Norway (Klochkova et al., 2013), freshwater fishpond in Romania (Dragos et al., 2010) and has even been witnessed in an arctic seashore habitat on the coastal rocks at Kost'yan Island in Russia (Chekanov et al., 2014). *H. pluvialis* is predominantly found in temperate regions of the globe, in natural or man-made water bodies such as rain pools, ponds and birdbaths (Suseela and Toppo, 2006; Gómez et al., 2015). Due to significant physiological and genetic variation (Mostafa et al., 2011) within the species yields the opportunity in biotechnological applications and thus allows for selection of fast-growing productive strains

that are adapted to various conditions which in turn could reduce the economic costs of production.

*H. pluvialis* is well suited for survival under extreme prevailing conditions regarding temperature, light, salt concentrations or nutrient deprivation, due to its ability to encyst in a rapid manner. Interesting isolates of *H. pluvialis* have shown the capability to grow and accumulate astaxanthin within temperatures (4 - 10°C), (Klochkova et al., 2013) and has demonstrated a salt tolerance of (up to 25%), (Chekanov et al., 2014). *H. pluvialis* deals with environmental oxidative stress via two mechanisms: antioxidative enzymes during the vegetative stage and the antioxidative ketocarotenoid accumulation in cysts, predominantly astaxanthin (Kobayashi et al., 1997). Such carotenoids are known to protect photosynthetic organisms by acting as light harvesting pigments to trap light and energy for chlorophylls and protection of light mediated stress (Young 1991).

Four types of cellular morphologies are observed during the life cycle of *H. pluvialis:* macrozooids (zoospores), microzooids, palmella and hematocysts (aplanospores). In the “green vegetative phase” the cells grow and accumulate biomass. Once a culture or environmental stressor is presented the cells lose their flagella, encapsulate and enter the “red nonmotile astaxanthin accumulated encysted phase”. In rare instances, gametogenesis occurs where aplanospores sexually reproduce themselves in extreme conditions such as complete lack of nutrients or freezing temperatures. During the life cycle several ultrastructural changes occur and the biochemical composition drastically varies between the “green” and the “red” stages of cultivation regarding protein, carbohydrate, lipid and carotenoid concentrations (Shah et al., 2016).

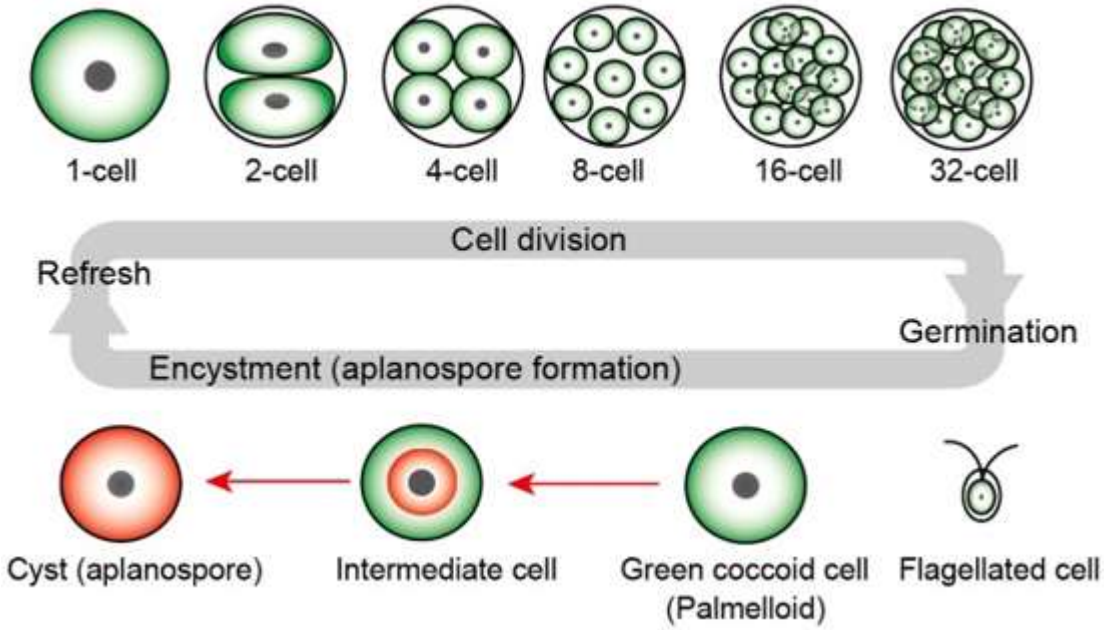


**Figure 1: Life cycle of *H. pluvialis.*** When older cultures are refreshed with new media flagellated cells form after cell division (germination) and can then settle and form coccoid cells. Environmental or laboratory stress conditions such as nutrient deprivation lead to carotenoid induction during encystment (red arrows). Figure presented from (Wayama et al., 2013).

## 1.3 Biological vs Synthetic astaxanthin

Several organisms are able to produce astaxanthin such as the microalgae *Chlorella zofungiensis*, the red yeast *Phaffia rhodozyma* and the marine bacterium *Agrobacterium aurantiacum*, however the content reported in these organisms ranged between 0.04% and 2.7% (DW), (Yokoyama et al., 1995; Kim et al., 2015;Wang and Peng, 2008). Strains of *H. pluvialis* considered for mass production of astaxanthin contain varying amounts ranging from (2.5 - 6.0 % DW) depending on the isolate used and the environmental or experimental conditions (Li et al., 2011; Wayama et al., 2013; Lemonie and Schoefs 2010). However, *H. pluvialis* is undoubtedly by far the richest known source of natural astaxanthin. In the study by (Kang et al., 2005) a reported astaxanthin content of up to 7% (DW) was achieved. Due to high production costs of biologically produced astaxanthin, synthetic astaxanthin currently dominates the market at around 95%. Rising concerns on several issues regarding synthetic production including the need for petrochemical sources, toxicities and lack of nutritional value are creating a higher demand for the natural product.

The main issue regarding synthetic production is the stereochemistry of astaxanthin, which have two chiral centers and thus the possibility of three stereoisomers (3S, 3′ S), (3R, 3′ S) and (3R, 3 ′R) generally found in a ratio of 1:2:1 (Lorenz and Cysewski, 2000). *H. pluvialis* predominantly biosynthesizes the 3S, 3′ S form which has a higher bioactivity than the

synthetic form and is the only form fit for direct human consumption (Gurein et al., 2003; Capelli et al., 2013, Higuera-Ciapara et al., 2006).

## 1.4 *H. pluvialis* cultivation in industry

A stable source of astaxanthin during the past few decades relies on synthetic production mainly for the pigmentation of salmon meat and crustacean shells in aquaculture resulting in a distinguishable bright red color. However to the high protein content whole biomass from *H. pluvialis* is often used in animal feed (Sirakov et al., 2015; Shields and Lupatsch, 2012) and the antioxidant properties of biologically produced astaxanthin have proven to enhance the growth and reproduction of commercially viable fish (Sommer et al., 1991; Choubert and Heinrich, 1993).

The main commercial application of biologically produced astaxanthin is for high value (>$10,000/t) human nutritional products (Benemann, 2013). Attributes such as antioxidant activity, anti-diabetes, anti-skin cancer and cardiovascular prevention abilities which have been reported using various in vitro and in vivo models (Ranga et al., 2013; Chan et al., 2012; Huangfu et al., 2013; Iizuka et al., 2012). Astaxanthin is like other carotenoids such as zeaxanthin, lutein and beta-carotene, and therefore has similar physiological and metabolic functions. However, keto and hydroxyl endings on each ionone ring enables the ability to be esterified and increases levels of antioxidant activity, making it one of the most preferred carotenoids (Lorenz and Cysewski, 2000). Astaxanthin produced from *H. pluvialis* has shown to have an antioxidant capacity 38-fold higher compared to beta-carotene and 500 times that of vitamin E (Shimidzu et al., 1996).Vast evidence shows oxidative stress is a factor in the pathogenesis of several prominent diseases such as Alzheimer's and Parkinson's, thus a diet rich in *H. pluvialis* derived astaxanthin could potentially lower the risks associated with common neurodegenerative diseases (Grant 1997; de Rijk, M. et al., 1997).

*H. pluvialis* it is an attractive source for biodiesel feedstock due to the high lipid and oil content in cells, however current production and extraction methods remain expensive and therefore non-profitable (Sheehan et al., 1998; Hu et al., 2006). However, due to the gradual depletion of fossil fuels, the quest for renewable fuel sources are likely to gain more probability in the future. Several other applications including cosmetics, dyes and raw materials for bio-refining have also been applied.

## 1.5 Culture conditions for *H. pluvialis* growth and astaxanthin production

Growth, biomass formation and astaxanthin accumulation is affected by culture parameters such as light, pH, temperature, salt concentration and medium composition. The ideal media composition depends on the application of either high growth rate or high accumulating astaxanthin, as the most efficient production strategy generally requires a two-stage process. Various types of growth media are commonly used including BMM (Bischoff and Bold, 1963), BG-11 (Rippka et al., 1979), OHM (Fábregas et al., 2000) and with KM1-basal medium (Kobayashi et al., 1991).Various studies indicate an optimal temperature between 20 to 28°C for growth and astaxanthin production (Fan et al., 1994; Yoo et al., 2012; Wan et al., 2014b). The optimal pH range for biomass and astaxanthin production was found to be between 7.0 - 7.85 (Sarada et al., 2002a; Hata et al., 2001).

Irradiation optimum during cultivation also ranges from 70 to 177 µmol photons $m^{-2}s^{-1}$ (Zhang et al., 2014; Fan et al., 1994; Domínguez-Bocanegra et al., 2004). Strain isolates, media composition, temperature or other cultivation parameters contribute to the variation among studies. White or blue LED lighting, or a combination of the two in a ratio of 3:1 using under constant illumination has shown to be the most efficient mode of illumination thus far (Saha et al., 2013). Higher light intensity than the corresponding light saturation point (LSP) induces carotenogenesis, however these values also range between studies from 150 µmol photons $m^{-2}s^{-1}$ to 480 µmol photons $m^{-2}s^{-1}$ (Zhang et al., 2014; Chekanov et al., 2014) variation between studies depend on the method used for carotenoid induction. Common carotenoid induction methods include addition of NaCl, nitrogen deprivation, sodium acetate along with NaCl , high PFD (photon flux densities) or several combinations thereof (Sarada et al., 2002; Kobayashi et al., 1993; Cifuentes et al., 2003).

## 1.6 Cultivation systems for *H. pluvialis* growth and astaxanthin production

*H. pluvialis* has the ability to grow in photoautotrophic, heterotrophic, or mixotrophic conditions. However, phototrophic growth is most commonly used in various cultivation systems such as closed photobioreactors (tubular or flat panel PBRs), open or closed raceway ponds or tanks (with or without aeration and stirring) and bubble or airlift columns (vertically, or less commonly horizontally). Batch, fed batch, or continuous modes of operation are employed with each mode having its advantages and disadvantages. However almost all commercially produced algal cultivation uses the open pond or closed photobioreactor method.

Photoautotrophic cultivation uses a common commercial two-step cultivation as culture conditions for maximum biomass and astaxanthin are exclusive. The first step being the optimal condition for growth and biomass formation during what is known as the "green stage" followed by a "red stage" where various stress conditions can be applied for carotenoid induction. A simpler one stage cultivation approach can also be applied however this method yields a significantly lower astaxanthin amounts.

Heterotrophic and mixotrophic cultures can also be used as the cost of high illumination is one of the main challenges of commercialization. Under heterotrophic conditions light is not needed as organic substrates serve as the carbon and energy source and acetate has been proved to be an efficient astaxanthin inducer. However, heterotrophic cultivation increases the risk of contamination (Hata et al., 2001; Olguín et al., 2012). Mixotrophic cultivation has shown promise in increasing biomass yields and astaxanthin contents (Krug, et al., 2020; Zhang et al., 1999; Wang et al., 2003). An astaxanthin content of 7% (DW) was reported using a sequential, heterotrophic- photoautotrophic culture mode achieving a 3.4 fold higher than autotrophic induction with a productivity of 6.25 mg $L^{-1}$ $d^{-1}$ (Kang et al., 2005). Overall photoautotrophic induction of astaxanthin production has shown to be more effective than heterotrophic induction and heterotrophic and mixotrophic cultures are less cost effective than photoautotrophic mass culture growth. More recently various new approaches such as "attached cultivation"(Wan et al., 2014b) and a "two-stage perfusion culture" combined with a stepwise increase of irradiance (Park et al., 2014) have advantages over traditional methods such as lower water consumption and smaller risk of contamination as well as higher astaxanthin productivity.

In recent years production of multiple products such as astaxanthin, triglycerides for biodiesel, and residual biomass for food or energy could further reduce the costs of biorefining. *H. pluvialis* fatty acid content of biomass (DW) ranges from 30-60% which makes *H. pluvialis* a viable candidate for biorefining (Solovchenko, 2015). *H. pluvialis* can utilize various carbon sources such as carbohydrates, carbon dioxide and carbonates thus speeding up cultivation by using various waste streams containing carbon and other nutrients (Wu et al., 2013). Furthermore, nutrients and energy can be recycled in auto-, hetero- and mixo-trophic cultivation methods, for instance recycling products from anaerobic digestion and utilizing carbohydrate-rich waste streams (Zhang, 2014). Once astaxanthin and triglycerides have been extracted residual biomass can further be used in feedstock for biogas which would return energy in this integrated process (Shah et al., 2016).

## 1.7 Current challenges in microalgae production

Current commercial cultivation is limited mainly due to high production costs with moderate productivities. Engineering designs and local environment largely determine the parameters of operation, furthermore conflicting studies regarding results and varying experimental designs cannot propose the most advantageous method of production. In large scale algal cultivation systems potential contaminations from bacteria, fungi, zooplankton, viruses or other unwanted microalgal species are frequently observed and can effect productivity of the cultivated species (Borowitzka, 2013; Bínová et al., 1998; Wang et al., 2016; Letcher et al., 2013). For instance, during cultivation of *Chlorella zofingiensis* a wild type strain *Scenedesmus* sp. FS was isolated as a contaminant and was able to quickly replace C. *zofingiensis* and form an ecological niche in an outdoor photobioreactor system (Huo et al., 2017). Recent studies indicate the co-occurrence of *Poterioochromonas malhamensis* with *Chlorella sorokiniana* have a significant impact on biomass yields as well (Ma et al., 2017). Rotifers and ciliates are of particular concern as they have shown the ability to decimate microalgal biomass in just a matter of days (Montemezzani et al., 2015; Moreno-Garrido et al., 2001). In many cases culture re-starts are often needed, and even a complete culture collapse or pond "crash" is often witnessed (Ma et al., 2017). Decontamination measures often require expensive control chemicals which can be disadvantageous to the process environment (Moreno-Garrido et al., 2001; Klapes and Vesley 1990; Johnston et al., 2005). Biological agents and physical treatments are also commonly used as decontamination measures (Carney and Lane, 2014) however, more sustainable replacements are required. Novel solutions are required to improve the efficiency and sustainability of microalgae production in the future. Recent advances and promising approaches for further improvements are introduced in the following chapter.

## 1.8 Recent advances in algal biomass and astaxanthin production

Regarding commercial economic viability, production costs remain a challenge and one significant contributing factor is insufficient biomass. Recent research concerning algae-bacterial symbiotic relationships could prove advantageous in biotechnological applications. In a recent study (Krug et al., 2020), co-cultivation experiments with plant growth-promoting species of *Methylobacterium* resulted in significantly enhanced biomass formation from 1.3-fold to 14 - fold higher yields in industrially relevant strains of *H. pluvialis* and *S. vacuolatus*, after 7 days of inoculation. Symbiotic bacteria have been observed near the surface of *H. plulialis*, which allows for direct metabolite exchange (Krug et al., 2020). This synergistic relationship is thought to be based on the ability of methylobacteria to grow solely on C-1

compounds that are discharged by algae and have been shown to form species specific relationships (Krug et al., 2020).Various bacterial genes with functions including nitrogen fixation, vitamin synthesis, siderophore and auxins synthesis, and other phytohormones have been shown to support algal growth, while algae can provide bacteria with dissolved organic matter (Okuda and Yamaguchi, 1960 ;Yu et al., 2017; Amin et al., 2009; Krug et al., 2020). Further exploration of natural strains of *H. pluvialis* as well as investigation of the natural microbiome could reveal more natural genetic variety and unveil insights into further beneficial bacterial-algal interactions. This information could be applied to create species specific synthetic communities which could push the industry toward more efficient algal biomass production without the side effects of competition for nutrients, light and space.

Krug and colleagues (2019) have explored the use of liquid and vaporized 5-isobutyl-2,3-dimethylpyrazine in microalgal cultures and found the treatments to be 100% effective in decontamination of three industrially relevant microalgal species *Scenedesmus vacuolatus, Chlorella vulgaris,* and *Haematococcus lacustris*. Furthermore, in between cultivation processes the use highly reactive agents such as hydrogen peroxide and sodium hypochlorite are commonly implied, which have shown to have deleterious effects on humans and the environment (Klapes and Vesley, 1990; Johnston et al., 2005). Pyrazine derivatives are generally considered safe for human consumption at certain concentrations (Adams et al., 2002) and occur naturally in various plants and bacteria ( Murray and Whitfeld, 1975; Bramwell et al., 1969; Buttery et al., 1969). 5-isobutyl-2,3- dimethylpyrazine is a model substance that simulates volatiles emitted by beneficial *Panenibacillus polymyxa* strains that are known as a potent biocontrol agents (Fürnkranz et al., 2012). In aforementioned study (Krug et al., 2019) the mechanism of pyrazines such as 5-isobutyl-2,3-dimethylpyrazine involves decreasing the stability of the algal cell wall which leads to cell rupture after alkylpyrazine applications. 5-isobutyl-2,3- dimethylpyrazine has previously been shown to be an effective means of decontaminating several species of bacteria commonly witnessed during meat processing (Schöck et al., 2018). Thus, further investigation of VOCs and other bioactive compounds as decontamination strategies in microalgae production could further improve biotechnological systems using environmentally friendly methods.

Genetic improvement could also provide the required characteristics for stable cultivation along with high productivity for feeds and fuel. Domestication of adding desired properties into the agal genome could help overcome important current challenges of production however, ongoing R&D is still needed to understand the complexities involved. However, genetic engineering of green eukaryotic microalgae has proven to be significantly difficult

and, in many instances, only transient transgene expression is obtained. Several transformation methods, vectors, promotors and strains have been investigated. Genetic improvements have long been limited to UV and chemical mutagenesis and screening techniques, however several improved mutants have been produced this way, many of which yield a two or three fold enhancement (Hu et al., 2008). More recently genetic engineering of the *H. pluvialis* chloroplast (Gutiérrez et al., 2012) and nuclear genomes (Sharon-Gojman et al., 2015) have been implied to improve product yield. However significant improvements still are needed.

As an additional strategy, several small molecules compounds such as plant hormones and their analongs have been tested as stress response mechanisms for astaxanthin production in *H. pluvialis*. The highest improvement was achieved with salicylic acid with 50 mg $L^{-1}$ and low light 25 μmol photons $m^{-2}$ $s^{-1}$ the content of astaxanthin was raised seven fold from 0.391 mg $L^{-1}$ to 2.74 mg $L^{-1}$(Gao et al., 2012b). mRNA transcript levels of 5 key enzymes of astaxanthin synthesis pathway (*ipi, psy, pds, crtO* and *crtR-b)* suggest a complex, multiple regulatory mechanisms at transcriptional, translational and post- transcriptional levels which control carotenoid synthesis (Li et al., 2010). Ongoing research regarding transformation vector technologies provides the opportunity of new metabolic engineering capabilities and a better understanding of the effects of small molecules on gene regulation have the possibility to enhance the likelihood of commercial production.

## 1.9 Objectives of the study

More efficient production of natural astaxanthin from *H. pluvialis* is in demand to meet higher commercial viability. Strains of the microalgae *H. pluvialis* currently used for astaxanthin production at BDI show no clear phenotype when analyzed with conventional methods. Therefore, the main objective of this study was to create an integrative characterization protocol of methods for BDI to better understand the variation within the species phylogeny, metabolic capabilities, biomass efficiency and volatile organic compound production. Methods used for characterization include: (I) Sanger sequencing of ITS and 18S rRNA genes of *H. pluvialis*, (II) fingerprinting analysis using BOX- PCR and ERIC PCR (III). Comparison of autotrophic and heterotrophic growth in varying media, (IV) observation of growth curves using aerated bioreactors with their corresponding biomass, and (V) investigation of secondary metabolites via GC-MS analysis (Figure 2).

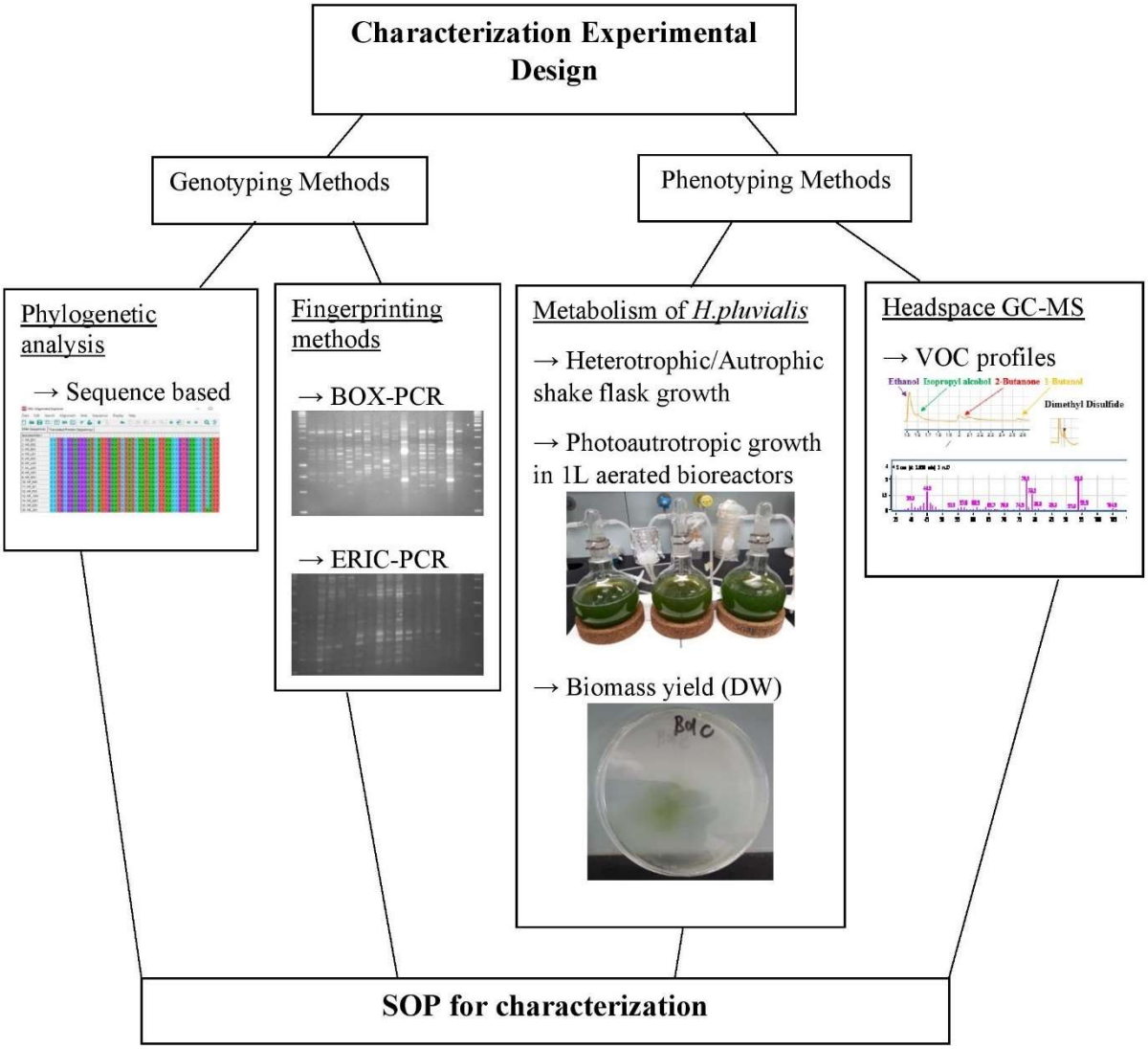


**Figure 2: Experimental design workflow**

# 2. Materials and Methods

## 2.1 Algal strains

The company BioLife Science GmbH (BDI) located in Styria, Austria, focuses on the production of the antioxidant astaxanthin (3,3'-dihydroxy- β, β -carotene-4,4'-dione) mostly based on the microalgae *H. pluvialis*, which is the richest natural source known thus far (Shah et al., 2016; Zhang et al., 2016). In this study 17 strains of *H. pluvialis* from the BDI strain collection were investigated for characterization (Table 1).

**Table 1: All strain names of *H. pluvialis* evaluated during characterization.** Strains derived from the strain collection at BDI.

| Isolate name | Strain |
|---|---|
| HL_ A01 | *Haematococcus pluvialis* |
| HP_ A01 | *Haematococcus pluvialis* |
| HP_ B01 | *Haematococcus pluvialis* |
| HP_ C01 | *Haematococcus pluvialis* |
| HP_ D01 | *Haematococcus pluvialis* |
| HP_ E01 | *Haematococcus pluvialis* |
| HP_ E02 | *Haematococcus pluvialis* |
| HP_ F01 | *Haematococcus pluvialis* |
| HP_ G01 | *Haematococcus pluvialis* |
| HP_ H01 | *Haematococcus pluvialis* |
| HP_ I01 | *Haematococcus pluvialis* |
| HP_ J01 | *Haematococcus pluvialis* |
| HP_ K01 | *Haematococcus pluvialis* |
| HP_ L01 | *Haematococcus pluvialis* |
| HP_ M01 | *Haematococcus pluvialis* |
| HP_ N01 | *Haematococcus pluvialis* |
| HP_ O01 | *Haematococcus pluvialis* |

## 2.2 Sequence based phylogenetic analysis

### 2.2.1 Sequence sample preparation

#### DNA extraction

To obtain genomic DNA, 300 µL of a 0.85% sterile NaCl solution was pipetted into 2-mL reaction tubes with glass beads. The tubes were inoculated with algal cells growing on BBM agar media and ribolyzed twice for 30 seconds at 6.5 m x $s^{-1}$. The tubes were then centrifuged for 3 min at 18°C and 4,000 rpm and the supernatant was transferred to new sterile tubes without touching cell debris.

#### PCR

Polymerase Chain Reaction was performed individually for each algal strain using three primer pairs with recommended program settings: SR1 and SR12 (Kim et al., 2015), NS1 and NS8 (White al., 1990), ITS1 and ITS4 (White al., 1990).

#### Gel electrophoresis

For conformation of the PCR products gel electrophoresis was performed using 0.5% TAE buffer and 0.8% agar. Program settings are as follows: 100 V, 200mA, 30 min. 3 µL of 1kb ladder added for reference. A mixture of 1.5 µL of dye and 4.5 µL of the PCR product were added to the following wells. The gel was then immersed in 0.8% ethidium bromide bath in

the dark for 20 - 30 min for staining. The gel was then immersed in a water bath to remove excess ethidium bromide. Gel bands were observed with the Quantity one® software program (Bio-Rad).

### PCR purification

Once the observed bands were confirmed, PCR purification was preformed via Wizard SV Gel and PCR Clean-Up System Quick Protocol FB072 (Promega, Fitchburg, USA) was used to remove unwanted components from the PCR tubes.

### DNA concentration

The DNA concentration for each PCR product was measured via Nanodrop™ 2000c. The concentration determined the amount of DNA needed for sequencing. The appropriate amount of DNA and ultrapure water (Table 2) was pipetted in an Eppendorf tube and sent to LCG Genomics (Berlin, Germany) for sequencing.

**Table 2: Sequencing preparations recommended by LGC Genomics (Berlin, Germany)**

| Template DNA | Concentration | Volume | Primer pair |
|---|---|---|---|
| 200-500 bp | 10 ng/ µL | 10 µL (DNA + $ddH_20$), 4 µL Primer (5mM) = 14 µL total | ITS1/4 |
| 500-1000 bp | 20 ng/ µL | | |
| 1000-2000 bp | 40 ng/ µL | | SR1/12, NS1/NS8 |

## 2.2.2 Sequence evaluation and extension

Sequences of each primer were evaluated for each strain by uploading the sequence file downloaded from LGC webpage into the program Seq Scanner 2. Once the files were imported the full sequences were viewed and bases were predicted with varying qualities indicated by their color. Only the sequence positions of high quality were used for evaluation. For each reverse primer SR12; NS8; and ITS4, a reverse compliment was created using the online tool https://www.bioinformatics.org/sms/rev_comp.html. A sequence of bases located near the end of the forward primer was selected. The same sequence was found in the reverse compliment of the reverse primer. Once the same sequence was found the following bases were added to increase the sequence length of the forward primer sequence. Extended sequences were created for all strains using each primer pair in this manner.

### 2.2.3 MEGA -X software for sequence alignments

The extended sequences were aligned using the MEGA -X software using ClustalW. Once aligned this tool allows you to see which positions you have a sequence for in all strains. For each primer pair all strains were aligned, and the sequence positions were chosen. Each primer now had the same position sequence and thus length. All three primer pair sequences were then put together to create one long sequence of 2,475 bp. This sequence consists of the following:

ITS1/ITS4 (White et al., 1990): 671 bp starting with sequence CCTGCGGAGGG ending with sequence AAACGTTGGCTTG

NS1/NS8 (White et al., 1990): 1,104 bp starting with sequence CCAGCAGCCGCGGTAA ending with sequence GGGTGTGCTGGTG

SR1/SR12 (Kim et al., 2015): 700 bp starting with sequence AGGATACTTT ending with sequence GGTCTGTGATGCCCTT

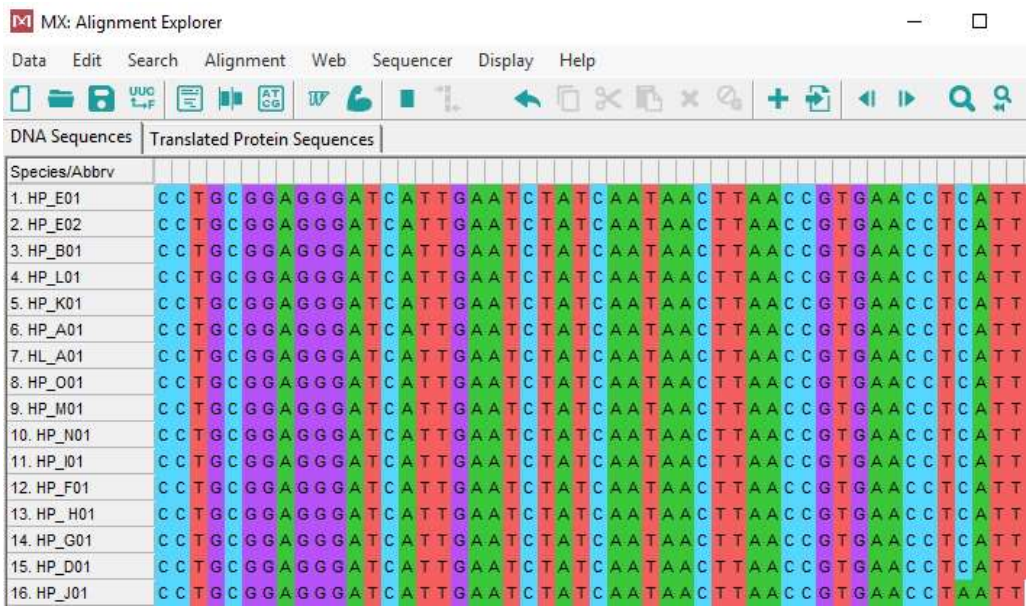


**Figure 3: Alignment of 2,475 bp partial sequences of *H. pluvialis*.** Derived from ITS1/4; NS1/NS8; and SR1/SR12 primer pairs aligned in MEGA-X.

### 2.2.4 Phylogenetic tree construction via maximum likelihood method of combined sequences

Using the MEGA-X program, a phylogenetic tree was constructed using the maximum likelihood method from the 2,475 bp sequences obtained for each strain. Thus, creating a visualization of the genetic divergence within the species *H. pluvialis*.

### 2.2.5 Percent identity matrix

For a compact overview of the 2,475 bp sequence similarities a percent identity matrix was created using the online website https://www.ebi.ac.uk/Tools/msa/clustalo/.

## 2.3 Phylogenetic analyses via fingerprinting methods

### 2.3.1 BOX-PCR and phylogenetic tree via neighbor joining method

A BOX-PCR was performed to further differentiate between the strains based on banding patters. Each PCR tube contained 16.5 µL $H_20$, 2.5 µL Box Primer A1, 1 µL DNA and 5 µL Taq & Go. The recommended PCR program was ran and is as follows:

1. 6 min 94°C
2. 1 min 94°C
3. 1 min 53°C
4. 8 min 65°C , (repeat steps 2-4 35x)
5. 16 min 65°C
6. Pause 10°C

To view banding patterns gel electrophoresis of the PCR products was ran using a gel consisting of 0.5% TBE buffer and 1.5% agar. All PCR product was used along with 2 µL dye and 1kb ladder for reference. The gel was ran at 100 V, 300 mA current, for 3 h; then the voltage was changed to 120 and ran for 2 h. Staining was performed with 0.8% ethidium bromide in the dark for 45 min. Gel bands were observed using the program Quantity one analysis software (Bio-Rad). Based on the banding patters from the BOX-PCR image a more divergent phylogenetic tree was constructed via the neighbor joining method using the program PyElph1.4.

### 2.3.2 ERIC-PCR

ERIC-PCR banding patters were evaluated to further characterize between the various strains. Each PCR tube contained 10 µL $H_20$, 2.5 µL forward and reverse primer, 2 µL DNA and 3 µL Taq & Go. The recommended PCR program was is as follows:

1. 5 min 95°C
2. 1 min 94°C
3. 5 min 51°C
4. 8 min 68°C , (repeat steps 2-4 30x)
5. 16 min 65°C
6. Pause 10°C

Banding patterns were observed via the same method as with BOX- PCR.

## 2.4 Metabolism of *H. pluvialis*

### 2.4.1 Heterotrophic/Autotrophic shake flask growth experiments

The metabolism of *H. pluvialis* was evaluated in various media in light and dark conditions. 10 mL of BBM media, BBM media + 0.8 g/L glucose or BBM media + 0.8 g/L sodium acetate was added to sterile 100mL Erlenmeyer flasks. The glucose and sodium acetate were filter sterilized with 0.2-micron filter. All flasks were inoculated with the same concentration of cells. For growth conditions in the dark the flasks were placed in a container completely covered with tin foil in a dark cabinet. Light conditions ranged from 6.7 - 8.6 Lux using fluorescent tube lighting and flask positions in the greenhouse at the Institute of Environmental Biotechnology were randomized daily with 18-h light/6-h dark cycles. The fluorescence intensity of 100 µL was measured with excitation 450 nm and emission 685 nm the day of inoculation and after day 7 and 14. CFU values were plated with 10 µL of culture grown in a petri dish containing BBM media with agar. Samples were plated after 7 and 14 days of growth. Once the culture was plated, the petri dishes were left to grow in the greenhouse until observable CFUs could be counted. Each strain in each condition was performed in triplicate to ensure reliable data.

### 2.4.2 Round bottom flask growth experiments

The purpose of this experiment was to observe growth curves over a 15-day period. 800 mL of BBM media was added to sterile 1L round bottom flasks. The flasks were then inoculated with the same number of cells and aerated at a psi of 2. Growth conditions consisted of a 24-h light cycle with intensities ranging from 5.2 - 8.0 Lux using white LED lighting. Flask positions were randomized daily for an equal light intensity distribution during the growing process. Fluorescence intensity of 100 µL of culture was measured with excitation 450 nm and emission 685 nm on the day of inoculation. Once there was an observable green tint (day 5), samples were then taken from day 5 - 9 and day 12 - 15 when the fluorescence intensity dropped. This indicates a transition from the green vegetative stage to the astaxanthin accumulating palmella cell in transition to an aplanospore. The CFU of 10 µL of culture was plated every day a sample was taken and left to grow in white LED lighting until observable CFUs could be counted. Each strain was grown in triplicate for data verification.

### 2.4.3 Biomass yield (DW) from round bottom flasks

Biomass via dry weight was measured once the round bottom flasks were harvested on day 15. Samples of 20 mL of a homogeneous mixture of the culture was sampled 4 times. From the 20mL samples, 10mL of the whole culture was poured into a petri dish and left at 60°C

until dry. 20mL of the culture was then centrifuged and 10mL of the supernatant was poured in a petri dish and left to dry at 60°C. The supernatant contains various trace salts from the media and thus was subtracted to obtain the algal biomass yield.

## 2.5 Headspace GC-MS Analyses

GC-MS combines gas chromatography which separates chemical mixtures, while the MS component recognizes the components by mass of the analyte molecule. A GC-MS was performed to investigate specific compounds produced by various strains of *H. pluvialis.* GC-MS vials were filled with 7mL of sterile BBM media and were left to dry in a slanted position. All 17 strains were inoculated in duplicate. The same day of inoculation BDI also inoculated 4 unanimous strains in duplicate. All vials grew in the green house at the Institute of Environmental Biotechnology under white LED lighting for 12 days and sample positions were randomized daily. Growth conditions occurred with 18-h light/6-h dark cycles, with a light intensity between 6.7 - 8.6 Lux. On day 12 all samples were ran under settings indicated in (Table 3), in randomized positions. Uninoculated vials of BBM media were also ran for comparison of the media prepared at BDI and the Institute Environmental Biotechnology.

**Table 3 : GC-MS method information.** Agilent 7890B Gas Chromatograph, 5977A Mass Spectrometer, PAL RSI Sampler

| | |
|---|---|
| **Mobile Phase** | Helium 6.0,<br>Flow: 1.2 mL/min |
| **Stationary Phase** | HP-5MS(= apolar): Dimensions: 30m x 250µm x 0,25µm |
| **Adsorbing Fiber** | Divinylbenzene/Carboxen/Polydimethylsiloxane (DVB/CAR/PDMS) coating |
| **GC Method** | Adsorbing Time: 30 min at 40°C<br>Extraction Time in Inlet: 36 min at 250°C<br>Oven: 40°C (2min)-5°C/min-110°C, 10°/min-280° (3min), Transfer Line Temperature: 280°C |
| **Stationary Phase** | HP-5MS (= apolar): Dimensions: 30m x 250µm x 0,25µm |

## 2.6 Growth media and primer pairs

### Sources of supply

All chemicals, culture media and hardware were produced from the following companies: Eppendorf (Hamburg, Germany), Carl Roth (Karlsruhe, Germany), Merck (Darmstadt, Germany).

## Bold's Basal Medium (BBM)

Per L:10 mL of each of the following stock solutions:

$NaNO_3$……....25 g/L

$MgSO_4$……. .....7.5 g/L

$KH_2PO_4$ ……...17.5 g/L

$CaCl_2$ x 2 $H_20$ ……2.5 g/L

NaCl …….....2.5 g/L

$NaHCO_3$ ……....1.6 g/L

$K_2HPO_4$ …….....7.5 g/L

Solutions were autoclaved at 121 °C for 15 min

## Trace element solution

Per L: 3 mL of the following stock solution

$Na_2EDTA$ …….....1.5 g/L

$FeSO_4$ x 7 $H_20$ ……....1.67 g/L

$MuCl_2$ x 4 $H_20$ …….....0.082 g/L

$ZnCl_2$ ……...0.01 g/L

$CoCl_2$ x 6 $H_20$ …….....0.004 g/L

$Na_2MoO_4$ x 2 $H_20$ ……..0.008 g/L

Trace solution was filter sterilized with a 0.2-micron filter

## Vitamin solution

Per L: 1 mL of the following stock solutions

Thiamin ……... 0.1 g/L

Biotin …….....0.0005 g/L

Trace solution was filter sterilized with a 0.2-micron filter

## Shake flask media

10 mL of various media in 100mL Erlenmeyer flasks:

BBM media

BBM media + 0.8 g/L glucose

BBM media + 0.8 g/L sodium acetate.

BBM media was autoclaved at 121 °C for 15 min. Glucose and sodium acetate were filter sterilized with a 0.2 - micron filter.

**Table 4: Primer Pairs used for Phylogenetic analysis**

| Primer | Sequence 5' to 3' | Distributor |
|---|---|---|
| ITS1 | TCCGTAGGTGAACCTGCGG | Sigma-Aldrich |
| ITS4 | TCCTCCGCTTATTGATATGC | Sigma-Aldrich |
| NS1 | GTAGTCATATGCTTGTCTC | Sigma-Aldrich |
| NS8 | TCCGCAGGTTCACCTACGGA | Sigma-Aldrich |
| SR1 | TACCTGGTTGATCCTGCCAG | Sigma-Aldrich |
| SR12 | CCTTCCGCAGGTTCACCTAC | Sigma-Aldrich |
| BOX A1R PCR | CTACGGCAAGGCGACGCTGACG | Sigma-Aldrich |
| ERIC1R | ATGTAAGCTCCTGGGGATTCAC | Sigma-Aldrich |
| ERIC 2 | AAGTAAGTGACTGGGGTGAGCG | Sigma-Aldrich |

# 3. Results

## 3.1 Sequence based phylogenetic analysis revealed variation in most strains of *H. pluvialis*

### 3.1.1 Constructed phylogenetic tree via maximum likelihood method for visualization of genetic divergence

The goal of this experiment was to differentiate sequences of genomic DNA in several strains of *H. pluvialis* using combined sequences obtained with primer pairs ITS1/4, NS1/NS8 and SR1/SR12. Based on the 2,475 bp sequences derived from the selected primer pairs a phylogenetic tree via maximum likelihood method was created using MEGA-X to view predicted evolutionary relationships among strains of the same species (Figure 4).

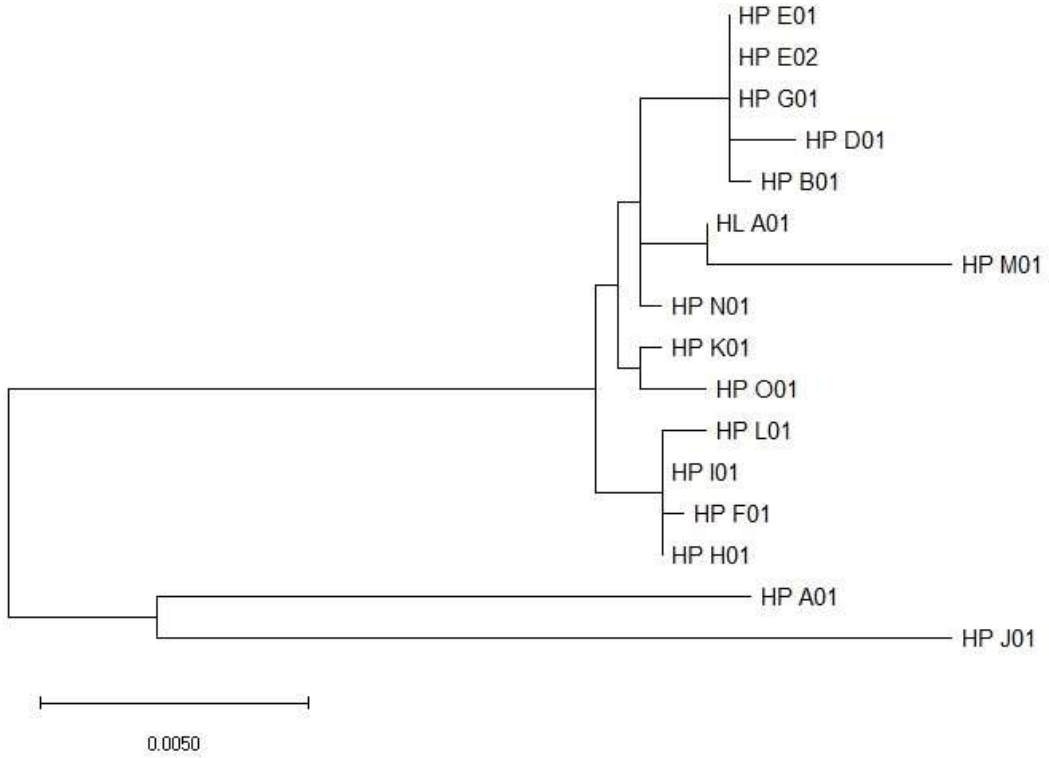


**Figure 4** : **Phylogenetic tree via maximum likelihood method**. Based on sequence data of combined 2,475 bp sequences constructed with MEGA-X.

### 3.1.2 Percent identity matrix uncovered significant variation among various strains

Sanger sequencing of the 2,475 bp derived from partial primer sequences of ITS1/ITS4, NS1/NS8, and SR1/SR12 revealed 96.02 - 100 % sequence identity between all strains tested. HP_E01, HP_E02 and HP_G01 were found to be 100% identical, while HP_B01 was found to have 99.96% identity to the following three strains, with only a single base change. Additionally, HP_I01 and HP_H01 were shown to have 100% sequence identity. An overview of specific percentage comparisons can be observed in (Table 5).

**Table 5: Percent identity matrix between strains of *H. pluvialis*.** Derived from sanger sequencing of combined 2,475 bp analysis using primer pairs ITS1/ITS4; NS1/NS8, and SR1/SR12

| | HP_ J01 | HP_ A01 | HP_ M01 | HP_ D01 | HP_ E01 | HP_ E02 | HP_ G01 | HP_ B01 | HP_ L01 | HP_ I01 | HP_ H01 | HP_ F01 | HP_ K01 | HP_ O01 | HL_ A01 | HP_ N01 |
|---|---|---|---|---|---|---|---|---|---|---|---|---|---|---|---|---|
| **HP_J01** | 100.0 | 96.89 | 96.02 | 96.35 | 96.47 | 96.47 | 96.47 | 96.43 | 96.47 | 96.47 | 96.47 | 96.43 | 96.47 | 96.43 | 96.47 | 96.47 |
| **HP_A01** | 96.89 | 100.0 | 96.81 | 97.39 | 97.43 | 97.43 | 96.43 | 96.47 | 97.31 | 97.39 | 97.39 | 97.35 | 97.43 | 97.39 | 97.27 | 97.35 |
| **HP_M01** | 96.02 | 96.81 | 100.0 | 99.13 | 99.25 | 99.25 | 99.25 | 99.21 | 99.21 | 99.21 | 99.21 | 99.17 | 99.30 | 99.38 | 99.54 | 99.38 |
| **HP_D01** | 96.35 | 97.39 | 99.13 | 100.0 | 99.88 | 99.88 | 99.88 | 99.83 | 99.46 | 99.54 | 99.54 | 99.50 | 99.59 | 99.50 | 99.59 | 99.67 |
| **HP_E01** | 96.47 | 97.43 | 99.25 | 99.88 | 100.0 | 100.0 | 100.0 | 99.96 | 99.59 | 99.67 | 99.67 | 99.63 | 99.71 | 99.63 | 99.71 | 99.79 |
| **HP_E02** | 96.47 | 97.43 | 99.25 | 99.88 | 100.0 | 100.0 | 100.0 | 99.96 | 99.59 | 99.67 | 99.67 | 99.63 | 99.71 | 99.63 | 99.71 | 99.79 |
| **HP_G01** | 96.47 | 97.43 | 99.25 | 99.88 | 100.0 | 100.0 | 100.0 | 99.96 | 99.59 | 99.67 | 99.67 | 99.63 | 99.71 | 99.63 | 99.71 | 99.79 |
| **HP_B01** | 96.43 | 97.47 | 99.21 | 99.83 | 99.96 | 99.96 | 99.96 | 100.0 | 99.54 | 99.63 | 99.63 | 99.59 | 99.75 | 99.67 | 99.67 | 99.75 |
| **HP_L01** | 96.47 | 97.31 | 99.21 | 99.46 | 99.59 | 99.59 | 99.59 | 99.54 | 100.0 | 99.92 | 99.92 | 99.88 | 99.67 | 99.59 | 99.67 | 99.67 |
| **HP_I01** | 96.47 | 97.39 | 99.21 | 99.54 | 99.67 | 99.67 | 99.67 | 99.63 | 99.92 | 100.0 | 100.0 | 99.96 | 99.75 | 99.67 | 99.67 | 99.75 |
| **HP_H01** | 96.47 | 97.39 | 99.21 | 99.54 | 99.67 | 99.67 | 99.67 | 99.63 | 99.92 | 100.0 | 100.0 | 99.96 | 99.75 | 99.67 | 99.67 | 99.75 |
| **HP_F01** | 96.43 | 97.35 | 99.17 | 99.50 | 99.63 | 99.63 | 99.63 | 99.59 | 99.88 | 99.96 | 99.96 | 100.0 | 99.71 | 99.63 | 99.63 | 99.71 |
| **HP_K01** | 96.47 | 97.43 | 99.30 | 99.59 | 99.71 | 99.71 | 99.71 | 99.75 | 99.67 | 99.75 | 99.75 | 99.71 | 100.0 | 99.83 | 99.75 | 99.83 |
| **HP_O01** | 96.43 | 97.39 | 99.38 | 99.50 | 99.63 | 99.63 | 99.63 | 99.67 | 99.59 | 99.67 | 99.67 | 99.63 | 99.83 | 100.0 | 99.67 | 99.75 |
| **HL_A01** | 96.47 | 97.27 | 99.54 | 99.59 | 99.71 | 99.71 | 99.71 | 99.67 | 99.67 | 99.67 | 99.67 | 99.63 | 99.75 | 99.67 | 100.0 | 99.83 |
| **HP_N01** | 96.47 | 97.35 | 99.38 | 99.67 | 99.79 | 99.79 | 99.79 | 99.75 | 99.67 | 99.75 | 99.75 | 99.71 | 99.83 | 99.75 | 99.83 | 100.0 |

## 3.2 Phylogenetic analysis via fingerprinting PCR methods indicate a powerful tool for strain differentiation in *H. pluvialis*

The aim of this experiment was to characterize strains based on banding patterns of the BOX-PCR gel image. Strain HP_E01, HP_E02 and HP_B01 were found to have the same banding patterns, while all other strains tested showed a unique profile (Figure 5). Banding pattern detection using PyElph 1.4 was used (Figure 6) to create a more divergent phylogenetic tree using the neighbor joining method (Figure 7) which distinguished HP_G01 from the previous cluster containing HP_E01, HP_E02 (Figure 4). Strain HP_I01 can also be distinguished from HP_H01 which previously was clustered together (Figure 4).

### 3.2.1 BOX-PCR profiles exhibit significant variation in many strains of *H. pluvialis*

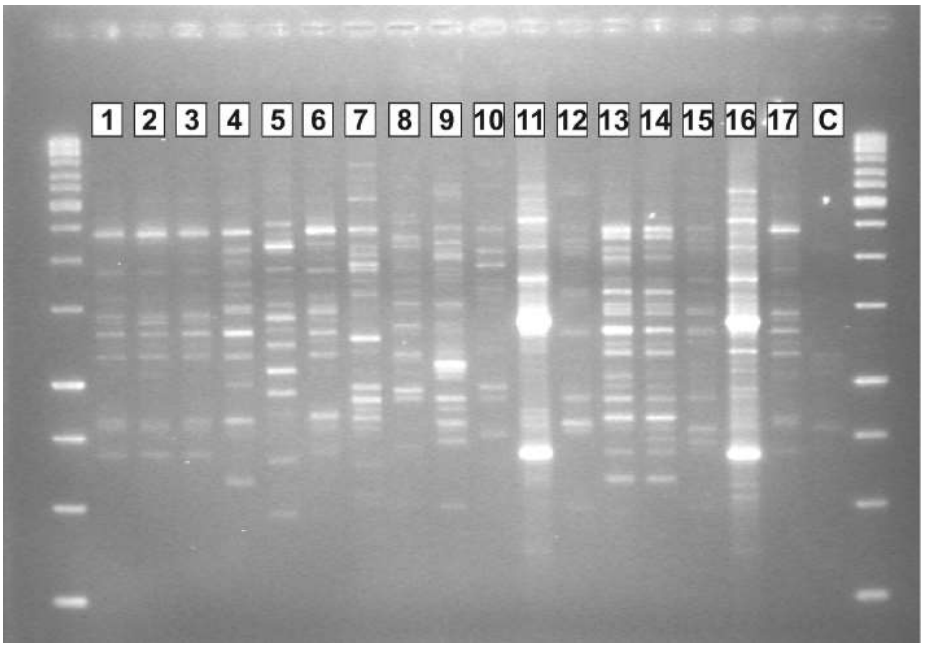


**Figure 5: BOX-PCR.** Gel image of various *H. pluvialis* strains from the BDI strain collection.

**Figure 5 Legend**

1kb ladder
1. HP_E01
2. HP_E02
3. HP_B01
4. HP_ L01
5. HP_K01
6. HP_A01
7. HL_A01
8. HP_O01
9. HP_M01
10. HP_N01
11. HP_I01
12. HP_F01
13. HP_H01
14. HP_G01
15. HP_C01
16. HP_D01
17. HP_J01
C. Negative control
1 kb ladder

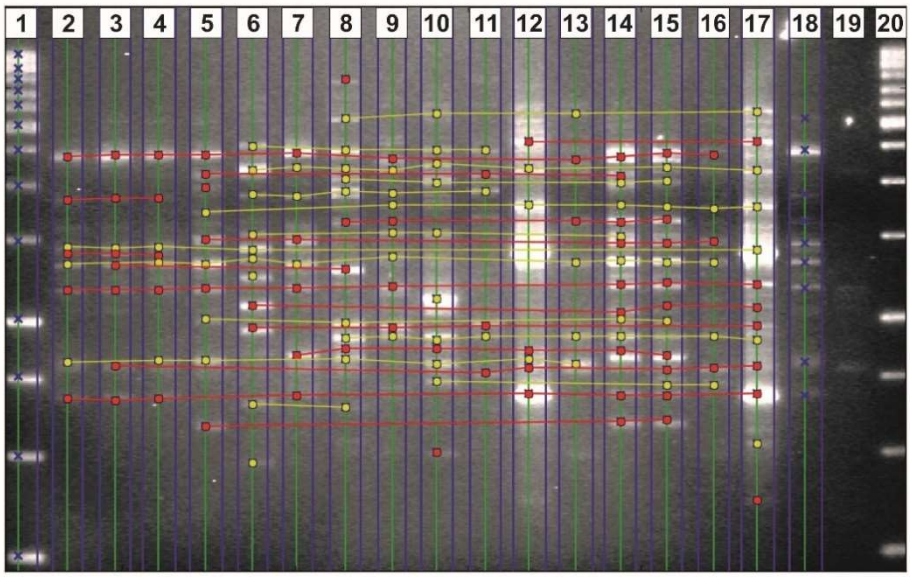


**Figure 6: BOX-PCR.** Banding patterns based on the gel image using detection software PyElph 1.4

**Figure 6 Legend**

1. 1kb Ladder
2. HP_E01
3. HP_E02
4. HP_B01
5. HP_L01
6. HP_K01
7. HP_A01
8. HL_A01
9. HP_O01
10. HP_M01
11. HP_N01
12. HP_I01
13. HP_F01
14. HP_H01
15. HP_G01
16. HP_C01
17. HP_D01
18. HP_J01
19.Negative control
20.1 kb ladder

### 3.2.2 Phylogenetic tree from BOX-PCR banding patterns resolves additional divergence

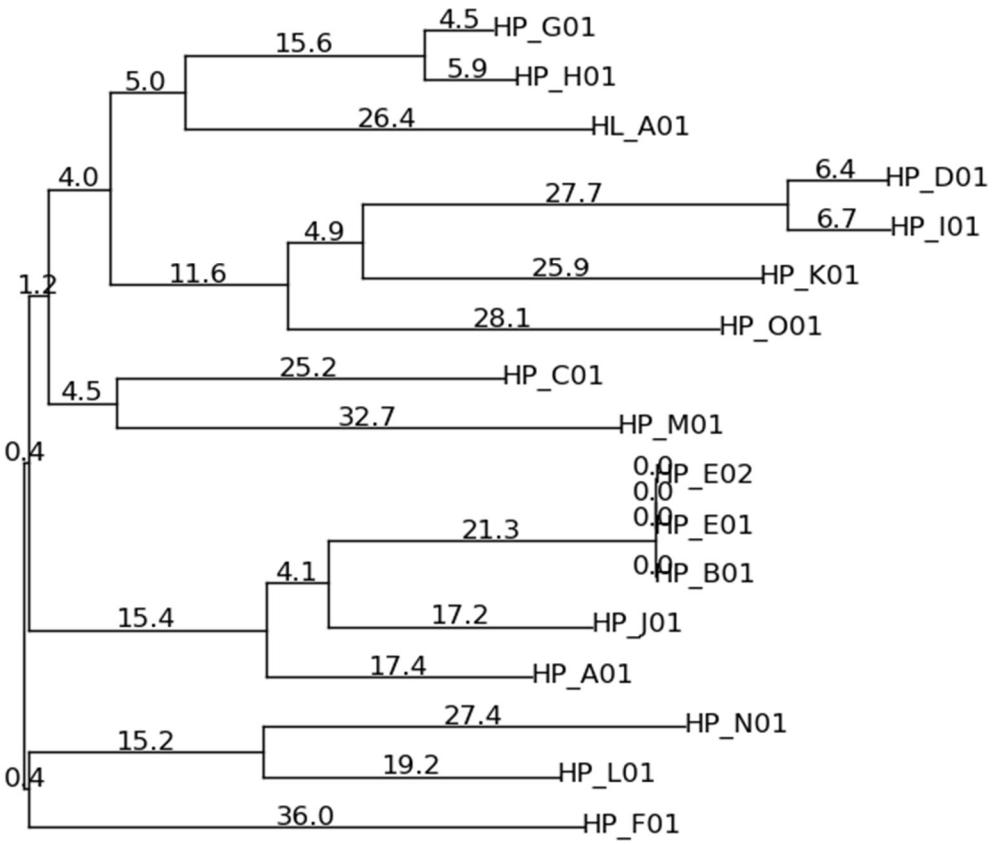


**Figure 7: Phylogenetic tree based on BOX-PCR banding pattern analysis using the neighbor joining method of PyElph 1.4.**

### 3.2.3 ERIC-PCR profiles reveal additional variance among strains

ERIC-PCR is another common fingerprinting tool for phylogenetic studies. Likewise, with BOX-PCR banning patterns were evaluated (Figure 8). Strain HP_E01 and HP_E02 showed the same banding pattern, while HP_B01 was distinguishable. All other strains showed a unique profile (Figure 8).

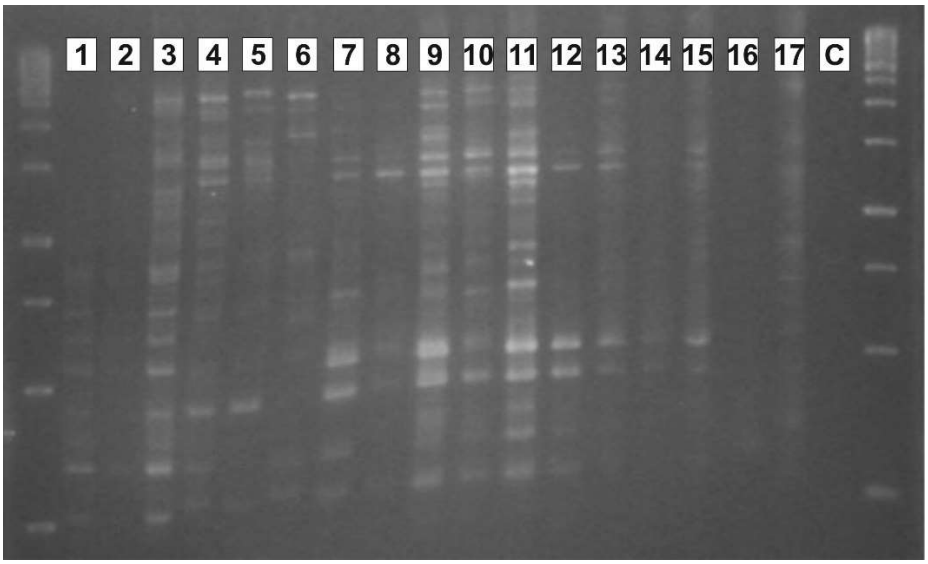


**Figure 8: ERIC-PCR** banding patterns of strains of *H. pluvialis* from the BDI strain collection

**Figure 8 Legend**

1kb Ladder
1. HP_E01
2. HP_E02
3. HP_B01
4. HP_L01
5. HP_K01
6. HP_A01
7. HL_A01
8. HP_O01
9. HP_M01
10. HP_N01
11. HP_I01
12. HP_F01
13. HP_H01
14. HP_G01
15. HP_C01
16. HP_D01
17. HP_J01
18. Negative control
1kb ladder

## 3.3 Heterotrophic/Autotrophic metabolism convey a range of phenotypic attributes

### BBM and BBM/glucose metabolism

The goal of this experiment was to characterize various strains based on their ability to grow in various media in light and dark conditions. Growth curves indicating CFU/10µL values were analyzed for all strains (Figures 11 - 27). Fluorescence curves using of 100µL of culture were also analyzed at an excitation of 450 nm and an emission value of 685 nm, which correlates to the chlorophyll B content. This determines which stage of the growth cycle the cells are during measurements taken after one and two weeks (Figures 28 - 44). Fluorescence curves correlate with CFU values in all cases, hence when the cells are growing the fluorescence intensity increases and when the CFU count is lower the fluorescence intensity decreases. The extent of this increase or decrease is unique to the strain (Figures 28 - 44). When comparing strains HP_E01 and HP_E02, no significant differences were found in all media and conditions tested since replica values commonly overlapped. The fluorescence values were also found to be nearly identical (Figures 11,12,28,29). Strains HP_E02, (443 CFU/10 µL), HP_N01 (430 CFU/10 µL), and HP_E01, (397 CFU/10 µL) were found to be the average top growing strains under shake flask growth conditions using fluorescent lamps and BBM media evaluated on day 14 (Figures 12,20,11). Under light conditions BBM with 0.8g/L glucose generally showed no significant advantage to BBM media was observed (Figures 11 - 27), except for strain HP_L01 in which BBM media averaged 147 CFU/10 µL

while with supplemental glucose an average of 242 CFU/10 µL was witnessed on day 14 (Figure 14). In almost all cases variation between replicas overlapped when grown in these two media. Under complete dark conditions no growth or very little growth was witnessed with BBM alone or with additional 0.8g/L glucose (Figures 11 - 27).

## Sodium acetate metabolism

Many strains indicated significant variations in growth patterns when an additional 0.8g/L sodium acetate was added to BBM media (Figures 11 - 27). Samples with additional 0.8g/L sodium acetate grown in light conditions ranged from 42 CFU/10 µL - 450 CFU/10 µL after one week, and 49 CFU/10 µL - 360 CFU/10 µL after two weeks (Figures 11 - 27). Significant variation was also witnessed with additional 0.8g/L sodium acetate in complete dark conditions (Figures 11 - 27). Growth after one week ranged from 10 CFU/10 µL - 203 CFU/10 µL and 8 CFU/10 µL - 193 CFU/10 µL after two weeks (Figures 11 - 27). Most strains CFU values increased from week one to week two in dark conditions with additional 0.8g/L sodium acetate, however in strains HP_K01, HL_A01, HP_O01 and HP_N01 the CFU count during week one in complete darkness was higher than week two (Figures 15,17,18,20). Most strains CFU values increased from week one to week two in light conditions with additional 0.8g/L sodium acetate, except in the case of HP_B01, HP_K01, HP_N01, and HP_F01 (Figures 13, 15, 20, 22). CFU counts after one week indicated strain HP_M01 had the largest growth advantage with additional 0.8g/L sodium acetate under light conditions when compared to BBM media alone, however after the second week the CFU counts were comparable to that of additional 0.8g/L glucose and BBM media (Figure 19).

When comparing flasks grown in the dark both BBM and BBM with 0.8g/L glucose showed no pigment, while in every case the flasks with 0.8g/L sodium acetate showed a noticeable green tint indicating growth (Figures 9, 28 - 44). When comparing the light conditions flasks with BBM and BBM with 0.8g/L glucose also showed a similar pigment, and thus comparable CFU and fluorescent measurements however, with additional 0.8g/L sodium acetate the flasks in many cases were a noticeably darker red indicating astaxanthin induction within a shorter time frame (Figures 10, 28 - 44).

**Figure 9: Shake flask growth for *H. pluvialis* strain HP_K01 in darkness after two weeks**. BBM media (left), BBM media with 0.8g/L glucose (middle), and BBM with 0.8g/L sodium acetate (right).

**Figure 10: Shake flask growth for *H. pluvialis* strain HP_K01 in 18 h light/ 6 h dark cycles after two weeks**. BBM media (left), BBM media with 0.8g/L glucose (middle), and BBM with 0.8g/L sodium acetate (right)

**Table 6: Legend for shake flask growth.** Conditions used for CFU/10µL curves (Figures 11 - 27) and fluorescence/100µL curves (Figures 28- 45).

| Legend | Media | Daily conditions |
|---|---|---|
| BBM L | BBM | 18-h light/6-h dark |
| BBM D | BBM | 24-h dark |
| Glu L | BBM+0.8g/L glucose | 18-h light/6-h dark |
| Glu D | BBM+0.8g/L glucose | 24-h dark |
| SA L | BBM+0.8g/L sodium acetate | 18-h light/6-h dark |
| SA D | BBM+0.8g/L sodium acetate | 24-h dark |

## 3.3.1 Heterotrophic/Autotrophic shake flask growth curves display a range of metabolic profiles

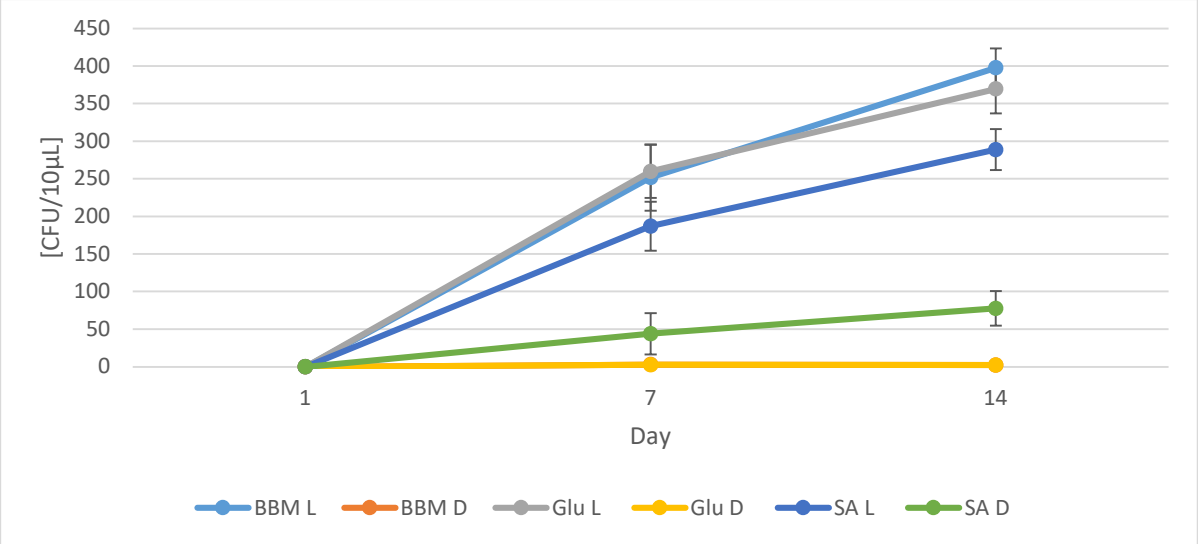


**Figure 11: Growth curves for *H. pluvialis* strain HP_E01.** Grown in various media in light and dark conditions.

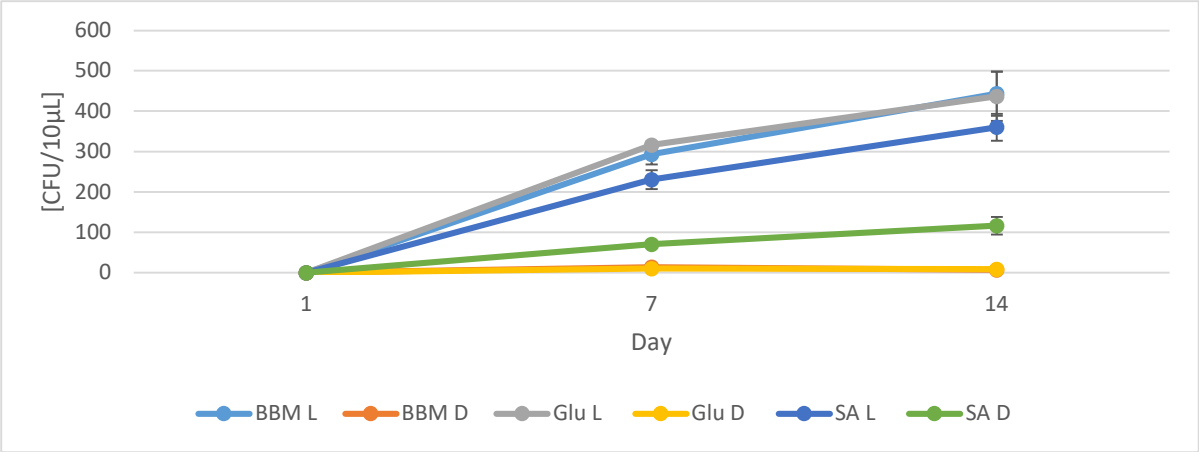


**Figure 12: Growth curves for *H. pluvialis* strain HP_E02.** Grown in various media in light and dark conditions.

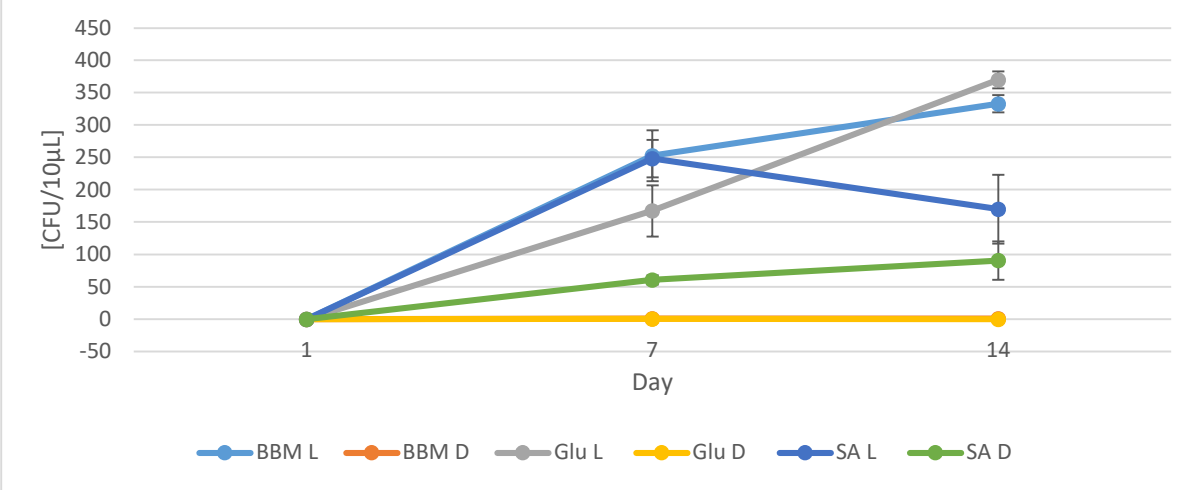


**Figure 13: Growth curves for *H. pluvialis* strain HP_B01.** Grown in various media in light and dark conditions.

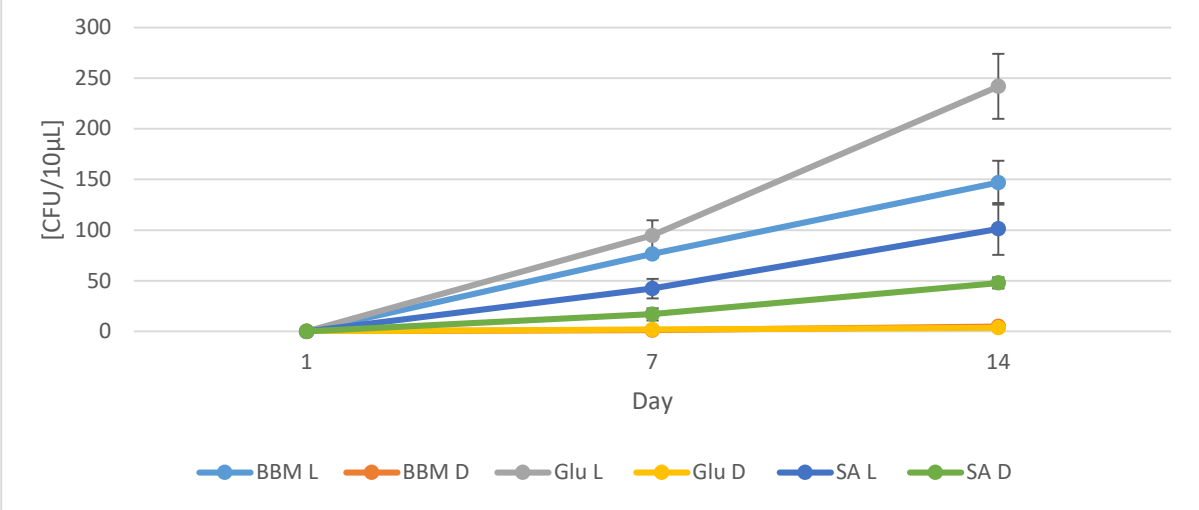


**Figure 14: Growth curves for *H. pluvialis* strain HP_L01.** Grown in various media in light and dark conditions.

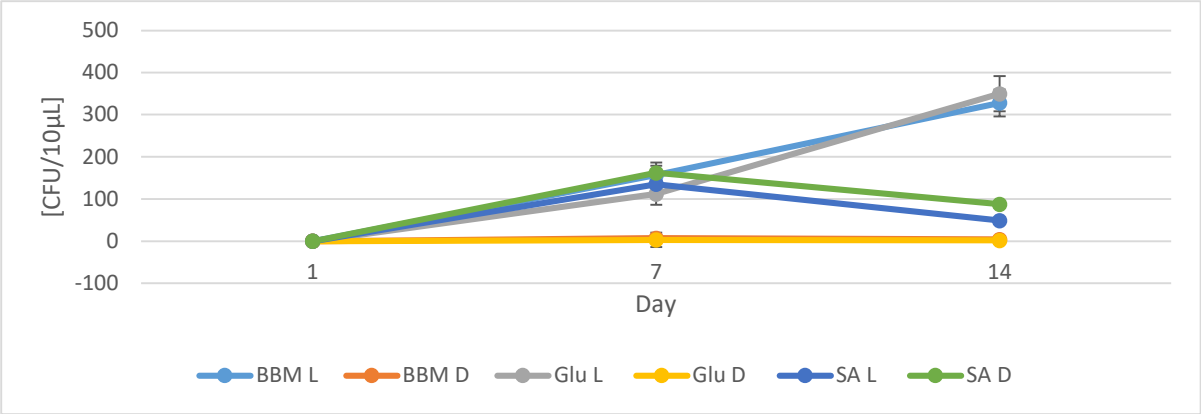


**Figure 15: Growth curves for *H. pluvialis* strain HP_K01.** Grown in various media in light and dark conditions.

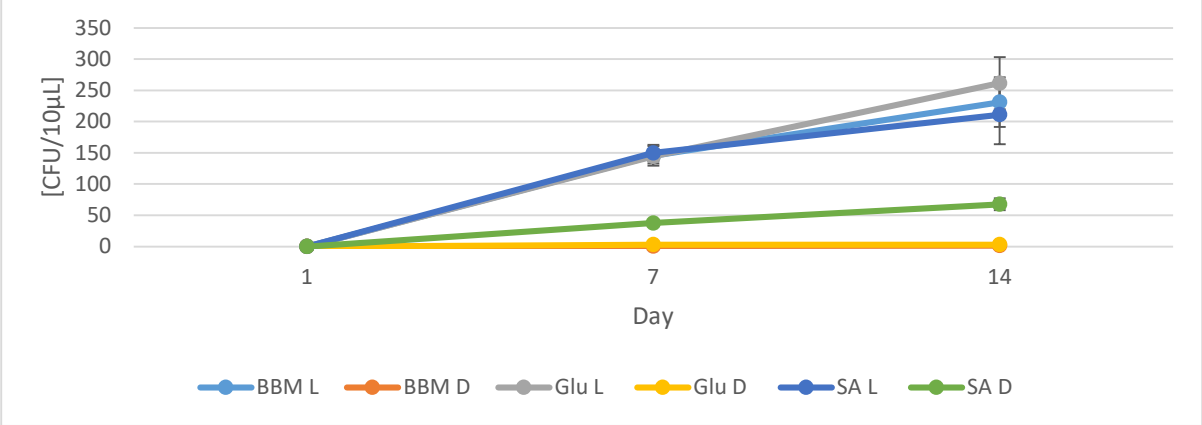


**Figure 16: Growth curves for *H. pluvialis* strain HP_A01.** Grown in various media in light and dark conditions.

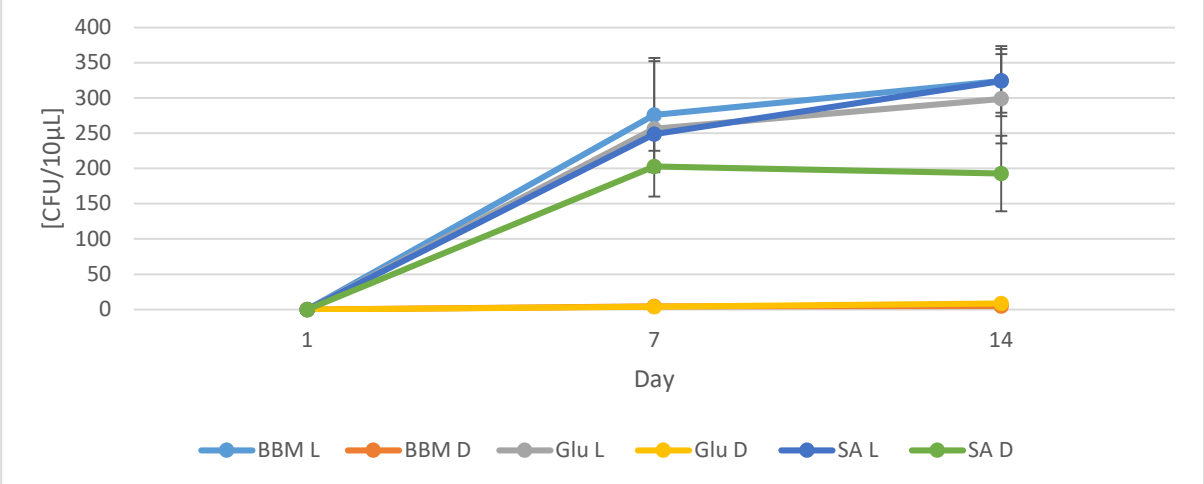


**Figure 17: Growth curves for *H. pluvialis* strain HL_A01.** Grown in various media in light and dark conditions.

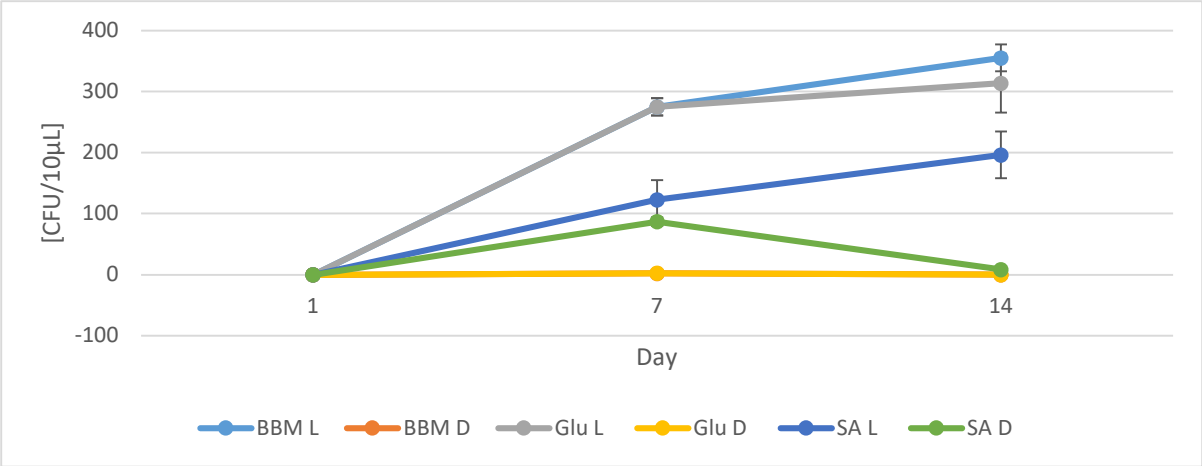


**Figure 18: Growth curves for *H. pluvialis* strain HP_O01.** Grown in various media in light and dark conditions.

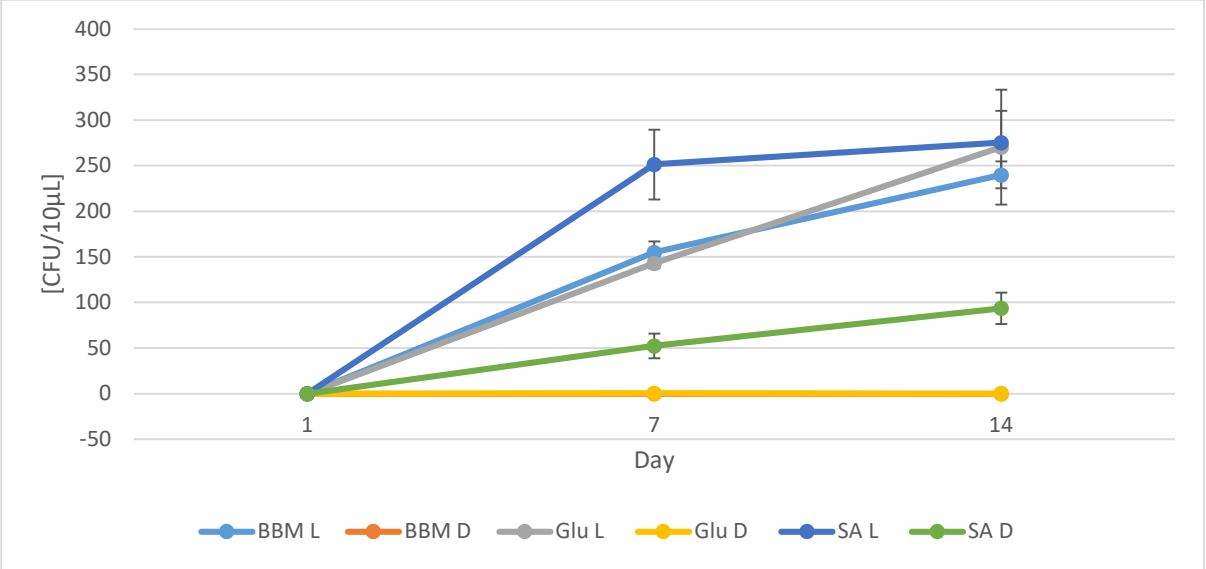


**Figure 19: Growth curves for *H. pluvialis* strain HP_M01.** Grown in various media in light and dark conditions.

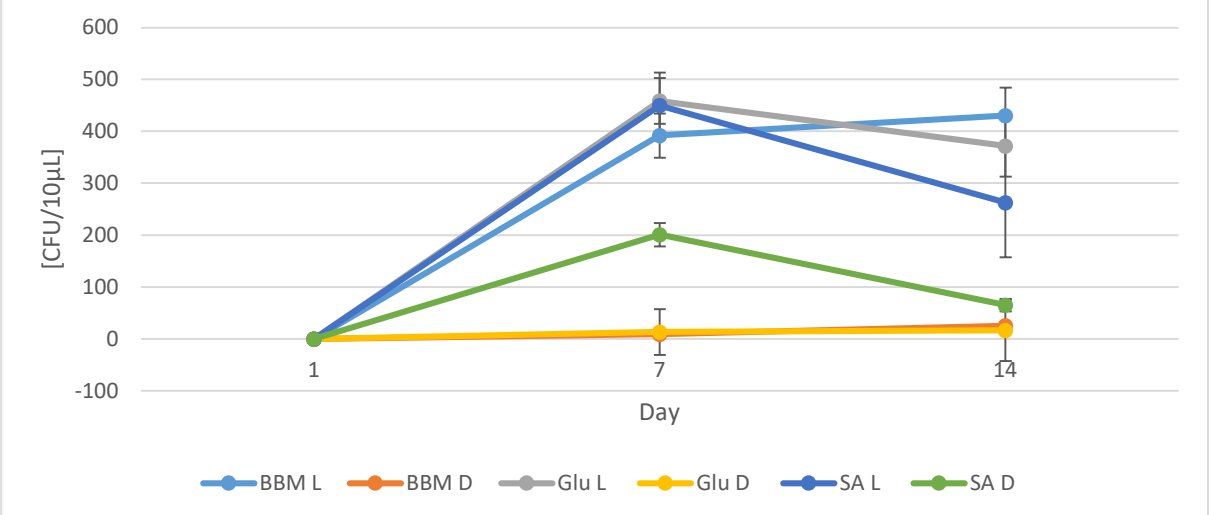


**Figure 20: Growth curves for *H. pluvialis* strain HP_N01.** Grown in various media in light and dark conditions.

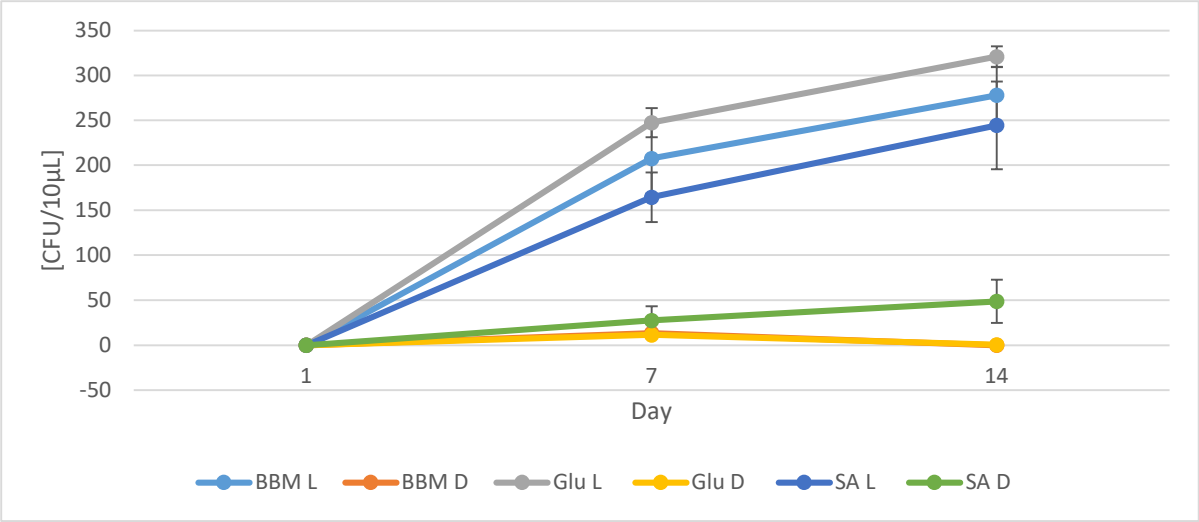


**Figure 21: Growth curves for *H. pluvialis* strain HP_I01.** Grown in various media in light and dark conditions.

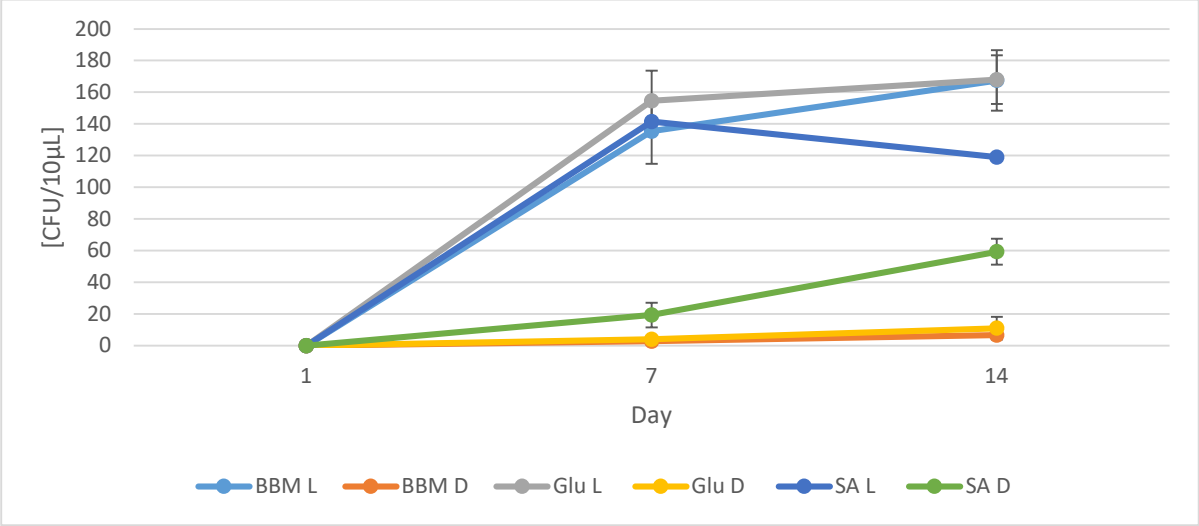


**Figure 22: Growth curves for *H .pluvialis* strain HP_F01.** Grown in various media in light and dark conditions.

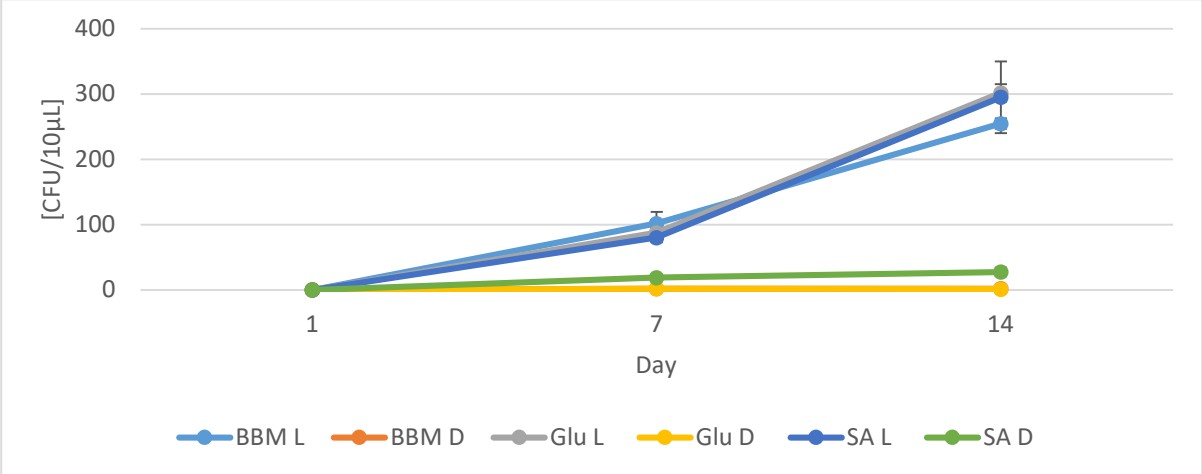


**Figure 23: Growth curves for *H. pluvialis* strain HP_H01.** Grown in various media in light and dark conditions.

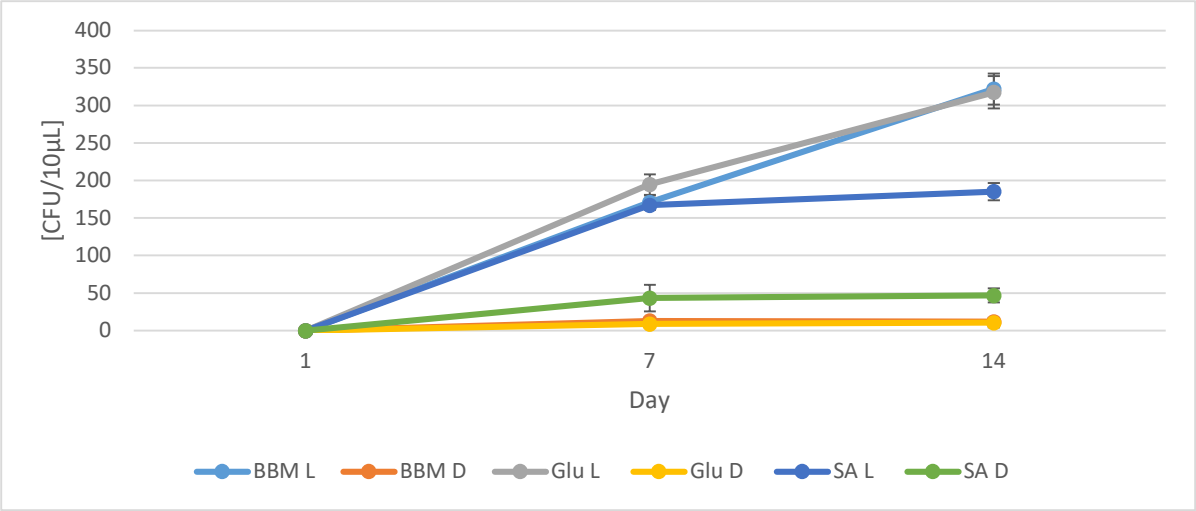


**Figure 24: Growth curves for *H. pluvialis* strain HP_G01.** Grown in various media in light and dark conditions.

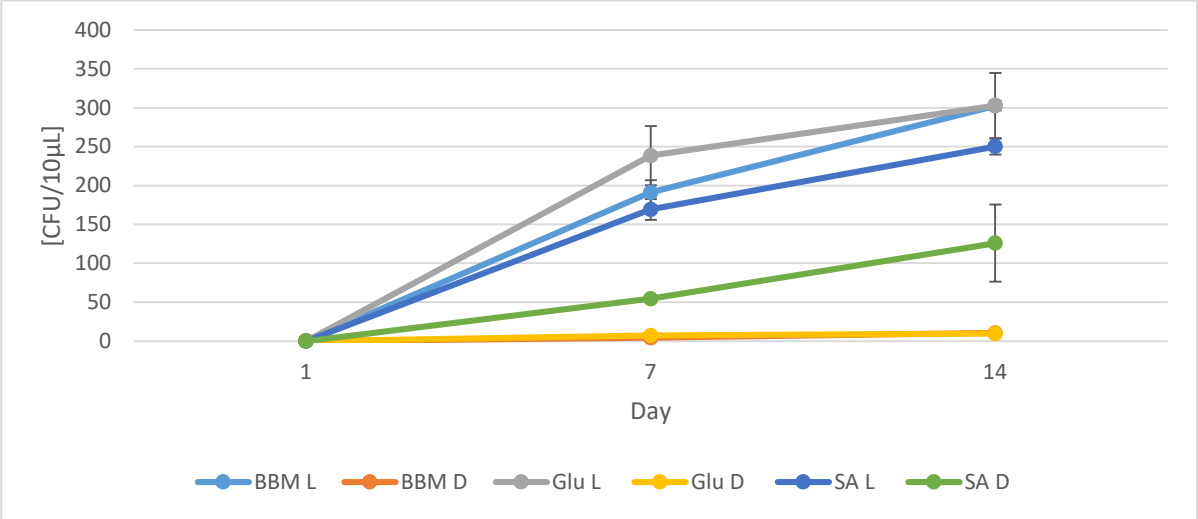


**Figure 25: Growth curves for *H. pluvialis* strain HP_C01.** Grown in various media in light and dark conditions.

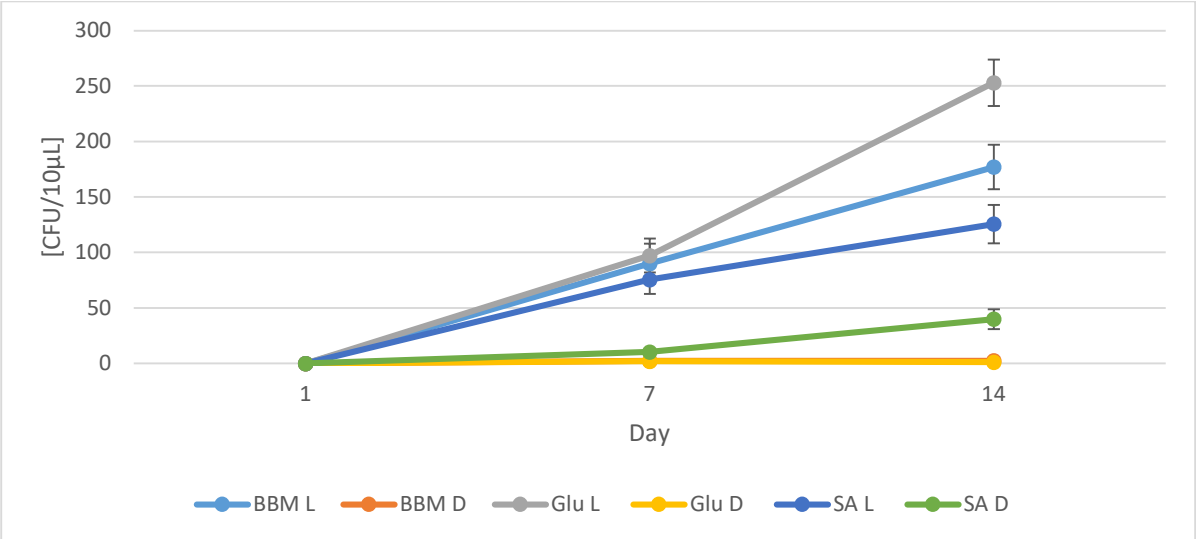


**Figure 26: Growth curves for *H. pluvialis* strain HP_D01.** Grown in various media in light and dark conditions.

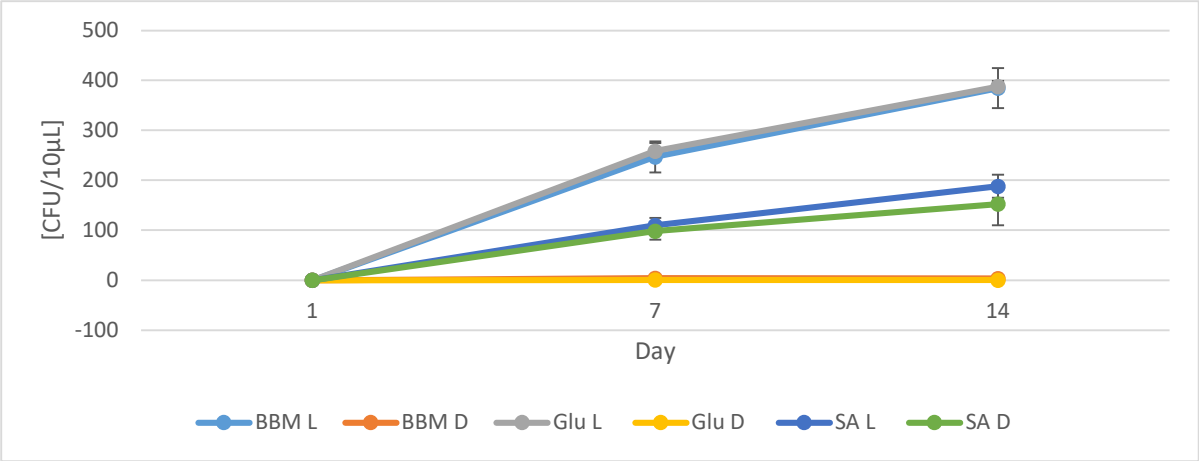


**Figure 27: Growth curves for *H. pluvialis* strain HP_J01.** Grown in various media in light and dark conditions.

### 3.3.2 Heterotrophic/Autotrophic shake flask fluorescence curves indicate significant variation in chlorophyll b profiles

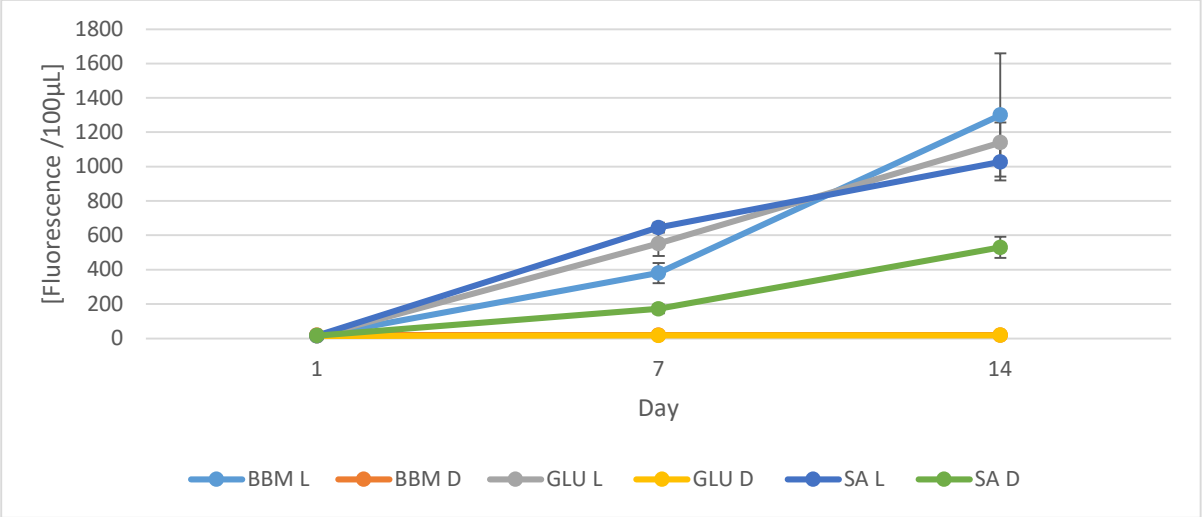


**Figure 28: Fluorescence curves for *H. pluvialis* strain HP_E01.** Grown in various media in light and dark conditions.

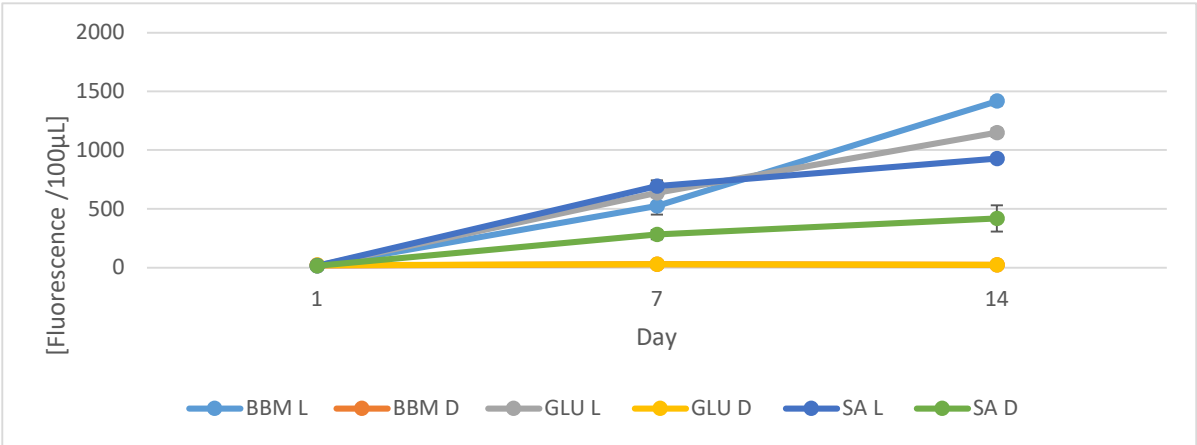


**Figure 29: Fluorescence curves for *H. pluvialis* strain HP_E02.** Grown in various media in light and dark conditions.

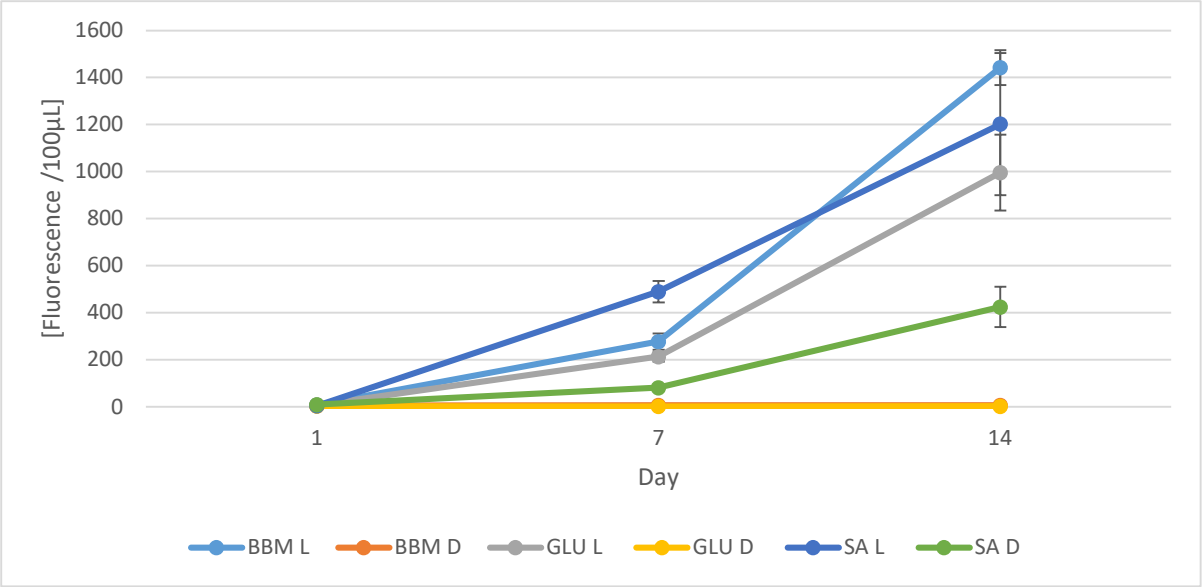


**Figure 30: Fluorescence curves for *H. pluvialis* strain HP_B01.** Grown in various media in light and dark conditions.

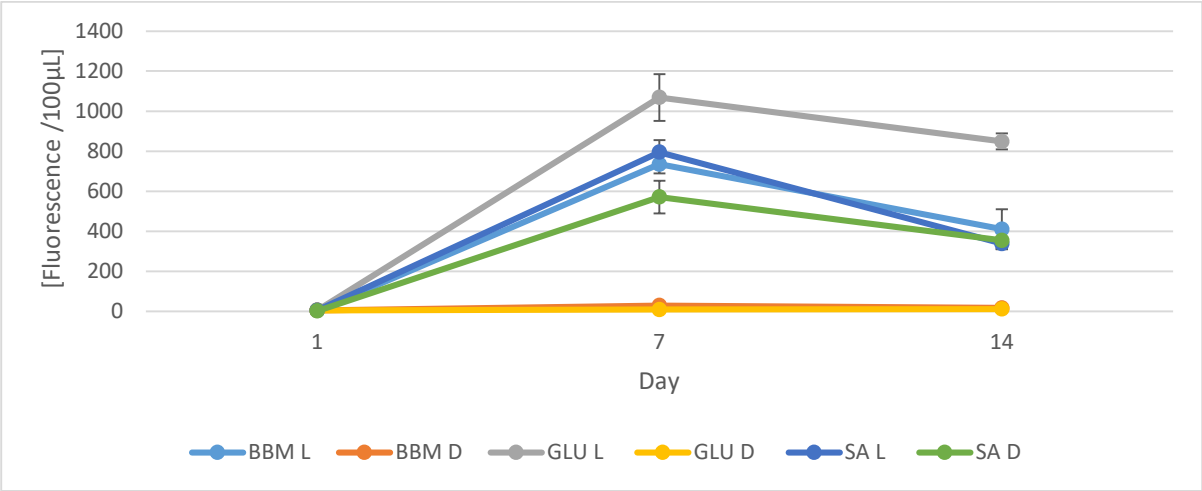


**Figure 31: Fluorescence curves for *H. pluvialis* strain HP_L01.** Grown in various media in light and dark conditions.

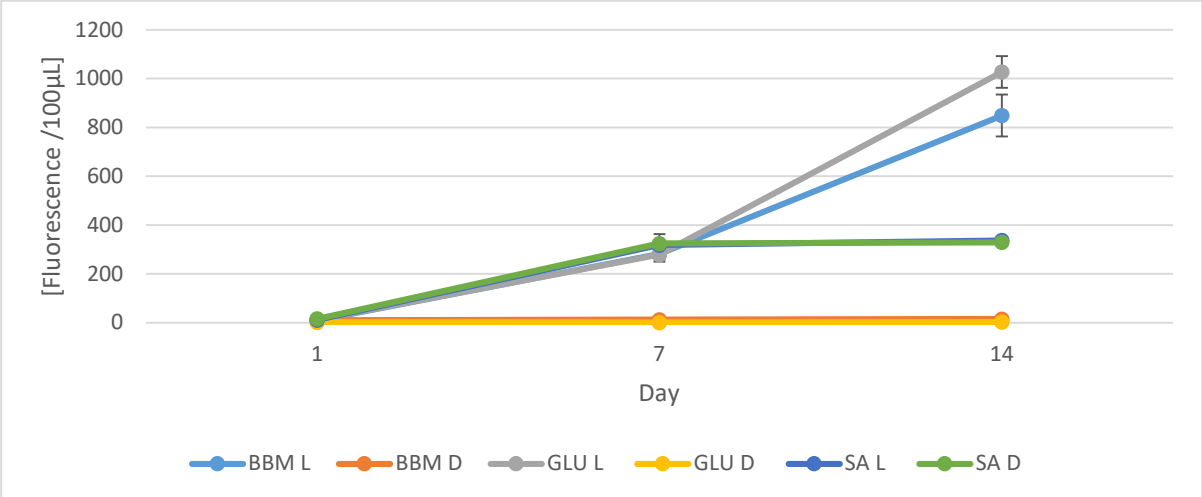


**Figure 32: Fluorescence curves for *H. pluvialis* strain HP_K01.** Grown in various media in light and dark conditions.

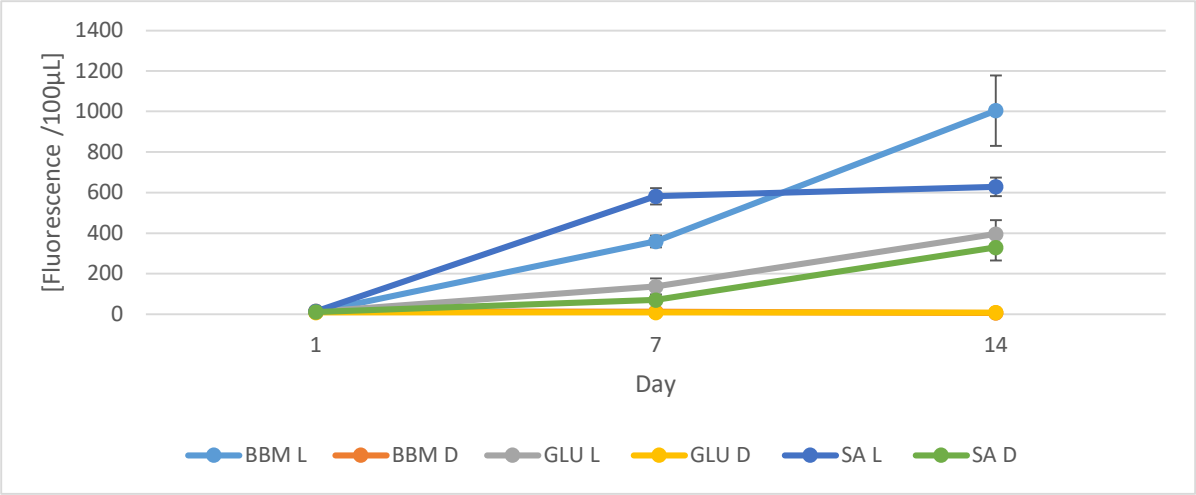


**Figure 33: Fluorescence curves for *H. pluvialis* strain HP_A01.** Grown in various media in light and dark conditions.

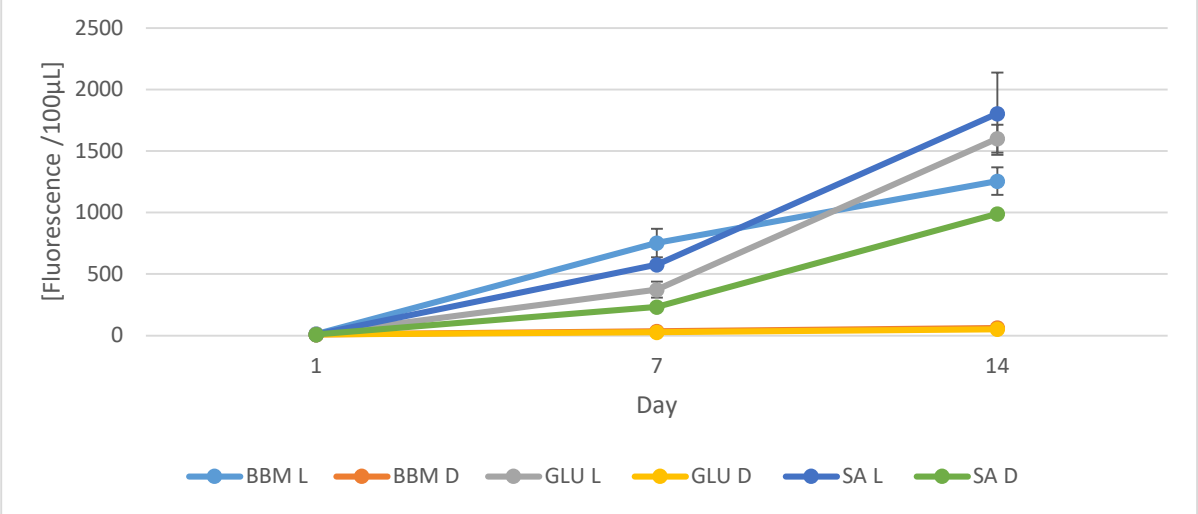


**Figure 34: Fluorescence curves for *H. pluvialis* strain HL_A01.** Grown in various media in light and dark conditions.

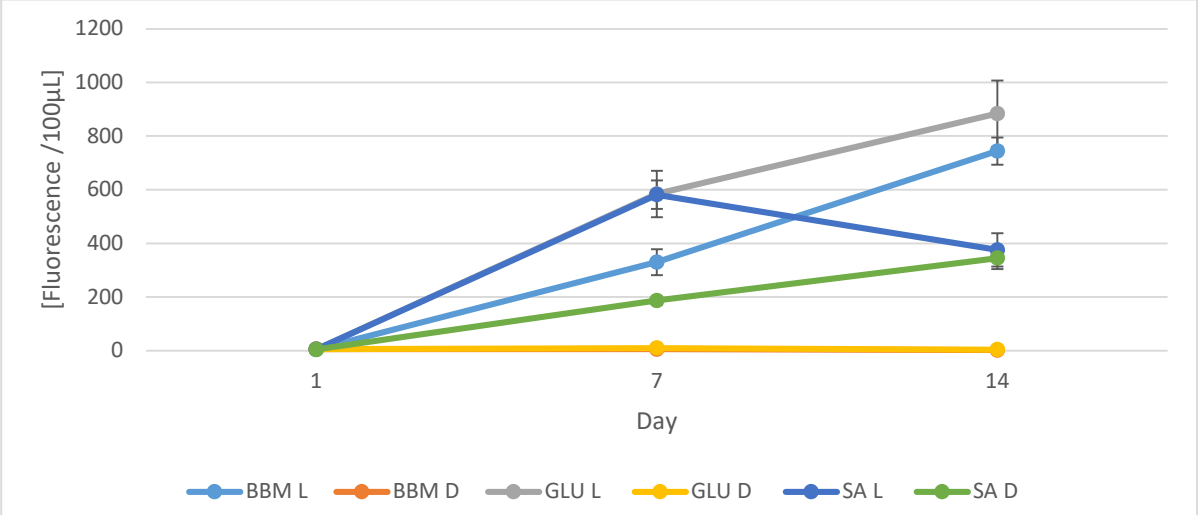


**Figure 35: Fluorescence curves for *H. pluvialis* strain HP_O01.** Grown in various media in light and dark conditions.

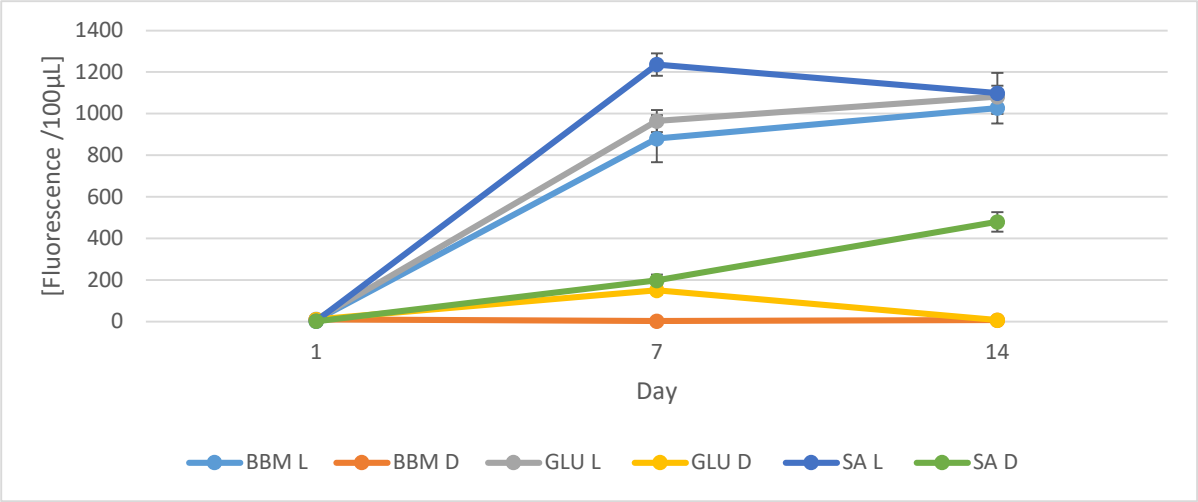


**Figure 36: Fluorescence curves for *H. pluvialis* strain HP_M01.** Grown in various media in light and dark conditions.

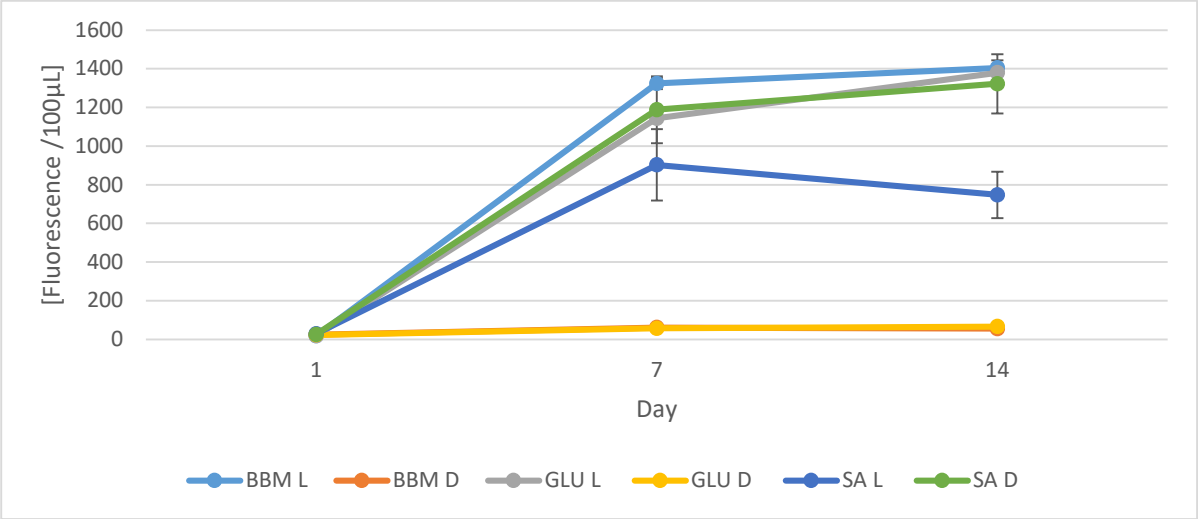


**Figure 37: Fluorescence curves for *H. pluvialis* strain HP_N01.** Grown in various media in light and dark conditions.

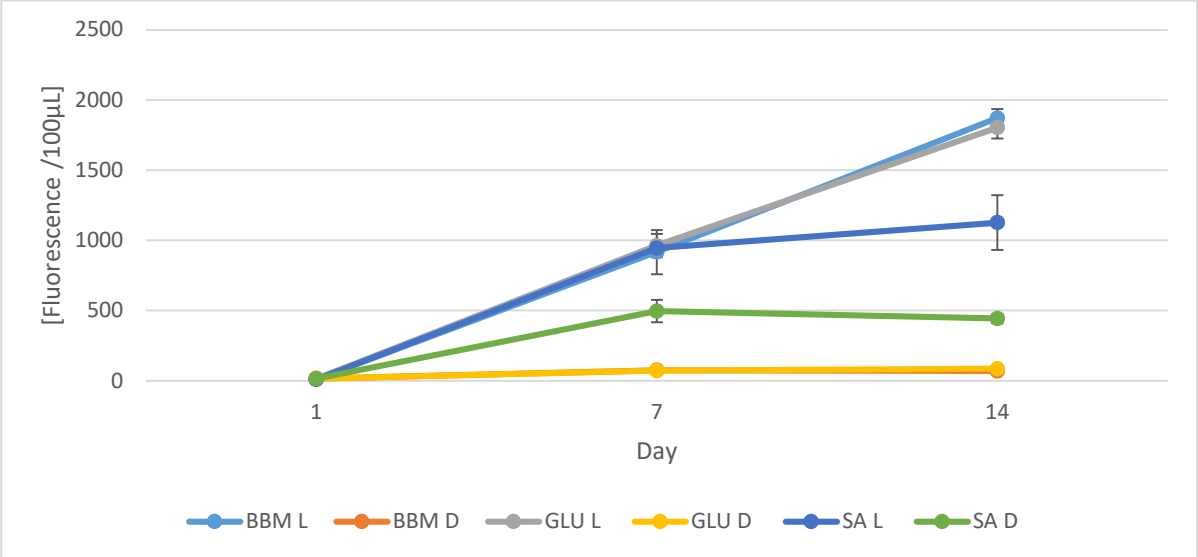


**Figure 38: Fluorescence curves for *H. pluvialis* strain HP_I01.** Grown in various media in light and dark conditions.

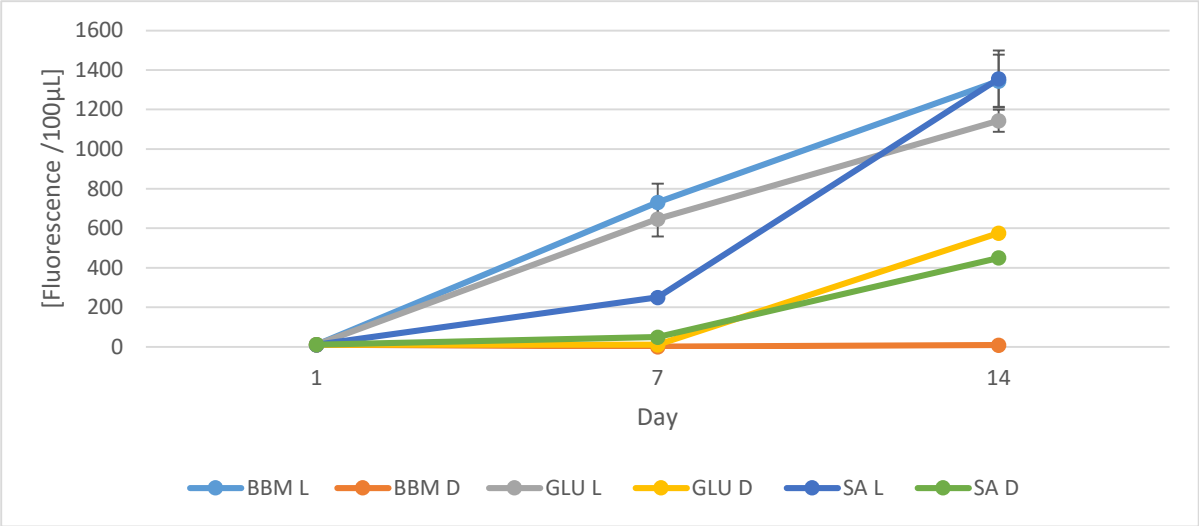


**Figure 39: Fluorescence curves for *H. pluvialis* strain HP_F01.** Grown in various media in light and dark conditions.

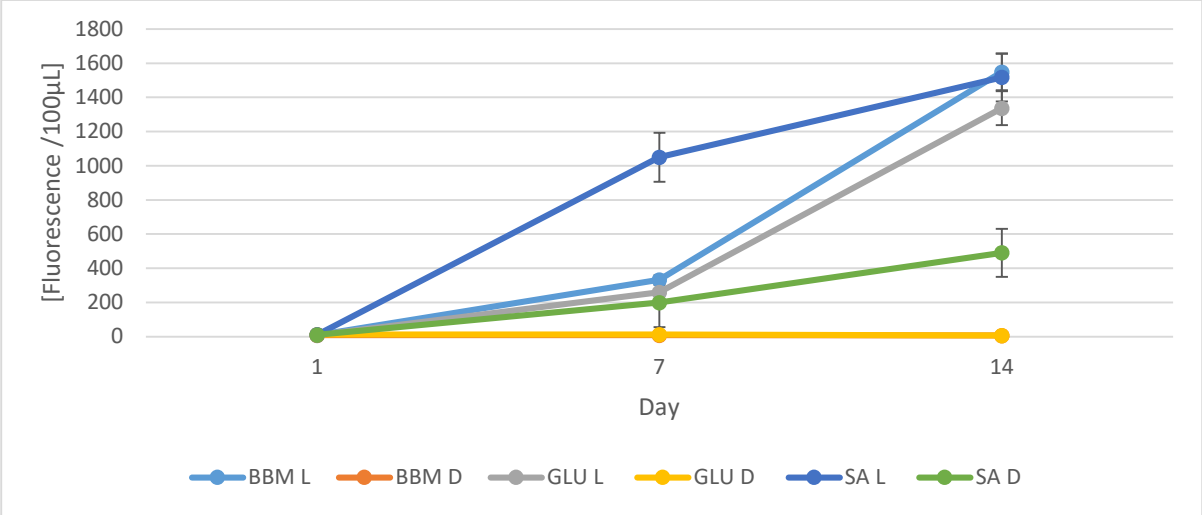


**Figure 40: Fluorescence curves for *H. pluvialis* strain HP_H01.** Grown in various media in light and dark conditions.

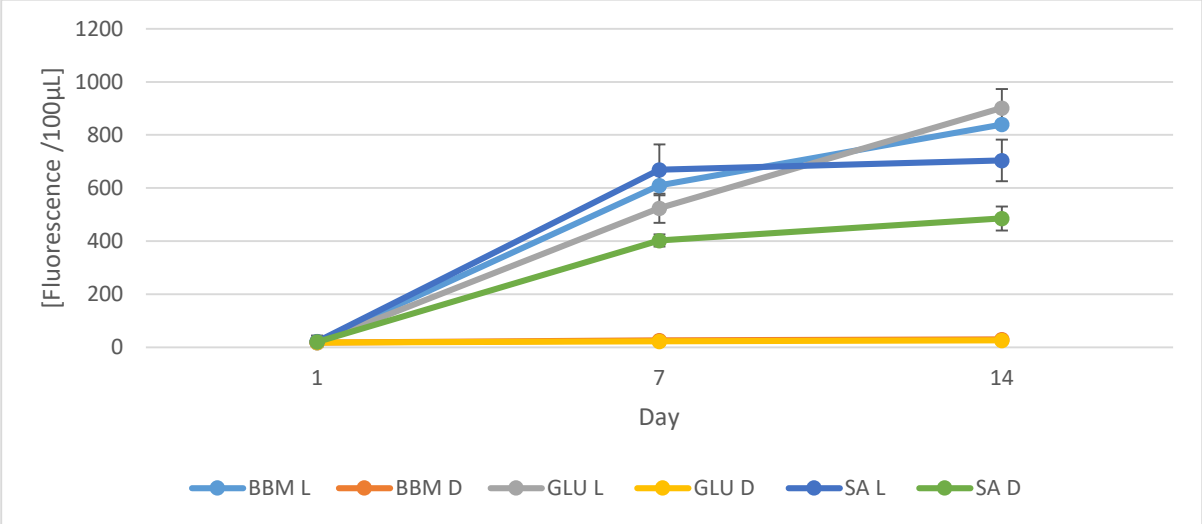


**Figure 41: Fluorescence curves for *H. pluvialis* strain HP_G01.** Grown in various media in light and dark conditions.

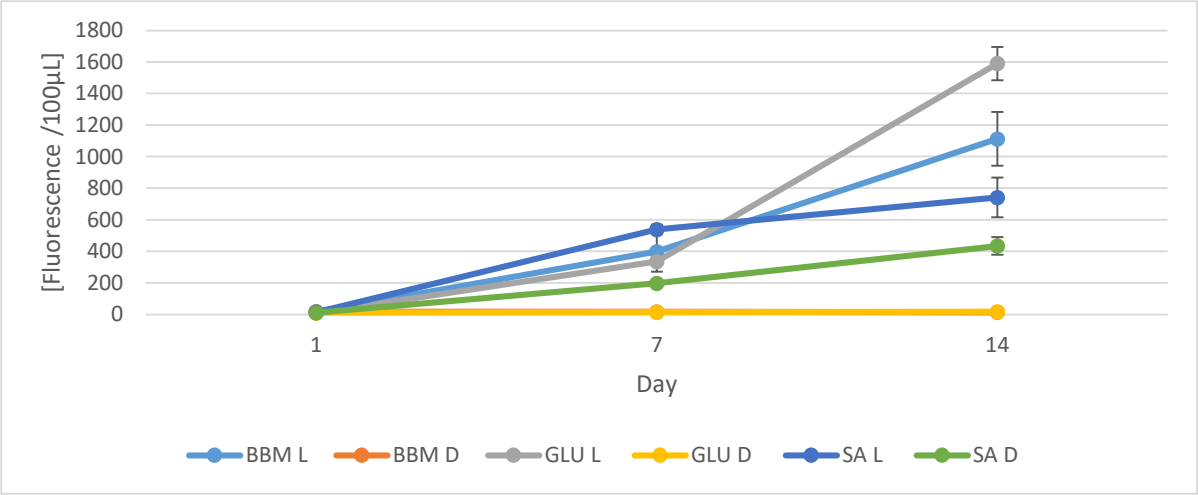


**Figure 42: Fluorescence curves for *H. pluvialis* strain HP_C01.** Grown in various media in light and dark conditions

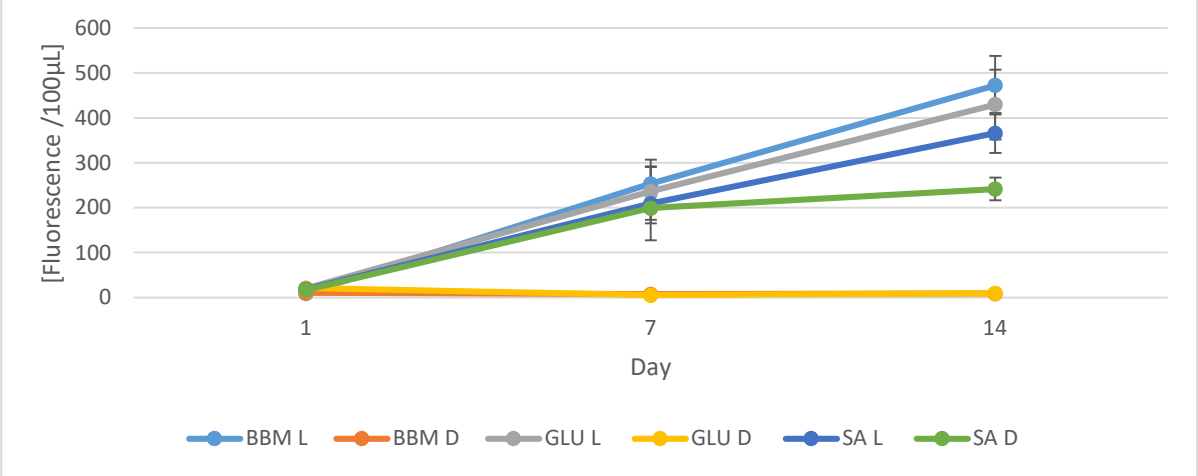


**Figure 43: Fluorescence curves for *H. pluvialis* strain HP_D01.** Grown in various media in light and dark conditions

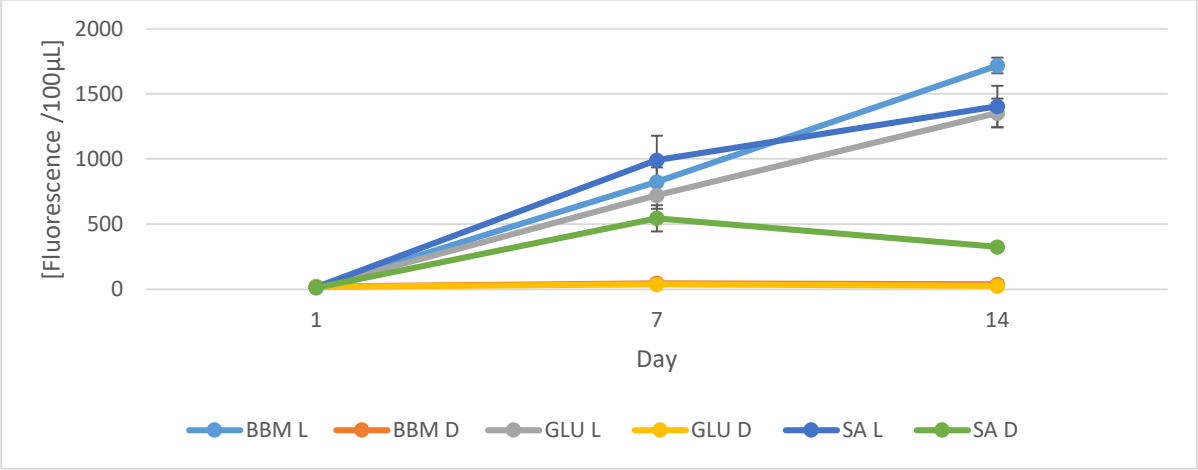


**Figure 44: Fluorescence curves for *H. pluvialis* strain HP_J01.** Grown in various media in light and dark conditions

## 3.4 Metabolism of *H. pluvialis* in round bottom flasks uncover fastest growing strains

The aim of this experiment was to create growth curves for strains of *H. pluvialis* when grown in aerated 1L round bottom flasks with 800 mL BBM media under 24-h white LED light conditions. Fluorescence intensity was also analyzed throughout the 15-day growth period to determine life cycle stage. Growth curves (Figures 45,46) and fluorescence intensity values (Figures 47,48) for all strains are presented based on the faster growing and slower growing strains. Strain HP_J01 showed a faster growth advantage up to day 9, however HP_B01 was found to have the highest CFU counts on day 15 followed by HP_E01 and HP_E02.

### 3.4.1 Round bottom flask growth curves reveal top producing strains

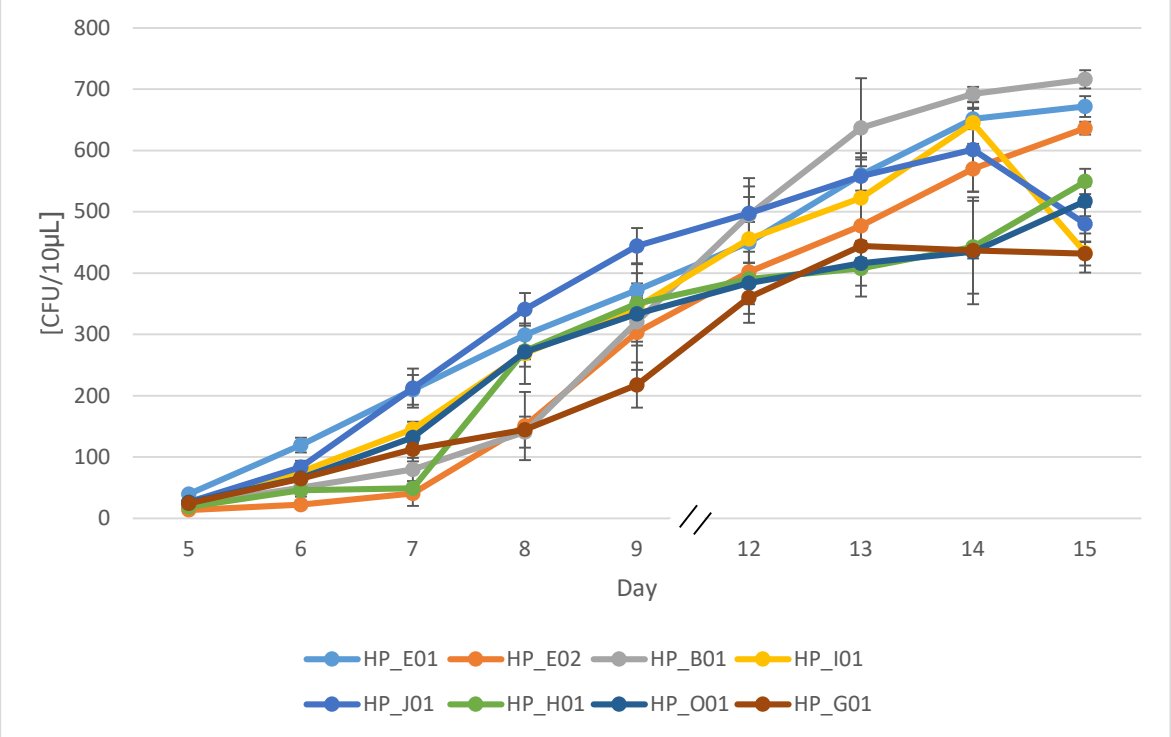


**Figure 45: Growth curves for the faster growing strains from the BDI strain collection.** Growth in 1L aerated round bottom flasks with 800 mL BBM media was used under constant white LED lighting.

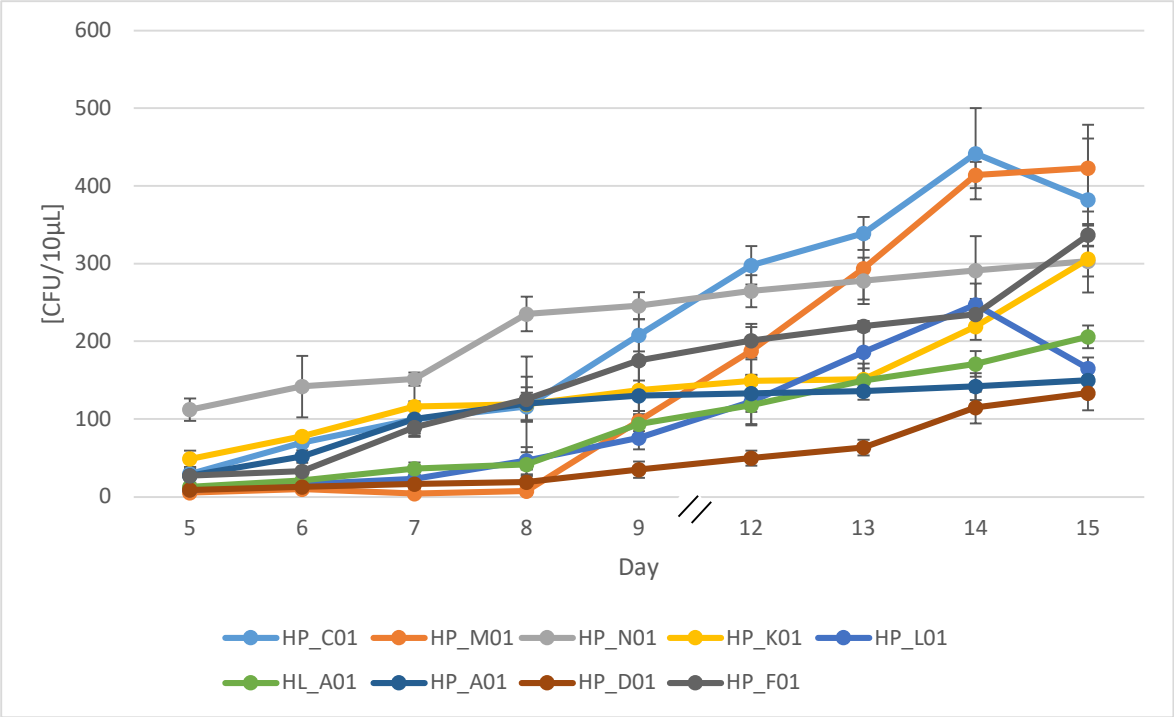


**Figure 46: Growth curves for the slower growing strains from the BDI strain collection.** Growth in 1L aerated round bottom flasks with 800 mL BBM media was used under constant white LED lighting.

### 3.4.2 Round bottom flask fluorescence curves reveal strain specific chlorophyll b profiles

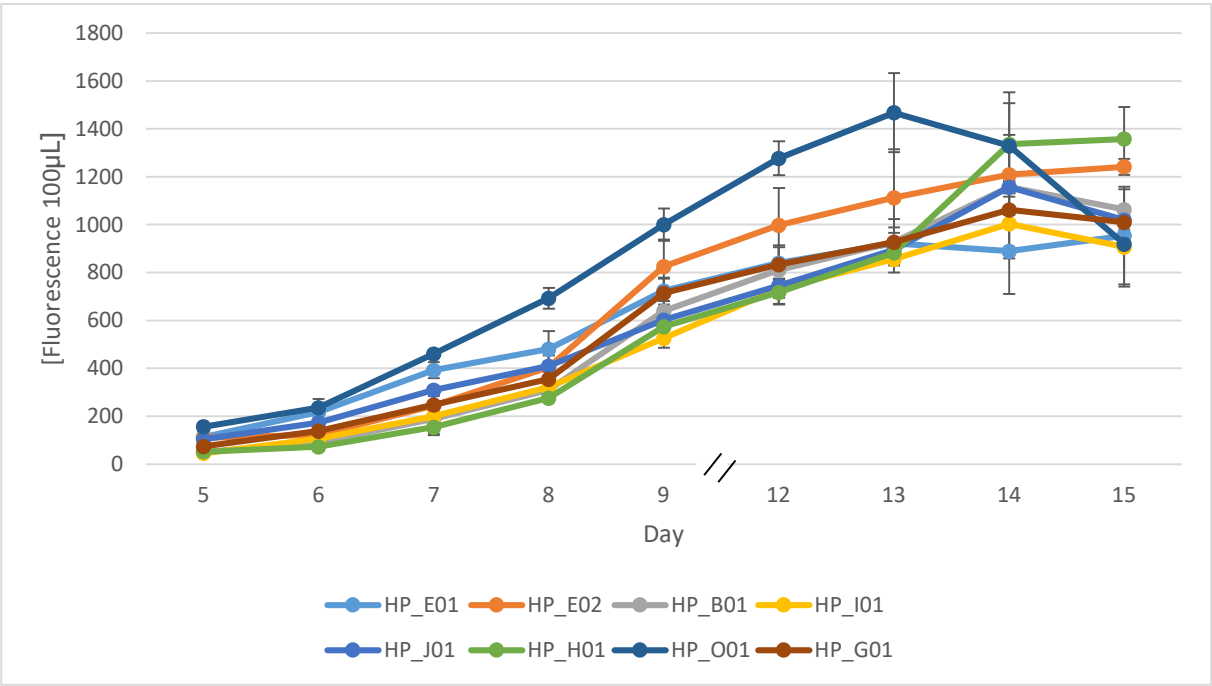


**Figure 47: Fluorescence curves for the faster growing strains from the BDI strain collection.** Growth in 1L aerated round bottom flasks with 800 mL BBM media was used under constant white LED lighting.

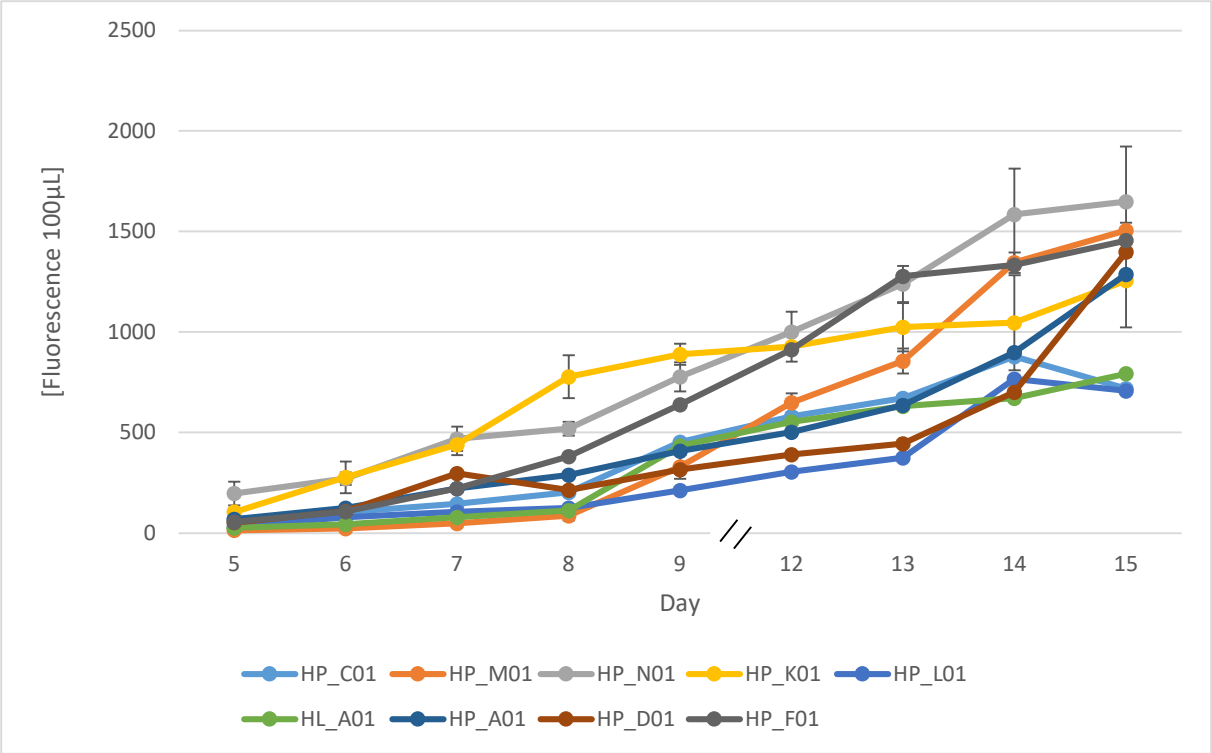


**Figure 48: Fluorescence curves for the slower growing strains from the BDI strain collection.** Growth in 1L aerated round bottom flasks with 800 mL BBM media was used under constant white LED lighting.

## 3.4.3 Biomass yield from round bottom flask growth indicate top producing strains

**Table 7: Round bottom flask biomass (DW) from *H. pluvialis*.** Cells were harvested after 15 days of growth in BBM media using aerated 1L round bottom flasks under constant white LED lighting

| Strain | Biomass range g/L | Average Biomass g/L | Strain | Biomass range g/L | Average Biomass g/L | Strain | Biomass range g/L | Average Biomass g/L |
|---|---|---|---|---|---|---|---|---|
| **HP_F01** | 0.450 – 0.550 | 0.518 | **HP_G01** | 0.450 – 0.600 | 0.516 | **HP_J01** | 0.400 -0.500 | 0.450 |
| **HP_N01** | 0.370 – 0.450 | 0.398 | **HP_H01** | 0.350 – 0.500 | 0.400 | **HP_B01** | 0.500 – 0.600 | 0.533 |
| **HP_K01** | 0.350 – 0.430 | 0.396 | **HP_O01** | 0.400 – 0.550 | 0.450 | **HP_M01** | 0.380 – 0.420 | 0.400 |
| **HL_A01** | 0.340 – 0.530 | 0.398 | **HP_E01** | 0.500 – 0.600 | 0.500 | **HP_D01** | 0.300 – 0.400 | 0.350 |
| **HP_A01** | 0.400 – 0.520 | 0.456 | **HP_L01** | 0.300 – 0.400 | 0.333 | **HP_E02** | 0.400 – 0.555 | 0.475 |
| **HP_I01** | 0.300 – 0.400 | 0.366 | **HP_C01** | 0.200 –0.300 | 0.266 | | | |

Biomass (DW) production of strains of *H. pluvialis* were evaluated after a 15-day growth period. Replicas of 3 were used for data analysis. The strains producing the highest average

biomass were found to be HP_B01, HP_E01, HP_F01, and HP_G01 (Table 7), however in many cases the biomass range between replicates overlapped for many strains.

## 3.5 Headspace GC-MS analyses provide first insights into VOC profiles of *H. pluvialis* strains

### 3.5.1 Analytical evaluation of *H. pluvialis* strains

Analysis of all randomized samples via headspace GC-MS revealed that *H. pluvialis* strains produced methyl furan, tetrahydrofuran and dimethyl disulfide in varying abundances (Table 8). Chromatographs for each sample (Figures 49 - 65) and mass spectrometry graphs (Figures 68-84) are presented for each chemical identified. Non-inoculated BBM media from the Institute of Environmental Biotechnology was found to contain 1-propanol (Figures 66 - 85), this chemical was also found in each inoculated sample. Non-inoculated BBM media prepared BDI indicated several chemicals including ethanol, isopropyl alcohol, 2-Butanone, and 1-Butanol (Figures 67,86-89) these chemicals were also found in every inoculated sample prepared at BDI (Figures 56,57,75,76).

**Table 8: GC-MS results from varying strains of *H. pluvialis* from the BDI strain collection.** The letter (a) next to the strain indicates the strain in duplicate.

| Chemical | Retention time | Area | Strain |
|---|---|---|---|
| **Methyl Furan** | 2.112 | 3.73 E+05 | HP_ L01 |
| | 2.105 | 7.10 E+05 | HP_ L01a |
| **Tetrahydrofuran** | 2.229 | 1.12E+06 | HP_ E01 |
| | 2.233 | 8.51E+04 | HP_ I01a |
| | 2.237 | 1.59E+05 | HP_ F01a |
| | 2.231 | 3.14E+05 | HP_ G01 |
| | 2.232 | 1.31E+05 | HP_ G01a |
| **Dimethyl Disulfide** | 3.639 | 9.61 E+05 | 2w BDI |
| | 3.669 | 2.84 E+04 | 8w BDI |
| | 3.694 | 6.61E+04 | HP_ O01a |
| | 3.675 | 2.16 E+05 | HP_ O01a |
| | 3.662 | 1.05E+06 | HP_ H01 |
| | 3.665 | 4.31E+05 | HP_ H01a |
| | 3.666 | 1.84E+05 | HP_ G01 |
| | 3.681 | 1.22E+05 | HP_ G01a |
| | 3.638 | 3.81E+05 | HP_ D01 |
| | 3.682 | 1.31E+05 | HP_ D01 |

**Table 9: GC-MS results for chemicals found in uninoculated media**. Uninoculated media from the Institute of Environmental Biotechnology and BDI. The same chemicals that were found in all inoculated samples are also listed.

| Chemical | Retention time | Area |
|---|---|---|
| **Ethanol** | 1.519 | 2.71E+07 |
| | 1.52 | 7.77E+06 |
| | 1.519 | 6.87E+06 |
| | 1.527 | 1.49E+05 |
| **Isopropyl alcohol** | 1.599 | 1.35E+07 |
| | 1.6 | 1.96E+06 |
| | 1.6 | 1.28E+06 |
| | 1.606 | 5.51E+06 |
| **1-Propanol** | 1.81 | 1.57E+06 |
| | 1.805 | 1.54E+06 |
| | 1.818 | 5.36E+05 |
| | 1.818 | 1.71E+05 |
| | 1.817 | 7.99 E+05 |
| | 1.808 | 7.76 E+05 |
| | 1.808 | 7.82 E+05 |
| | 1.816 | 7.81 E+05 |
| | 1.822 | 1.29 E+06 |
| | 1.814 | 3.70 E+05 |
| | 1.811 | 1.09 E+06 |
| | 1.809 | 6.70 E+05 |
| | 1.807 | 4.94 E+05 |
| | 1.819 | 4.68 E+05 |
| **2-Butanone** | 1.99 | 1.36E+06 |
| | 1.994 | 1.89E+06 |
| | 1.991 | 7.41E+06 |
| | 2.006 | 1.03E+06 |
| **1-Butanol** | 2.551 | 3.59E+05 |
| | 2.551 | 8.23E+05 |
| | 2.545 | 9.39E+05 |
| | 2,555 | 1.08E+06 |

## 3.5.2 Chromatographs of the analyzed strains indicate VOCs in uninoculated and inoculated samples

### Methyl Furan

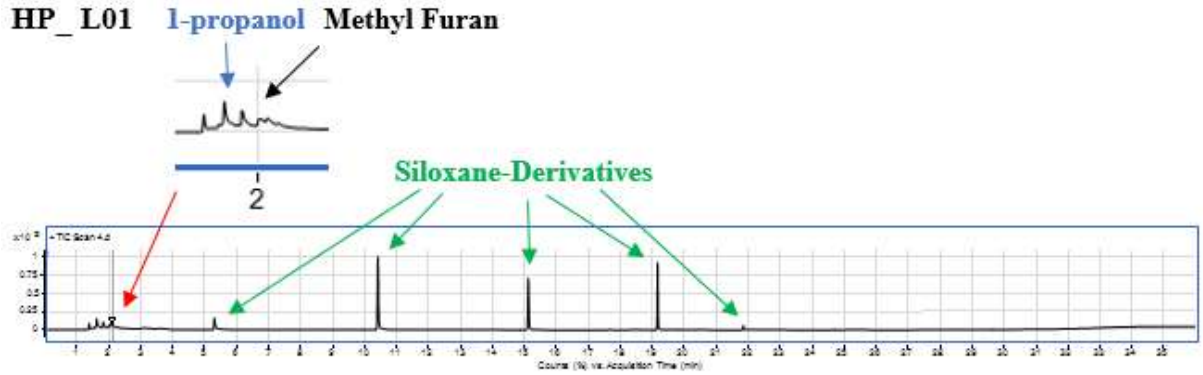


**Figure 49: Chromatogram of *H. pluvialis* strain HP_L01.** Enhanced image of peak detection indicated by the red arrow. Siloxane-derivatives from the fiber and column are indicated by the green arrows and these same peaks apply to all further samples.

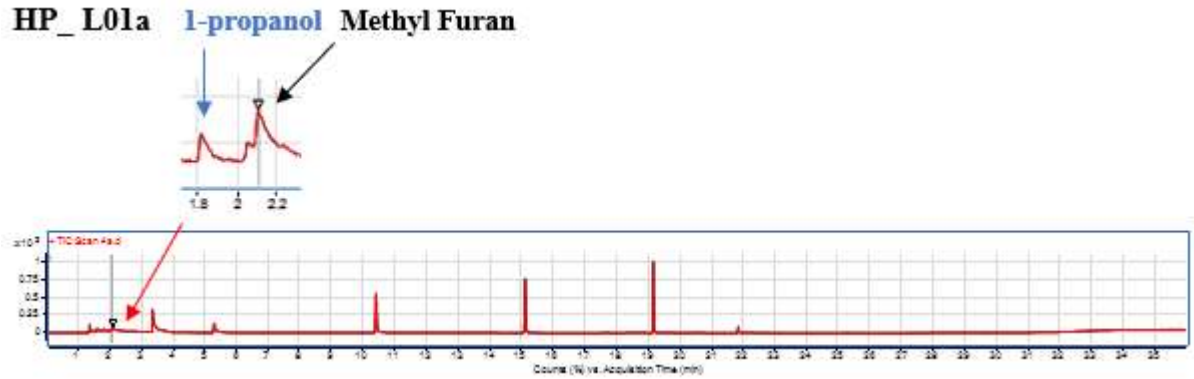


**Figure 50: Chromatogram of *H. pluvialis* strain HP_L01a.** Enhanced image of peak detection indicated by the red arrow.

### Tetrahydrofuran

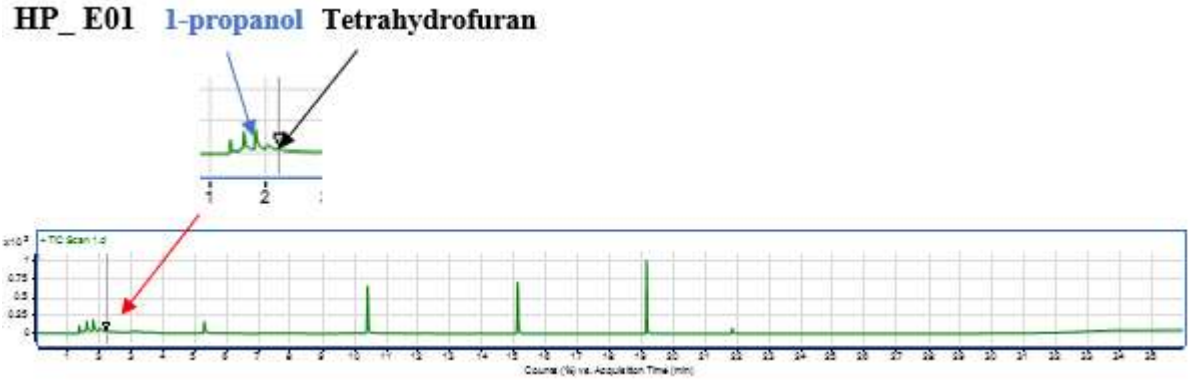


**Figure 51: Chromatogram of *H. pluvialis* strain HP_E01.** Enhanced image of peak detection indicated by the red arrow.

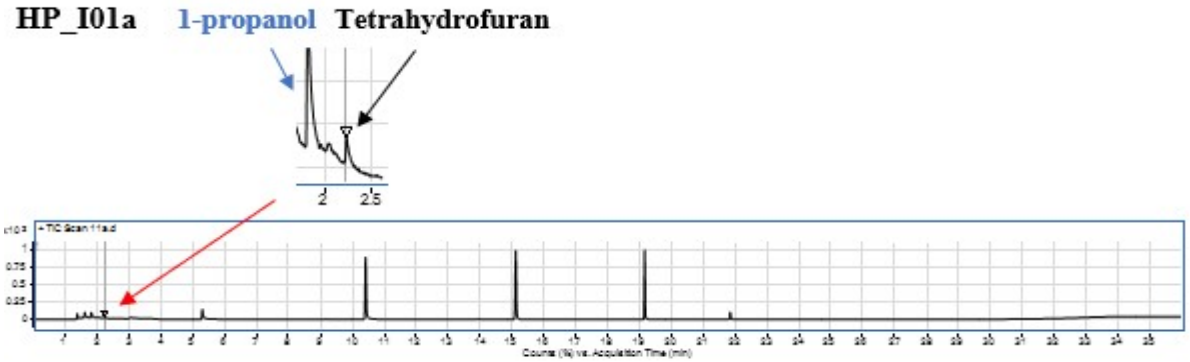


**Figure 52: Chromatogram of *H. pluvialis* strain HP_I01a.** Enhanced image of peak detection indicated by the red arrow.

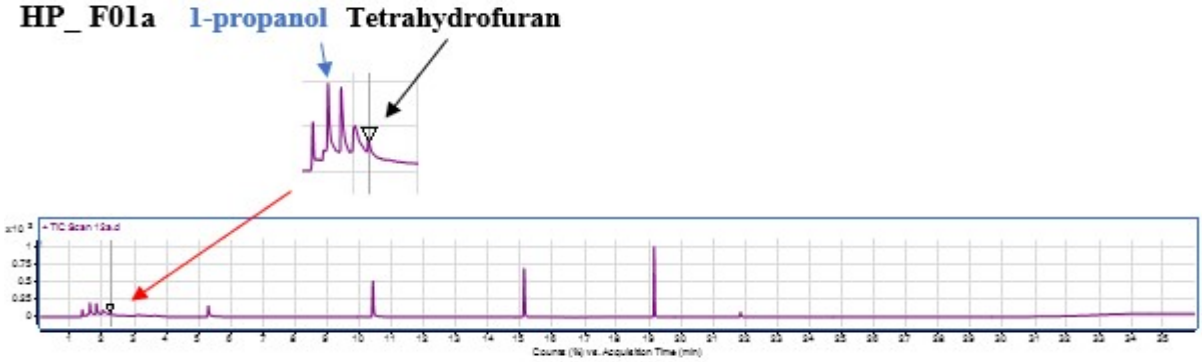


**Figure 53: Chromatogram of *H. pluvialis* strain HP_F01a.** Enhanced image of peak detection indicated by the red arrow.


**Figure 54: Chromatogram of *H. pluvialis* strain HP_G01.** Enhanced image of peak detection indicated by the red arrow.

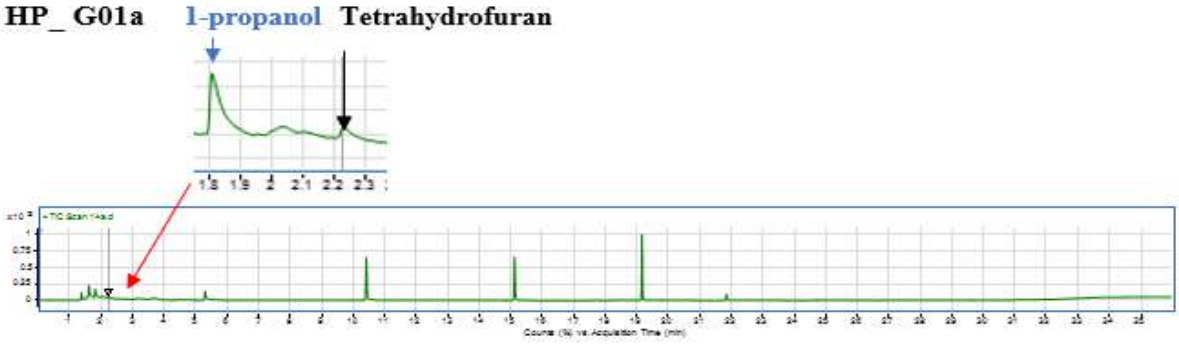


**Figure 55: Chromatogram of *H. pluvialis* strain HP_G01a.** Enhanced image of peak detection indicated by the red arrow.

## Dimethyl Disulfide

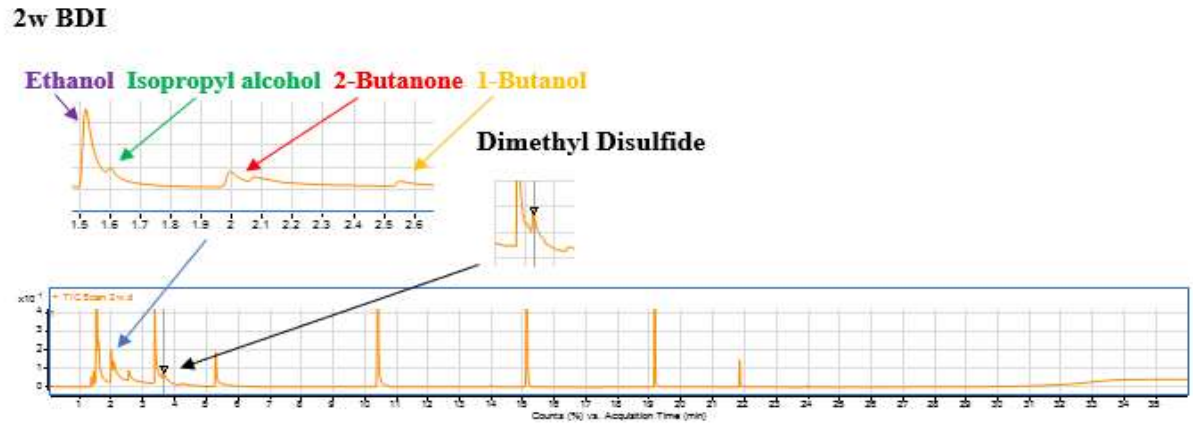


**Figure 56: Chromatogram of *H. pluvialis* unknown BDI strain named 2w.** Enhanced image of peak detection indicated by the blue and black arrows.

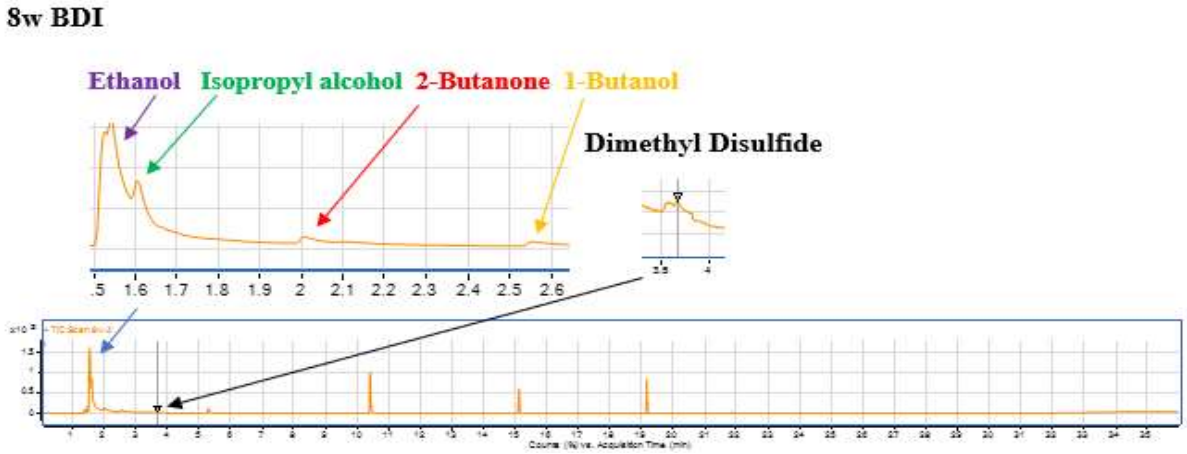


**Figure 57: Chromatogram of *H. pluvialis* unknown BDI strain named 8w.** Enhanced image of peak detection indicated by the blue and black arrows.

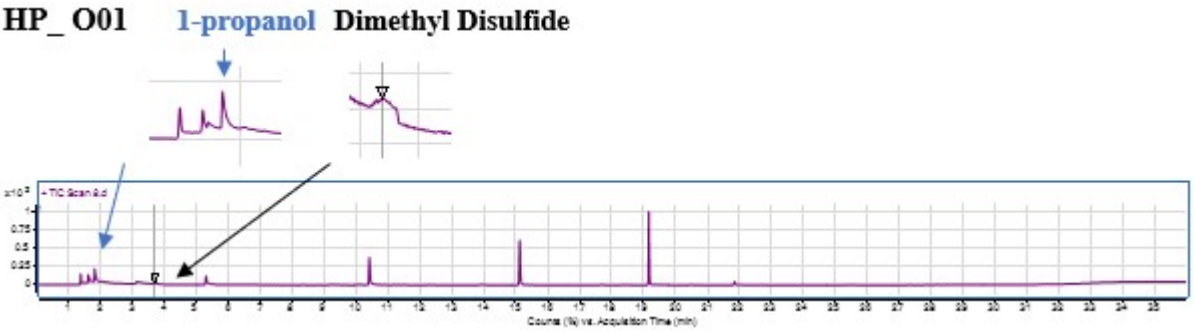


**Figure 58: Chromatogram of *H. pluvialis* strain HP_O01.** Enhanced image of peak detection indicated by blue and black arrows.

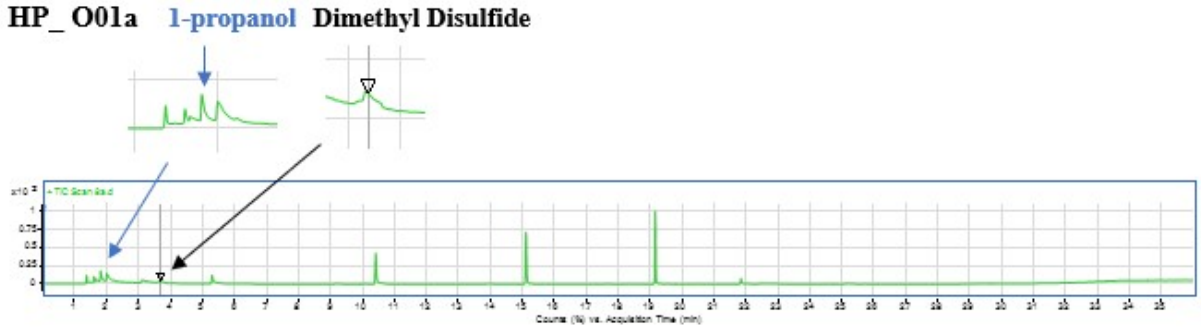


**Figure 59: Chromatogram of *H. pluvialis* strain HP_O01a.** Enhanced image of peak detection indicated by blue and black arrows.

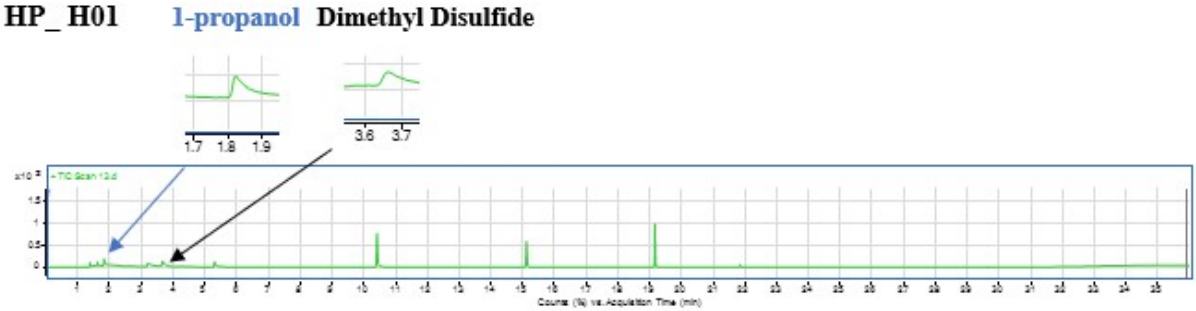


**Figure 60: Chromatogram of *H. pluvialis* strain HP_H01.** Enhanced image of peak detection indicated by blue and black arrows.

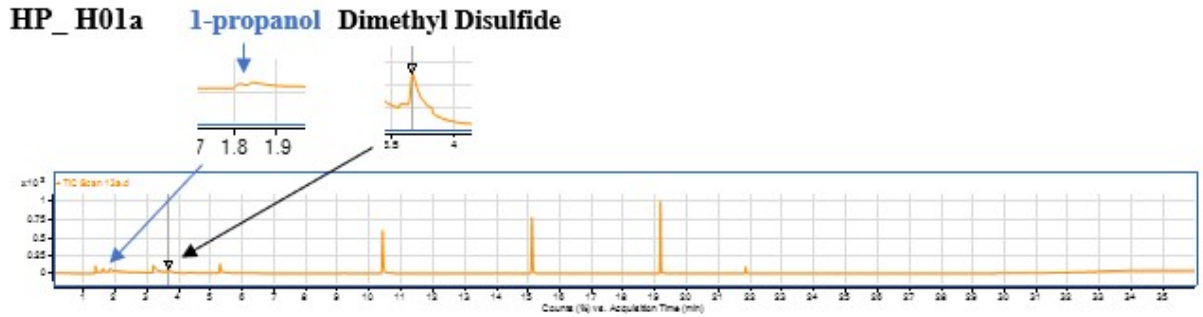


**Figure 61: Chromatogram of *H. pluvialis* strain HP_H01a.** Enhanced image of peak detection indicated by blue and black arrows.

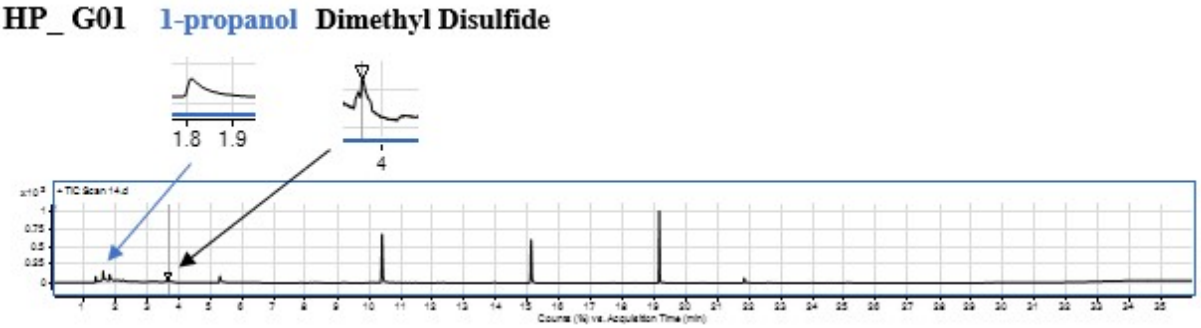


**Figure 62: Chromatogram of *H. pluvialis* strain HP_G01.** Enhanced image of peak detection indicated by blue and black arrows.

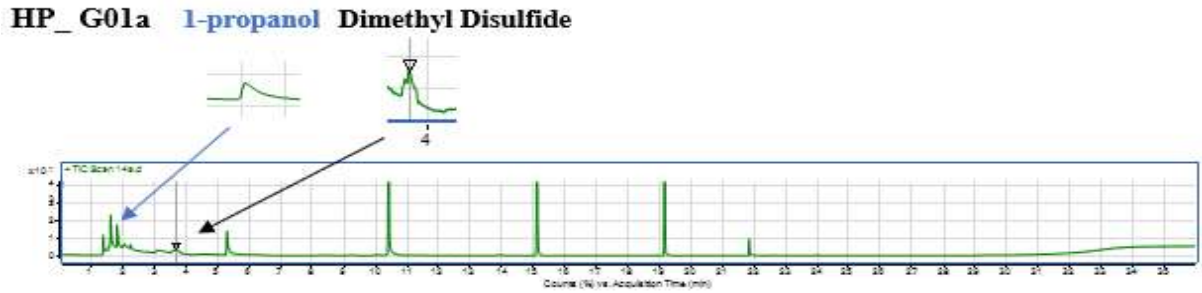


**Figure 63: Chromatogram of *H. pluvialis* strain HP_G01a.** Enhanced image of peak detection indicated by blue and black arrows.

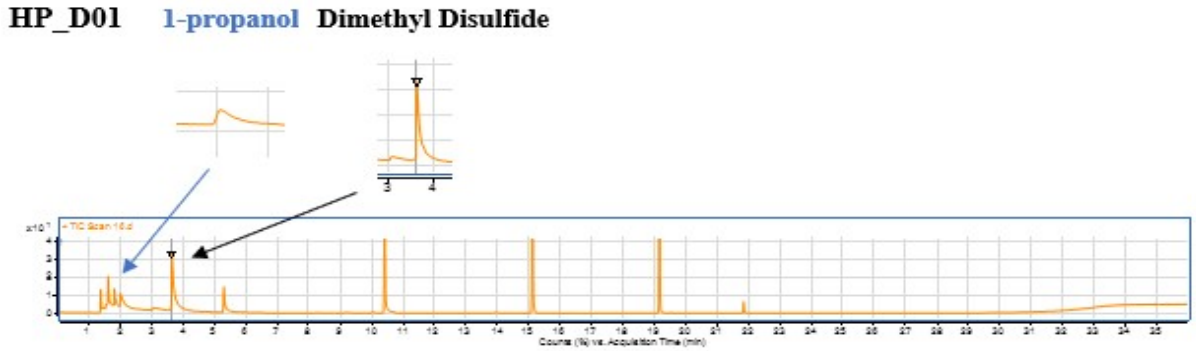


**Figure 64: Chromatogram of *H. pluvialis* strain HP_D01.** Enhanced image of peak detection indicated by blue and black arrows.

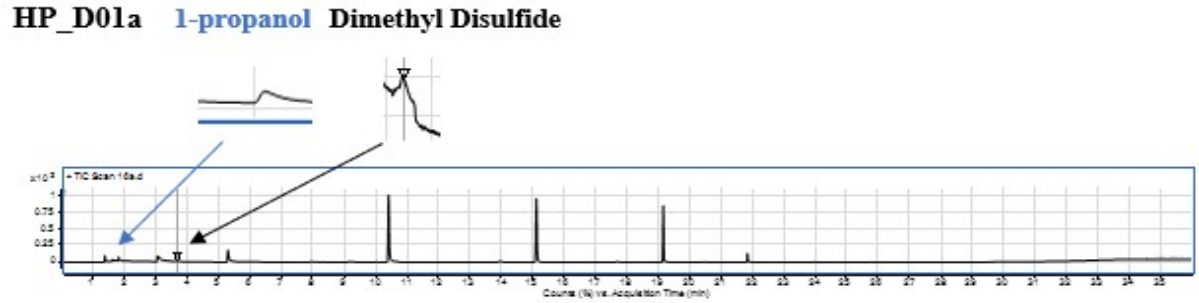


**Figure 65: Chromatogram of *H. pluvialis* strain HP_D01.** Enhanced image of peak detection indicated by blue and black arrows

## Uninoculated media

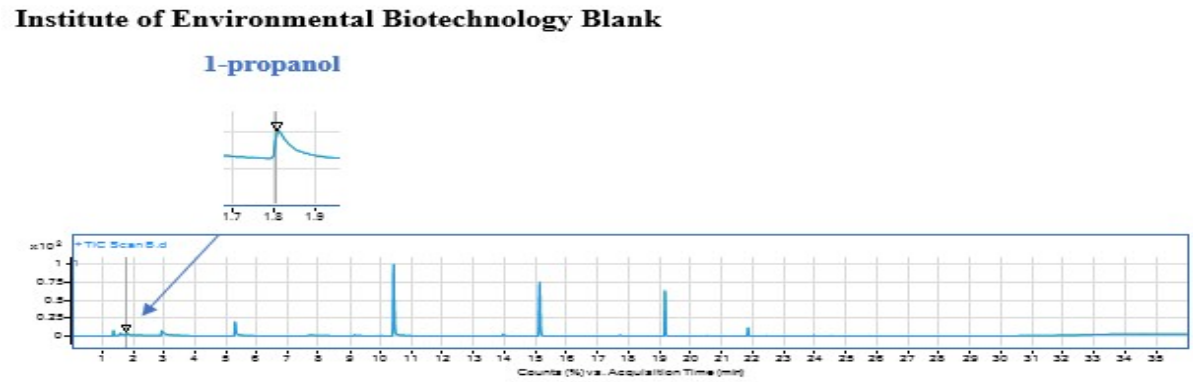


**Figure 66: Chromatogram of uninoculated BBM media produced at the institute of environmental biotechnology at TU Graz.** Enhanced image of peak detection indicated by the blue arrow.

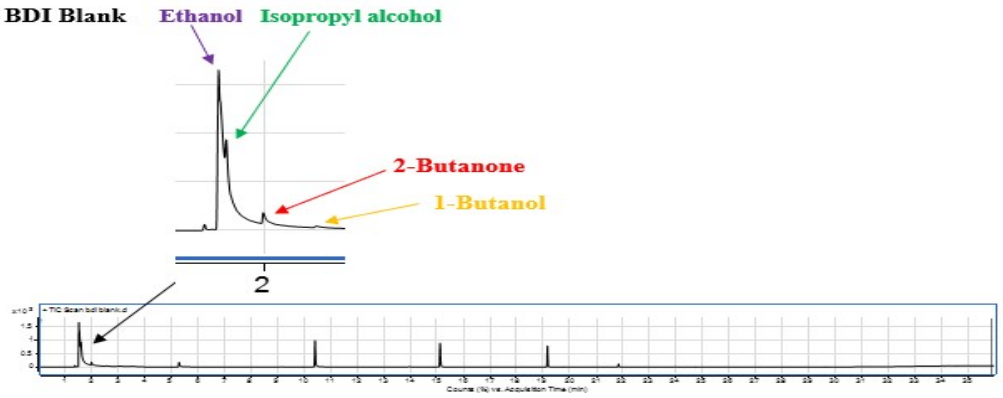


**Figure 67: Chromatogram of uninoculated BBM media produced at BDI.** Enhanced image of peak detection indicated by the black arrow.

## 3.5.3 Mass spectrometry graphs further verify identities of VOCs

### Methylfuran

**HP_L01**

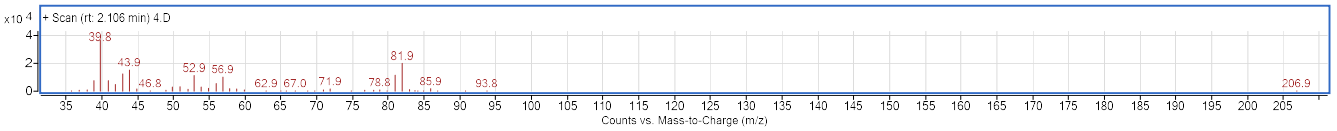


**Figure 68: Mass spectrum of methylfuran detected in *H. pluvialis* strain HP_D01 sample.**

**HP_L01a**

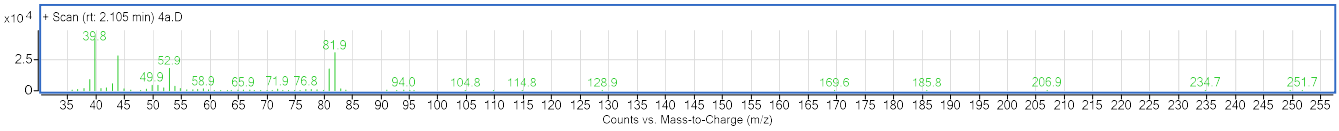


**Figure 69: Mass spectrum of methylfuran detected in *H. pluvialis* strain HP_L01a sample.**

### Tetrahydrofuran

**HP_E01**

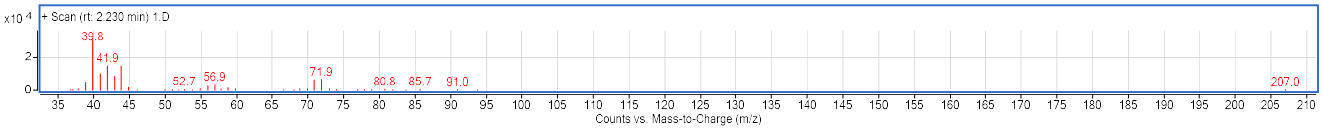


**Figure 70: Mass spectrum of tetrahydrofuran detected in *H. pluvialis* strain HP_E01 sample.**

**HP_I01**

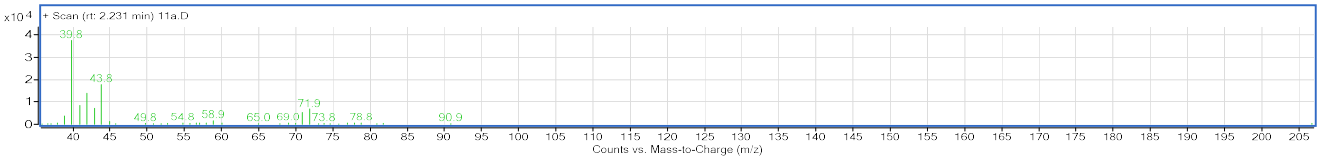


**Figure 71: Mass spectrum of tetrahydrofuran detected in *H. pluvialis* strain HP_I01 sample.**

### HP_F01a

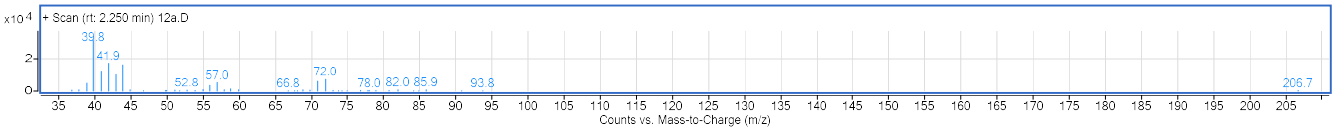


**Figure 72: Mass spectrum of tetrahydrofuran detected in *H. pluvialis* strain HP_F01a sample.**

### HP_G01

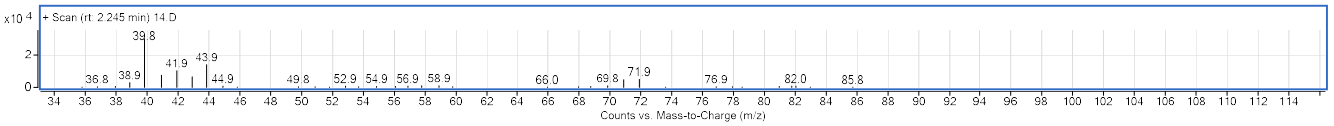


**Figure 73: Mass spectrum of tetrahydrofuran detected in *H. pluvialis* strain HP_G01 sample.**

### HP_G01a

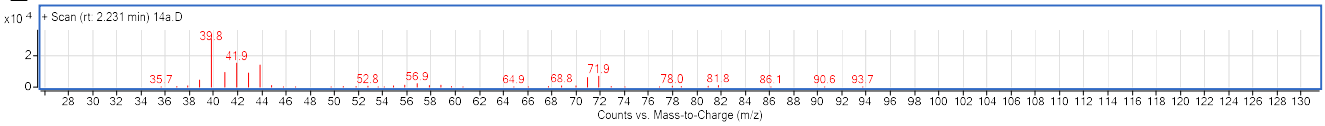


**Figure 74: Mass spectrum of tetrahydrofuran detected in *H. pluvialis* strain HP_G01a sample.**

## Dimethyl disulfide

### 2w BDI

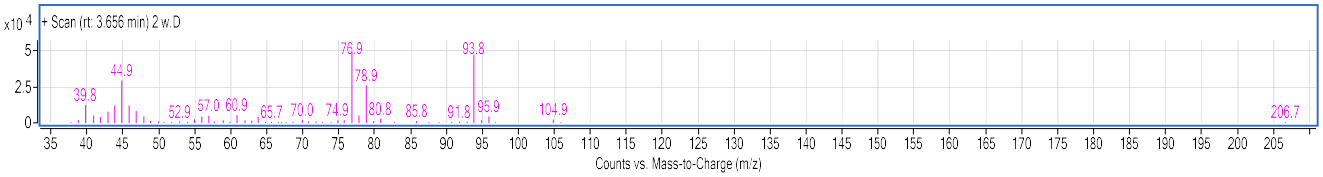


**Figure 75: Mass spectrum of dimethyl disulfide detected in unknown sample named 2w produced at BDI.**

### 8w BDI

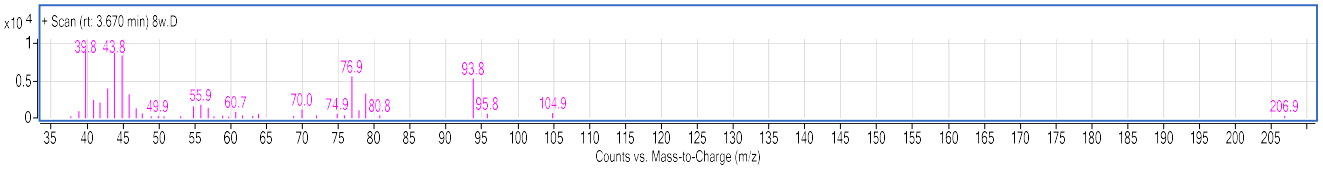


**Figure 76: Mass spectrum of dimethyl disulfide detected in unknown sample named 8w produced at BDI.**

### HP_O01

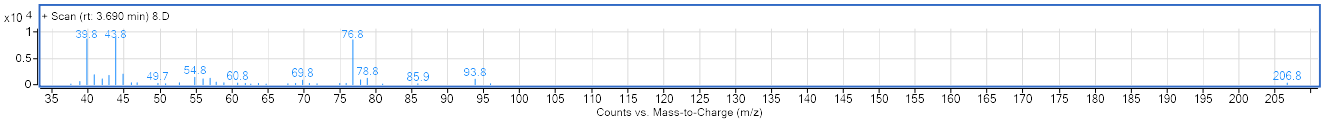


**Figure 77: Mass spectrum of dimethyl disulfide detected in *H. pluvialis* strain HP_O01 sample.**

## HP_O01a

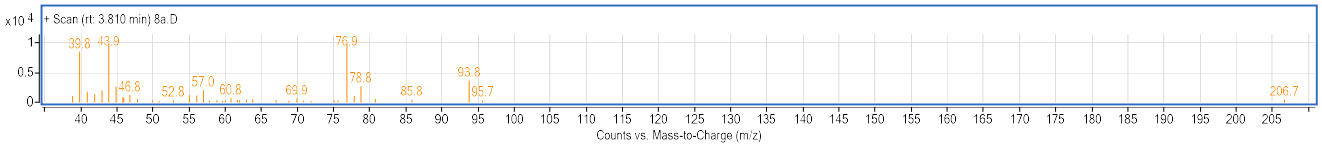


**Figure 78: Mass spectrum of dimethyl disulfide detected in *H. pluvialis* strain HP_O01a sample.**

## HP_H01

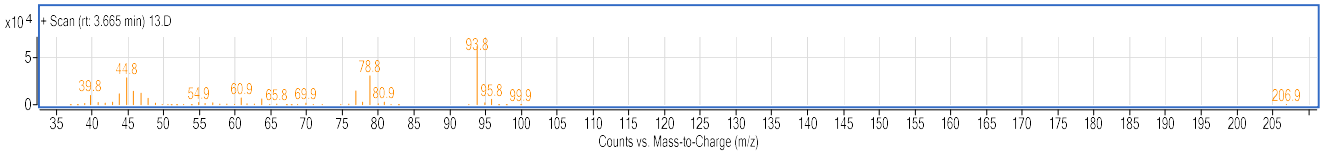


**Figure 79: Mass spectrum of dimethyl disulfide detected in *H. pluvialis* strain HP_H01 sample.**

## HP_H01a

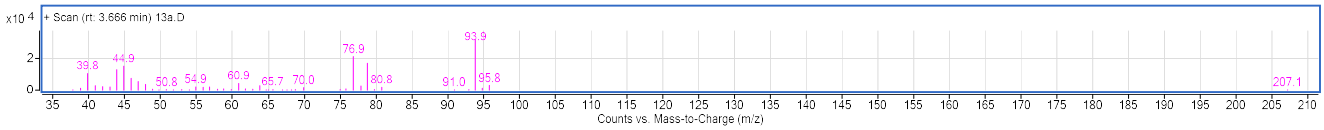


**Figure 80: Mass spectrum of dimethyl disulfide detected in *H. pluvialis* strain HP_H01a sample.**

## HP_G01

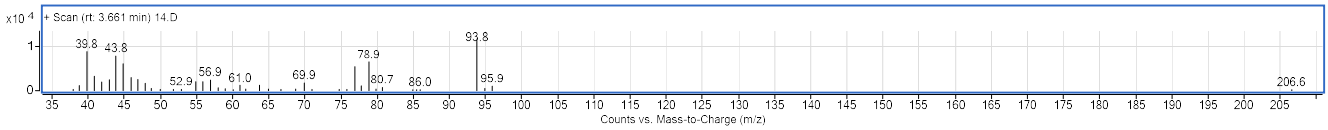


**Figure 81: Mass spectrum of dimethyl disulfide detected in *H. pluvialis* strain HP_G01 sample.**

## HP_G01a

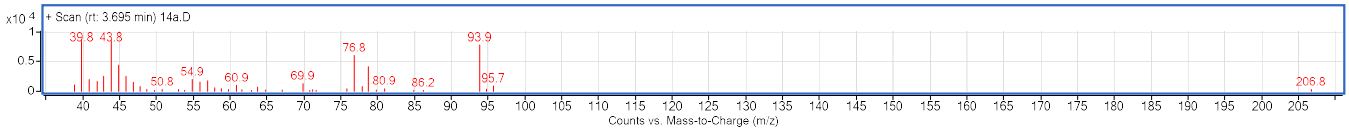


**Figure 82: Mass spectrum of dimethyl disulfide detected in *H. pluvialis* strain HP_G01a sample.**

## HP_D01

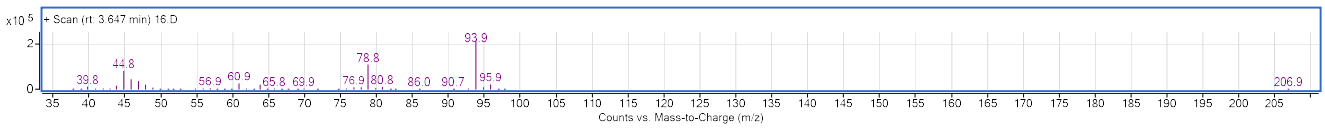


**Figure 83: Mass spectrum of dimethyl disulfide detected in *H. pluvialis* strain HP_D01 sample.**

### HP_D01a

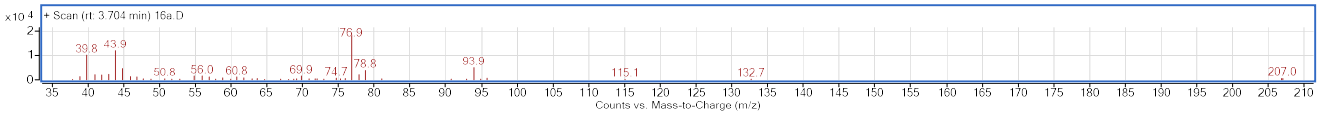


**Figure 84: Mass spectrum of dimethyl disulfide detected in *H. pluvialis* strain HP_D01a sample.**

## Institute of Environmental Biotechnology blank

### 1-propanol

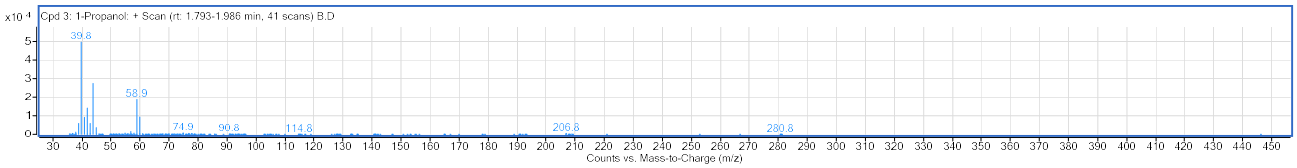


**Figure 85: Mass spectrum of 1-propanol detected in uninoculated BBM media produced at the institute of environmental biotechnology at TU Graz.**

# BDI blank

## Ethanol

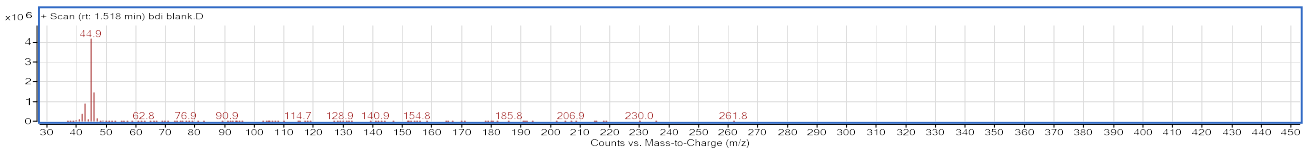


**Figure 86: Mass spectrum of ethanol detected in uninoculated BBM media produced at BDI.**

## Isopropyl alcohol

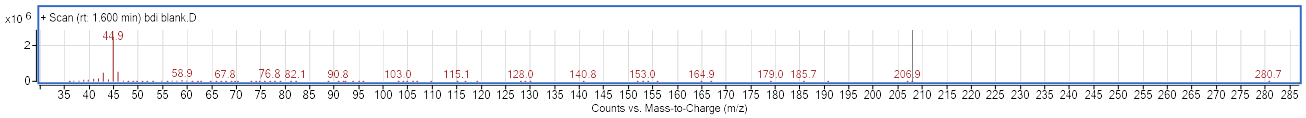


**Figure 87: Mass spectrum of isopropyl alcohol detected in uninoculated BBM media produced at BDI.**

## 2-Butanone

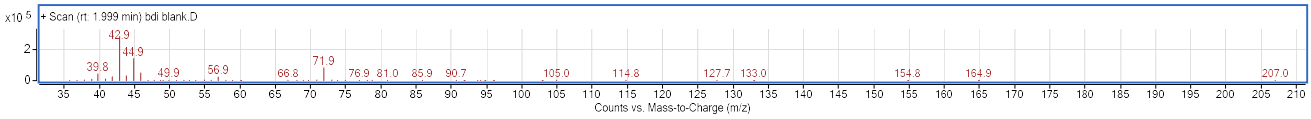


**Figure 88: Mass spectrum of 2-butanone detected in uninoculated BBM media produced at BDI.**

## 1-Butanol

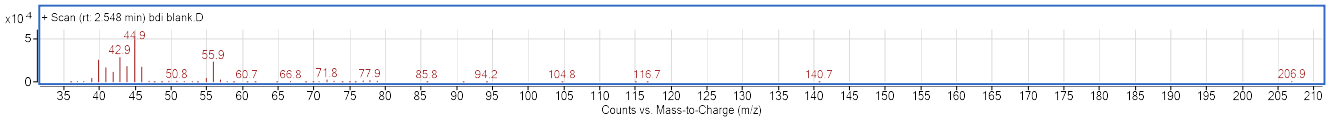


**Figure 89: Mass spectrum of 1-butanol detected in uninoculated BBM media produced at BDI.**

# 4. Discussion

## 4.1 Sequence based phylogenetic analysis for strain distinction

In the present thesis various primer sets for molecular phylogenetic analyses were tested and compared to results from previous studies. Although originally studied in fungi, ITS rDNA phylogeny has been performed throughout numerous studies including algae, plants and yeast and is recognized as a common molecular marker for intra and interspecies discrimination (Bellemain et al., 2010; Mitchell et al., 1994; Kroken and Taylor, 2000; Ownley et al., 2008; Ruiz-Barba et al., 2005). Primer pairs NS1/NS8 (White et al., 1990; Uemura et al., 2008; Dong et al., 2010), and SR1/12 (Uwai et al., 2005; Kimura and Tomaru, 2013) have also been previously used in various phylogenetic studies regarding 18S rRNA genes. SR1/12 primers have been used to classify a new species of marine green algae termed *N. viridis* from the genus *Nephroselmis,* which had previously been known as an undescribed species sharing some ultrastructural characters witnessed only with the freshwater species *N. olivacea* (Yamaguchi et al., 2010). Primer pairs from SR1- SR12 have also been used to investigate not only algal species but also the bacterial genus *Streptomyces* (Khalid et al., 2017). Molecular analysis of the industrially relevant microalga *Chlorella vulgaris* has been previously investigated using primer pairs NS1/NS8 and ITS1/ITS4 (Hong et al., 2016).

Taxonomical studies regarding the *Haematococcus* genus have previously been evaluated based on the sequencing of 18S rRNA genes for characterization (Kim et al., 2015; Klochkova et al., 2013). When the strain *Haematococcus* sp. KORDI03 originating from Korea was characterized and compared to *H. lacustris* from GenBank a 99.9% - 99.6% sequence identity was reported (Kim et al., 2015). Taxonomic identity of the 18S rRNA gene from an *H. pluvialis* isolate in Russia indicated a (99 - 100%) sequence identity to several known *H. pluvialis* strains using the basic logical alignment search tool (BLAST), (Chekanov et al., 2014). In the frame of the present study a combined 2,475 bp sequence analysis from ITS and 18S rRNA genes also revealed significant variation between 96.02 - 100% (Table 5). There has been previous debate among algal systematicts on the status of *Haematococcus* and *Stephanosphaera*, as previous phylogenetic investigations affirmed a phylogenetic alliance amongst the two genera. In the study by (Buchheim et al., 2013) new molecular phylogenetic analysis of 18S and 26S rRNA data revealed a separate genus *Balticola*. Therefore, *Haematococcus* remains a genus with *H. pluvialis* being its only member. Furthermore, *H. lacustris* is formally phylogenetically embedded within *H. pluvialis* and is

known as taxonomic synonym thereof. Such evidence is supported by molecular evolution in the ITS2 sequences of *H. pluvialis* strains, which indicate ITS as a highly variable region among geographically diverse isolates (Buchheim et al., 2013). In the study by (Allewaert et al., 2015) six lineages of *H. pluvialis* were resolved from ITS rDNA phylogeny, three of which formally described by (Buchheim et al., 2013). In this study most of this variation resulted within the ITS regions, which coincides with previous phylogenetic studies regarding *H. pluvialis*. Further phylogenetic characterization of *H. pluvialis* strains can provide credible phylogenetic framework for further comparative physiological studies and can be used regarding selection criteria for strains that are adapted to specific climatic conditions applicable to production facilities around the globe (Allewaert et al., 2015).

## 4.2 Phylogenetic analysis via fingerprinting PCR methods display significant variance

### 4.2.1 BOX-PCR phylogeny profiles indicate significant variation in many strains of *H. pluvialis*

BOX-PCR is a common fingerprinting technique originally derived from the BOX dispersed-repeat motif of the bacteria *Streptococcus pneumoniae* (Koeuth et al., 1995), however it has been reported in the analysis of several different bacterial genera (Meintanis et al., 2008; Proudy et al., 2007; Osek and Gallien, 2012). The study by (Saluja and Weiser, 1995) showed that the BOX element was associated with colony opacity in the species *Pneumococcus*. Another study reported the location and vicinity of genes could be involved in bacterial competence, genetic transformation and virulence (Martin et al., 1992). The BOX repeat can be used to discriminate 3 regions *boxA*, *boxB*, and *boxC*, However, only *boxA* which consists of 59 bp was used in this study. Throughout literature the BOX element focuses on bacterial discrimination and has previously proved be a distinguishing factor when closely related strains of *Pseudomonas* were not able to be discriminated by the ITS or *aclB* genes (Cho and Tiedje, 2000). Furthermore, 16S rRNA and ITS regions could not show a strong degree of endemicity but observed strict endemicity when fingerprinting with BOX-PCR genes (Cho and Tiedje, 2000). The BOX element has been used to evaluate genetic differences between the cyanobacterium *Cylindrospermopsis raciborskii* which is the closest organism to *H. pluvialis* that has been evaluated by BOX-PCR banding patterns (Piccini et al., 2011). However, no instance thus far has used BOX-PCR to access the genetic diversity in any species of algae thus far. Therefore, this study was the first instance of the use of BOX-PCR banding patterns as an efficient way of detecting interspecies variation within *H. pluvialis.*

### 4.2.2 ERIC-PCR phylogeny profiles reveal additional variance among strains

ERIC- PCR is another common PCR method of molecular typing and was used for further strain discrimination. The method is based on short repetitive sequences of (127 bp) that are imperfect palindromes which have been found in multiple copies of the genomes of various bacterial species (Lupski and Weinstock, 1992; Wilson, 2006). However, shorter sequences have been described through internal deletions (Sharp and Leach, 1996) as well as longer sequences at internal sites (Cromie, Collins, and Leach 1997). Little is known about the function of these elements however due their diversity among bacterial species it's unlikely they are aspects of conserved areas of the genome regarding growth, survival or replication and in many cases are likely to be non-functional junk DNA. Likewise with BOX-PCR, ERIC-PCR has been evaluated thoroughly throughout bacterial species, and has shown to be a prominent tool in distinguishing various toxic and non-toxic strains of Cyanobacteria, which remain the closest relatives to green algae evaluated by this technique (Lyra et al., 2001; Valério et al ., 2009; Bruno 2006). There have been no reports thus far using ERIC-PCR for discrimination in algal species, however, in this study significant variation between strains of *H. pluvialis* was identified (Figure 7). Furthermore, in the study by (Peng et al., 2007) indicated optimization of ERIC-PCR suggest that $Mg^{2+}$, dNTP, Primer and polymerase concentrations play a significant role on the ERIC-PCR fingerprinting patterns with optimal conditions. Therefore, further optimization could have improved the ERIC-PCR banding patterns in the present study.

## 4.3 Heterotrophic/Autotrophic shake flask growth and fluorescence indicate significant variation in metabolic capabilities

### Autotrophic shake flask growth

When analyzing the metabolism of various strains of *H. pluvialis* in BBM media the average top growing strains evaluated on day 14 in BBM media were found to be similar to the top growing strains with additional glucose. Some strains indicated slightly higher average CFU values, however common overlap between replicas of the two medias frequently appeared (Figures 11 - 27). However, some interesting trends were witnessed in a few strains with additional glucose. When measured on day 7 strain HP_B01 grew to a significantly higher density in BBM media than with additional glucose, however on day 14 BBM growth was lower than that of additional glucose. Also, during the growth of strain HP_N01 with additional glucose cell densities on day 7 were higher than on day 14, indicating that the strain grows to a higher cell density in a shorter amount of time with additional 0.8g/L glucose

since this was not witnessed during the growth with BBM media (Figure 20). Under shake flask autotrophic growth conditions, no additional $CO_2$ was implemented for photosynthetic growth, therefore strains could also metabolize glucose, thus making use of organic and inorganic carbon. During mixotrophic growth it is not clear which carbon source is preferred or used first, or if a combination of photosynthesis and glucose metabolism is simultaneous. The study by (Howieson, 2001) found that utilization of different organic substrates was strain specific during mixotrophic cultivation. These results correlate with this study as glucose metabolism was significantly different than with BBM media alone in some strains, while in most other strains no significant difference was witnessed. Furthermore, variations throughout literature regarding growth parameters and nutritional requirements vary with the strains, and thus optimum values for culture conditions and carotenoid production could be strain specific.

Unlike most green algae, *H. pluvialis* can perform photosynthesis and utilize the oxidative metabolism of acetate during mixotrophic growth (Kobayashi et al., 1992; Orosa et al., 2001). Several studies indicate early encystment of *H. pluvialis* with acetate supplementation under autotrophic, mixotrophic, and heterotrophic growth conditions (Orosa et al., 2001; Kobayashi et al., 1991; Tripathi et al., 1999; Cifuentes et al., 2003). These findings correlate with some strains in this study as autotrophic growth in BBM media supplemented with sodium acetate indicated a higher CFU value in some of the strains on the 7$^{th}$ day of growth (Figures 11 - 27) and a faster decrease in fluorescence (Figures 28 - 44) in many strains compared to BBM media alone or BBM supplemented with glucose. An increase in cell density was observed on day 7 compared to day 14, for 13 of the 17 strains with additional sodium acetate. These results indicate that 13 strains initially grew faster in a shorter time compared to BBM media alone, but do not show a growth advantage when measured at day 14 (Figures 11 - 27).

## Heterotrophic shake flask growth

Concerning heterotrophic growth conditions BBM media and BMM with glucose showed no or very little growth. Some algal strains can assimilate with various carbon sources under heterotrophic conditions a supplemental organic acid or carbohydrate source such as glucose, glycerol, sucrose, lactose, mannose, or acetate (Liang et al., 2009; Kobayashi et al, 1993). However, this study indicated no heterotrophic growth with 0.8 g/L glucose in *H. pluvialis*. In the study by (Howieson, 2001) none of the strains of *H. pluvialis* tested were able to grow heterotrophically in any media other than sodium acetate. Interestingly, the same study reported that when glucose and sodium acetate were supplied together during heterotrophic

cultivation one strain metabolized both carbon sources even though glucose alone was an ineffective heterotrophic substrate (Howieson, 2001). Unlike *Chlorella protothecoides* CS-41, and *Chlorella vulgaris* which have the capability of growth in various glucose concentrations heterotrophically (Shi et al., 1999; Shi et al., 2002; Liang et al., 2009). Furthermore, in the study by (Shi et al., 1999) the concentration of glucose was shown to have a significant effect on biomass concentrations and lutein productivities as a maximum biomass concentration was reached from 4-9 to 31-2 g/L (DW) with an increase in initial glucose concentration from 10 to 80 g/L . Interestingly a concentration of 100 g/L was shown to be significantly lower concerning many factors such as biomass concentration, growth rate coefficient, and contributed to a significantly longer lag phase, which was suspected to be due to substrate inhibition. However, it is well known that *H. pluvialis* can grow and produce photosynthetic pigments as well as astaxanthin under heterotrophic conditions on acetate (Kobayashi et al., 1992; Tripathi et al., 1999; Chen et al., 2011). Therefore, the concentration of sodium acetate could also significantly affect growth and astaxanthin production under heterotrophic conditions, and perhaps a specific optimum concentration would have been beneficial for growth and differentiation. Day 14 values indicate a wide range from 8 – 193 CFU/10µL and thus the best way of distinguishing strains based on metabolism alone. Previous reports regarding *H. pluvialis* indicate the importance of acetate as a carbon source enabling the enhancement of growth and carotenogenesis (Borowitzka et al., 1991; Orosa et al., 2001) these results correlate with this study, due to additional 0.8 g/L sodium acetate to BBM media resulted in several strains growing to a higher cell density on day 7 compared to day 14 (Figures 11 - 27). This could prove advantageous as a higher biomass can be obtained in a shorter time frame. Heterotrophic growth has also been proven to be useful in some species regarding biodiesel production as a higher lipid content has been observed by changing cultivation conditions from phototrophic to heterotrophic (Xu et al., 2006; Xiong et al., 2008). However, some studies indicate that encystment is retarded when a high nitrate concentration is added together with supplemental acetate, indicating that encystment is triggered via a high C/N ratio and not only by the acetate concentration (Kakizono et al., 1992; Borowitzka et al., 1991). Heterotrophic growth avoids limited light that hinder high cell density during large scale phototrophic cultivation (Huang et al., 2010). However, the main drawback is a sugar-based system is expensive and more frequently contaminated.

## 4.4 Metabolism of *H. pluvialis* in round bottom flasks revealed top producing strains

### 4.4.1 Round bottom flask growth and fluorescence profiles

The highest average CFU/10µL value was witnessed on day 15 with strain HP_B01 (716) followed by HP _E01 (672), and HP_E02 (636), (Figure 45). HP _E01, and HP_E02 were also the top growing strains for the shake flask experiments (Figures 11 - 12). Strain HP _E01 and HP_E02 showed replicas of three frequently overlapped and therefore these strains could in fact still be the same. Interestingly strain HP_N01 (Figure 20) was a top growing strain in previous shake flask experiments however when grown under the conditions of constant white LED lighting and aeration this strain was not of high performance (Figure 46). This indicates varying experimental designs have a significant influence on the growth advantages of different strains of *H. pluvialis*. Strains HP_E01 and HP_E02 were some of the top growing strains in all autotrophic experimental conditions (Figures 11 - 12,45).

When comparing cell densities to shake flask growth, round bottom flask growth indicated higher cell densities (Figures 45 - 46). This was to be expected as strain conditions such as a higher inoculum value, longer growth period, larger amount of BBM media, constant white LED illumination and aeration were implied. Similar cell densities of 3.5 x $10^5$ CFU/mL were witnessed in the study of (Domínguez-Bocanegra et al., 2004) which used similar conditions to the round bottom flask conditions in this study and identified the optimal environmental factors for the growth rate of *H. pluvialis*. Maximum growth after 12 days was obtained through BBM media at 28°C under constant illumination of white fluorescent light (177 µmol photon $m^{-2}$ $s^{-1}$), with continuous aeration (1.5 v.v.m) (Domínguez-Bocanegra et al., 2004).

### 4.4.2 Biomass yield (DW) from round bottom flask growth indicated top producers

When the (DW) of the cells were harvested on day 15, no clear top producer was prevalent as replicas of 3 common overlapped between 0.55 - 0.6 g/L (DW). In industry, faster growing strains could be favored for producing a higher amount of biomass and possibly a higher astaxanthin content in a shorter time frame. However, After 15 days of biomass accumulation, the highest overall biomass cannot be evaluated. Once carotenoid induction occurs a decrease in fluorescence is observed. During the growth period the fluorescence was measured for all strains until the first notice of a fluorescent decrease was observed for one strain, however all needed to be harvested at the same time for comparison. This indicated

that not all strains finished their growth stage when the biomass was evaluated. Throughout literature biomass accumulation is commonly measured daily however, due to the limited amount of media daily samples would have decreased the amount of media significantly throughout the experiment, therefore biomass (DW) was only measured the day of harvest (15 days of growth).

Regarding *H. pluvialis* biomass and astaxanthin productivities greatly vary depending on the strain, culture time, and condition. Biomass yields and productivities in the green and red stage, as well as astaxanthin content and yield in the red stage also significantly varies between studies. Since the BDI strains analyzed in this study were harvested during the very first instance of a decrease in fluorescence of one of the 17 strains, for comparison to literature biomass yields are evaluated in the green stage. When considering various strains in various conditions a biomass range of (0.2 - 7g $L^{-1}$ DW) have been reported during the green stage with productivities ranging from (0.036 - 1.9 g $L^{-1}$ $d^{-1}$ (DW); Olaizola et al., 2003; Hata et al., 2001; Del Río et al., 2005; Butler et al., 2017). Astaxanthin yields in the red stage range from (6.2 – 10.69 mg $L^{-1}$ $D^{-1}$ (DW), (Torzillo et al., 2003; Sarada et al., 2002; Butler et al., 2017). It must be noted that a strain with an advantage for growth and thus biomass formation in the green stage cannot be correlated directly to astaxanthin production in the red stage due to specific concentrations of astaxanthin being unique to a specific strain. Furthermore, some studies even indicate up to three-fold variations in growth rate, biomass production, and/or astaxanthin production when grown under identical conditions (Gao et al., 2015; Mostafa, 2012; Zhang et al., 2009). Biomass obtained in study could be lower than some reported in literature due to the lack of $CO_2$ when grown in round bottom flasks, as photosynthetic organisms consume $CO_2$ and produce biomass. Thus, adding $CO_2$ to the bioreactor could potentially have increased the biomass yield.

## 4.5 Headspace GC-MS analyses for VOC profiles of *H. pluvialis* strains

### 4.5.1 Detection of strain-specific VOCs in numerous strains of *H. pluvialis*

Analysis of GC-MS samples revealed methyl furan ,tetrahydrofuran, and dimethyl disulfide in various strains and in varying abundancies (Figures 49 - 65, 68 - 84). Each strain was analyzed in duplicate in random order to confirm the identification of the chemical. However, abundances often were too low to accurately be detected by the instrument. This is the case for very small molecules with a retention time lower than 1.5 hence, the first chemical that could be accurately detected by the instrument was ethanol which has a retention time of around 1.519 (Table 9). When analyzing samples that contained tetrahydrofuran, samples

HP_E01, HP_I01a and HP_F01a showed some abundance however, the duplicate samples of HP_I01 and HP_F01 did not (Table 8). This could be due to low abundance or perhaps a potential contamination present in one vial, but not in the duplicate sample. Peaks occurring at a retention times of ~5.3, 10.4, 15.2, 19.2, 21.9 are all siloxane-derivatives which are components of the fiber and the column and is known as "bleeding" (Behan, 2006). Siloxane-derivative peaks are labeled in the first chromatogram with green arrows (Figure 49), but apply to all the following samples (Figures 49 - 67).

GC-MS evaluation of the uninoculated BBM media that was used as a blank indicated that 1-propanol (Figure 85) as well in all inoculated samples produced from the Institute of Environmental Biotechnology at TU Graz (48 - 54). This procedure was also performed at BDI however several compounds were found in every BDI sample as well as in the uninoculated media, that were not found in the samples produced at the Institute of Environmental Biotechnology at TU Graz. These chemicals include: 1-butanol, 2-butanone, isopropyl alcohol, and ethanol (Figures 56 - 57,67,75 -76,86 - 89). It is possible that chemicals present in the uninoculated samples could be the result of contamination or could derive from a disinfection agent, as some of these compounds such as propan-1-ol, propan-2-ol, and ethanol are commonly found in laboratory cleaning products such as Bacillol®.

Volatile organic sulfur compounds (VOSCs) such as dimethyl sulfide (DMS) are known to play a role in the global sulfur cycle, especially in marine environments as DMS is often released from oceans to the atmosphere and is oxidized to form various sulfur degradation products. Like dimethyl disulfide (DMDS) dimethyl sulfide (DMS) differs only in the oxidation states and are -1, and -2 respectively. Gaseous forms of DMS and DMDS have been reported in axenic cultures of blue-green algae from various soil types, and eutrophic waters (Rasmussen, 1974). Several multicellular algae have also been shown to produce dimethyl sulfide such as the red algae *Polysiphonia fastigiate*, (Challaenger and Simpson, 1948; Haas, 1935) green algae such as *enteromorpha intestinalis* (Baywood and Challenger, 1953; Obata et al., 1951) and *Ulva pertusa* (Obata et al., 1951; Katayama and Tomiyama, 1951). Production of DMS during growth is a characteristic of marine algae and its precursor dimethyl- β- propiothetin has been shown to play a certain role in the metabolism of unicellular algae which inhabit waters of high salinity concentration (Kadota and Ishida, 1967 a). In the unicellular eukaryotic phytoplankton *Emiliania huxleyi* conversion of dimethyl sulfoniopropionate (DMSP) to DMS via DMSP lyase is minimal, however during agal grazing with a species of dinoflagellates such as *Oxyrrhis marina*, disruption of *E. huxleyi*

leads to the release of DMSP in solution in which DMSP lyases including those of bacteria will catalyse the conversion of DMSP to DMS (Wolfe and Steinke, 1996; Wolfe et al., 1994). DMS has also shown to damper predation of the marine heterotroph *Oxyrrhis marina* (Wolfe et al., 1997). Unlike marine algae, there was no previous evidence of freshwater green microalgae producing DMS thus far (Kadota and Ishida, 1968). Dimethyl disulfide is also a known decomposition product of a variety of bacteria and fungi (Segal and Starkey, 1969; Kadota and Ishida, 1972; Zinder et al., 1977).

Samples containing methyl furan could not be distinguished from 2-methyl- furan or 3-methyl- furan by the instrument. There have been no reports thus far indicating methyl furans being produced by algae however, VOC profiles of plant bacteria interactions report strains of plant dwelling rhizobacteria such as *Bacillus amyloliqefaciens* (IN937a) and *B. subtilis* (GB03) producing 2-methyl- furan (Farag et al., 2006). Therefore, it is possible that the furans found in this study are due to bacterial contamination and are not produced by strains of *H. pluvialis*. *Bacillus* strains are noted for their nitrogen- fixing capabilities and have been linked to beneficial effects on plants (Amavizca et al., 2017) and thus the co-occurrence with *H. pluvialis* could provide growth-promoting abilities for the algae. There has been a report of tetrahydrofuran being produced from a species of marine brown algae *(Notheia Anomaliz*), the cis-dihydroxy tetrahydrofuran produced was reported for the first time as a potent inhibitor of larval development of parasitic nematodes (Capon et al., 1998). An isolated endophyte from the plant-dwelling fungus *Muscodor albus* has been shown to produce several extremely bioactive VOCs including 2-methyl furan, tetrahydrofuran, 2-butanone etc., which are lethal to various plant and human pathogenic fungi and have shown to be effective against nematodes and certain insects (Strobel, 2010). Therefore, the function of the DMS and furans found in this study could possibly be a mechanism against parasitic organisms, however contamination from either a bacterial or fungal source cannot be ruled out.

# 5. Conclusions and Outlook

When characterizing strains of *H. pluvialis* the most effective method in this study was found to be analysis from 18rRNA and ITS regions of the genome in combination with the molecular typing tools of BOX-PCR and ERIC-PCR. These methods in unison are an effective means for a quick and robust means of differentiation for every strain evaluated, and thus should be the first steps in the SOP for characterization (Figure 90). The metabolic

growth capabilities of autotrophic and heterotrophic growth indicated the most variation when 0.8 g/L sodium acetate was added to the commonly used Bold Basal Media (BBM), especially during heterotrophic growth. However, autotrophic growth in BBM media alone and BBM supplemented with 0.8 g/L glucose showed significant variation for 11.76% of the implemented strains. Strains grown with the same media in varying experimental designs show certain strains can outperform others depending on the cultivation strategy. Furthermore, biomass yields (DW) indicated top producers however, was not a clear distinguishing factor. Headspace GC-MS analyses led to the detection of VOCs that are potentially formed due to a co-occurrence of microalgae with other microorganisms. The conducted experiments have confirmed that a combination of phylogenetic analyses, fingerprinting PCR methods, assessment of various cultivation strategies, biomass yields and investigation of VOCs could provide significant insights into more efficient biomass and astaxanthin production in *H. pluvialis* and thereby increasing the likelihood for increased economic viability.

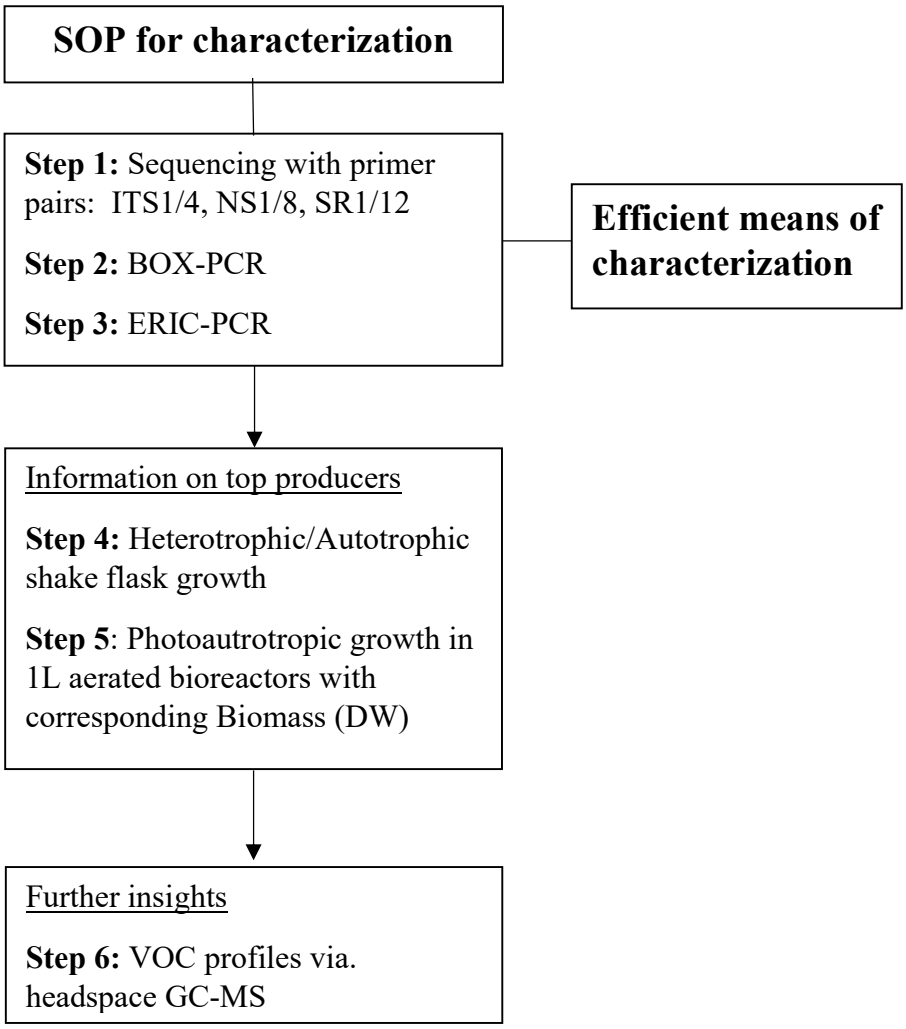


**Figure 90: SOP for *H. pluvialis* characterization**

# IV. References

Adams, T. B. et al. The FEMA GRAS assessment of pyrazine derivatives used as favor ingredients. Flavor and Extract Manufacturers Association. Food Chem. Toxicol. Int. J. Publ. Br. Ind. Biol. Res. Assoc. 40, 429–451 (2002).

Allewaert, Céline C., et al. "Species Diversity in European Haematococcus Pluvialis (Chlorophyceae, Volvocales)." Phycologia, vol. 54, no. 6, 2015, pp. 583–598., doi:10.2216/15-55.1

Amavizca, E., Bashan, Y., Ryu, C.-M., Farag, M. A., Bebout, B. M., and de-Bashan, L. E. (2017). Enhanced performance of the microalga Chlorella sorokiniana remotely induced by the plant growth-promoting bacteria Azospirillum brasilense and Bacillus pumilus. Sci. Rep. 7:41310. doi: 10.1038/srep41310

Amin, S. A., Green, D. H., Hart, M. C., Küpper, F. C., Sunda, W. G., and Carrano, C. J. (2009). Photolysis of iron–siderophore chelates promotes bacterial–algal mutualism. Proc. Natl. Acad. Sci. U.S.A. 106, 17071–17076. doi: 10.1073/pnas.0905512106

Behan, A. (2006). Books: Mass Spectrometry – A Textbook. By Jürgen H. Gross. *Biotechnology Journal, 1*(2), 226-226. doi:10.1002/biot.200690028

Benemann, J. (2013). Microalgae for Biofuels and Animal Feeds. Energies, 6(11),5869-5886. Doi:10.3390/en6115869

Bellemain, E., Carlsen, T., Brochmann, C., Coissac, E., Taberlet, P., & Kauserud, H. (2010). ITS as an environmental DNA barcode for fungi: An in-silico approach reveals potential PCR biases. BMC Microbiology, 10(1), 189. doi:10.1186/1471-2180-10-189

Bentley, R., & Chasteen, T. G. (2004). Environmental VOSCs—formation and degradation of dimethyl sulfide, methanethiol and related materials. Chemosphere, 55(3), 291-317. doi:10.1016/j.chemosphere.2003.12.017

Bínová, J., Tichý, V., Lívanský, K. & Zahradník, J. Bacterial contamination of microalgal biomass during outdoor production and downstream processing. *Algol. Stud. Für Hydrobiol. Suppl. Vol*. 151–158 (1998).

Bischoff, H. W., and Bold, H. C. (1963). "Phycological studies IV," in Some Soil Algae from Enchanted Rock and Related Algal Species. (Austin, TX: University of Texas Publications), 95.

Borowitzka, M. A. High-value products from microalgae—their development and commercialisation. *J. Appl. Phycol.* 25, 743–756 (2013).

Borowitzka, M. A., Huisman, J. M., & Osborn, A. (1991). Culture of the astaxanthin-producing green alga Haematococcus pluvialis 1. Effects of nutrients on growth and cell type. Journal of Applied Phycology, 3(4), 295-304. doi:10.1007/bf02392882

Bramwell, F. A., Burrell, K. J. W. & Riezebos, G. Characterisation of pyrazines in Galbanum oil. | Article Information | J-GLOBAL. Tetrahedron Lett 3215–3216 (1969).

Brennan, L, Owende, P., 2010. Biofuels from microalgae- a review of technologies for production, processing, and extractions of biofuels and co-products. Renew. Sust. Energ. Rev. 14, 557-577.

Bruno, L., Billi, D., Albertano, P., & Urzí, C. (2006). Genetic Characterization of Epilithic Cyanobacteria and Their Associated Bacteria. *Geomicrobiology Journal, 23*(5), 293-299. doi:10.1080/01490450600760732

Buchheim, M. A., Sutherland, D. M., Buchheim, J. A., & Wolf, M. (2013). The blood alga: Phylogeny ofHaematococcus(Chlorophyceae) inferred from ribosomal RNA gene sequence data. *European Journal of Phycology, 48*(3), 318-329. doi:10.1080/09670262.2013.830344

Butler, T., Mcdougall, G., Campbell, R., Stanley, M., & Day, J. (2017). Media Screening for Obtaining Haematococcus pluvialis Red Motile Macrozooids Rich in Astaxanthin and Fatty Acids. Biology, 7(1), 2. doi:10.3390/biology7010002

Buttery, R. G., Seifert, R. M., Guadagni, D. G. & Ling, L. C. Characterization of some volatile constituents of bell peppers. J. Agric. Food Chem. 17, 1322–1327 (1969).

Bywood, H. and F. Challenger. 1953: The evolution of dimethyl sulphide by Enteromorpha intestinalis " Isolation of dimethyl-ft-carboxyethyl sulphonium chloride from the alga. Biochem. J., 53, XXVI.

Capelli, B.; Bagchi, D.; Cysewski, G.R. Synthetic astaxanthin is significantly inferior to algal-based astaxanthin as an antioxidant and may not be suitable as a human nutraceutical supplement. Nutrafoods 2013, 12, 145–152.

Capon, R. J., Barrow, R. A., Rochfort, S., Jobling, M., Skene, C., Lacey, E., . . . Wadsworth, D. (1998). Marine nematocides: Tetrahydrofurans from a southern Australian brown alga, Notheia anomala. Tetrahedron, 54(10), 2227-2242. doi:10.1016/s0040-4020(97)10432-x

Carney, L. T. & Lane, T. W. Parasites in algae mass culture. *Front. Microbiol*. 5 (2014).

Challenger, F. And M. I. Simpson. 1948: Studies on biological methylation. Part XIII: A precursor of the dimethyl sulfide evolved by Polysiphonia fastigiata. Dimethyl-2-carboxethyl sulphonium hydroxide and its salts. J. Chem., Soc., 1948; 1591-1597

Chan K.C., Pen P.J., Yin M.C. Anti-coagulatory and anti-inflammatory effects of astaxanthin in diabetic rats. J. Food Sci. 2012;77:H76–H80. doi: 10.1111/j.1750-3841.2011.02558.x.

Chekanov, K., Lobakova, E., Selyakh, I., Semenova, L., Sidorov, R., and Solovchenko, A. (2014). Accumulation of astaxanthin by a new Haematococcus pluvialis strain BM1 from the White Sea coastal rocks (Russia). Mar. Drugs. 12, 4504–4520. doi: 10.3390/md12084504

Chen, C., Yeh, K., Aisyah, R., Lee, D., & Chang, J. (2011). Cultivation, photobioreactor design and harvesting of microalgae for biodiesel production: A critical review. *Bioresource Technology, 102*(1), 71-81. doi:10.1016/j.biortech.2010.06.159

Cho JC, Tiedje JM (2000) Biogeography and degree of endemicity of fluorescent Pseudomonas strains in soil. Appl Environ Microbiol 66:5448–5456

Choubert, G., and Heinrich, O. (1993). Carotenoid pigments of the green alga Haematococcus pluvialis: assay on rainbow trout, Oncorhynchus mykiss, pigmentation in comparison with synthetic astaxanthin and canthaxanthin. Aquaculture 112, 217–226. doi: 10.1016/0044-8486(93)90447-7

Cifuentes, A. S., González, M. A., Vargas, S., Hoeneisen, M., & González, N. (2003). Optimization of biomass, total carotenoids and astaxanthin production in Haematococcus pluvialis Flotow strain Steptoe (Nevada, USA) under laboratory conditions. Biological Research, 36(3-4). doi:10.4067/s0716-97602003000300006

de-Bashan, L., Antoun, H., and Bashan, Y. (2008). Involvement of indole-3-acetic acid produced by the growth-promoting bacterium Azospirillum spp. promoting growth of Chlorella vulgaris. J. Phycol. 44, 938–947. doi: 10.1111/j.1529-8817.2008.00533.x

de-Bashan, L. E., and Bashan, Y. (2010). Immobilized microalgae for removing pollutants: review of practical aspects. Bioresour. Technol. 101, 1611–1627. doi: 10.1016/j.biortech.2009.09.043

Del Río, E., Acién, F. G., García-Malea, M. C., Rivas, J., Del Rio, E., Acién, F. G., et al. (2005). Efficient one-step production of astaxanthin by the microalga Haematococcus pluvialis in continuous culture. Biotechnol. Bioeng. 91, 808–815. doi: 10.1002/bit.20547

de Rijk, M. et al. (1997) Dietary antioxidants and Parkinson disease. The Rotterdam Study. Arch. Neurol. 54, 762–765

Domínguez-Bocanegra, A. R., Guerrero Legarreta, I., Martinez Jeronimo, F., and Tomasini Campocosio, A. (2004). Influence of environmental and nutritional factors in the production of astaxanthin from Haematococcus pluvialis. Bioresour. Technol. 92, 209–214. doi: 10.1016/j.biortech.2003.04.001

Dong, S., Pang, K., Bai, X., Yu, X., & Hao, P. (2010). Identification of Two Species of Yeast-like Symbiotes in the Brown Planthopper, Nilaparvata lugens. Current Microbiology, 62(4), 1133-1138. doi:10.1007/s00284-010-9830-z

Dragos, N., Bercea, V., Bica, A., Druga, B., Nicoara, A., and Coman, C. (2010). Astaxanthin production from a new strain of Haematococcus pluvialis grown in batch culture. Ann. Roman. Soc. Cell Biol. 15, 353–361.

Fábregas, J., Dominguez, A., Regueiro, M., Maseda, A., and Otero, A. (2000). Optimization of culture medium for the continuous cultivation of the microalga Haematococcus pluvialis. Appl. Micobiol. Biotechnol. 53, 530-535. Doi: 10.1007/s002530051652

Fan, L., Vonshak, A., and Boussiba, S. (1994). Effect of temperature and irradiance on growth of Haematococcus pluvialis (Chlorophyceae). J. Phycol. 30, 829–833. doi: 10.1111/j.0022-3646.1994.00829.x

Farag MA, Ryu CM, Summer LW, Pare PW (2006) GC-MS SPME profiling of rhizobacterial volatiles reveals prospective inducers of growth promotion and induced systemic resistance in plants. Phytochemistry 67:2262–2268

Flotow, J. (1844). Beobachtungen über Haematococcus pluvialis. Verhandlungen der Kaiserlichen Leopoldinisch-Carolinischen Deutschen Akademie der Naturforscher 12 (Abt. 2): 413-606, 3 pls.

Fürnkranz, M. et al. Microbial diversity inside pumpkins: microhabitat-specifc communities display a high antagonistic potential against phytopathogens. Microb. Ecol. 63, 418–428 (2012).

Gao Z., Meng C., Chen, Y.C et al. Comparison of astaxanthin accumulation and biosynthesis gene expression of three Haematococcus pluvialis strains upon salinity stress. J Appl Phycol 27, 1853-1860 (2015). https://doi.org/10.1007/s10811-014-0491-3

Gao, Z., Meng, C., Zhang, X., Xu, D., Zhao, Y., Wang, Y., et al. (2012b). Differential expression of carotenogenic genes, associated changes on astaxanthin production and photosynthesis features induced by JA in H. pluvialis. PLoS ONE 7:e42243. doi: 10.1371/journal.pone.0042243

Gómez, P. I., Haro, P., Lagos, P., Palacios, Y., Torres, J., Sáez, K., . . . González, M. A. (2015). Intraspecific variability among Chilean strains of the astaxanthin-producing microalga Haematococcus pluvialis (Chlorophyta): An opportunity for its genetic improvement by simple selection. Journal of Applied Phycology, 28(4), 2115-2122. doi:10.1007/s10811-015-0777-0

Gong X, Chen F (1997) Optimization of culture medium for growth of Haematococcus pluvialis. J appl Phycol 9: 437-444. doi:10.5353/th_b3123690

Guerin, M.; Huntley, M.E.; Olaizola, M. Haematococcus astaxanthin: Applications for human health and nutrition. Trends Biotechnol. 2003, 21, 210–216.

Gutiérrez, C. L., Gimpel, J., Escobar, C., Marshall, S. H., and Henríquez, V. (2012). Chloroplast genetic tool for the green microalgae Haematococcus pluvialis (Chlorophyceae, Volvocales)1. J. Phycol. 48, 976–983. doi: 10.1111/j.1529-8817.2012.01178.x

Grant, W.B. (1997) Dietary links to Alzheimer's disease. J. Alzheimers Dis. 2, 42–55

Haas, P. (1935). The liberation of methyl sulphide by seaweed. Biochemical Journal, 29(6), 1297-1299. doi:10.1042/bj0291297

Hata, N., Ogbonna, J. C., Hasegawa, Y., Taroda, H., and Tanaka, H. (2001). Production of astaxanthin by Haematococcus pluvialis in a sequential heterotrophic-photoautotrophic culture. J. Appl. Phycol. 13, 395–402. doi: 10.1023/A:1011921329568

Hausner, G., & Wang, X. (2005). Unusual compact rDNA gene arrangements within some members of the Ascomycota: evidence for molecular co-evolution between ITS1 and ITS2. Genome, 48(4), 648–660. doi: 10.1139/g05-037

Hazen, T. E. (1899). The life history of Sphaerella lacustris. Mem. Torrey Bot. Club 6, 211–244.

Higuera-Ciapara, I.; Felix-Valenzuela, L.; Goycoolea, F.M. Astaxanthin: A review of its chemistry and applications. Crit. Rev. Food Sci. Nutr. 2006, 46, 185–196.

Hong, J. W., Kim, O. H., Jo, S., Kim, H., Jeong, M. R., Park, K. M., Yoon, H. (2016). Biochemical Composition of a Korean Domestic Microalga Chlorella vulgaris KNUA027. Microbiology and Biotechnology Letters, 44(3), 400-407. doi:10.4014/mbl.1512.12008

Howieson, Janet Rosalind (2001) Nutrition and carotenogenesis in Haematococcus pluvialis. PhD thesis, Murdoch University.

Hu, Q., Zhang, C.W., Sommerfeild, M., 2006. Biodiesel from algae: lessons learned over the past 60 years and future perspectives. J. Phycol.42,12.

Hu, Z., Li, Y., Sommerfeld, M., Chen, F., and Hu, Q. (2008). Enhanced protection against oxidative stress in an astaxanthin-overproduction Haematococcus mutant (Chlorophyceae). Eur. J. Phycol. 43, 365–376. doi: 10.1080/09670260802227736

Huang, G., Chen, F., Wei, D., Zhang, X., & Chen, G. (2010). Biodiesel production by microalgal biotechnology. *Applied Energy, 87*(1), 38-46. doi:10.1016/j.apenergy.2009.06.016

Huangfu J., Liu J., Sun Z., Wang M., Jiang Y., Chen Z.Y., Chen F. Anti-ageing effects of astaxanthin-rich alga Haematococcus pluvialis on fruit flies under oxidative stress. J. Agric. Food Chem. 2013;6:7800–7804.

Huo, S., Shang, C., Wang, Z., Zhou, W., Cui, F., Zhu, F., … Dong, R. (2017). Outdoor Growth Characterization of an Unknown Microalga Screened from Contaminated Chlorella Culture. BioMed Research International, 2017, 1–7. doi: 10.1155/2017/5681617

Iizuka M., Ayaori M., Uto-Kondo H., Yakushiji E., Takiguchi S., Nakaya K., Hisada T., Sasaki M., Komatsu T., Yogo M., et al. Astaxanthin enhances ATP-binding cassette transporter A1/G1 expressions and cholesterol efflux from macrophages. J. Nutr. Sci. Vitaminol. (Tokyo) 2012;58:96–104. doi: 10.3177/jnsv.58.96.

Johnston, M. D., Lawson, S. & Otter, J. A. Evaluation of hydrogen peroxide vapour as a method for the decontamination of surfaces contaminated with Clostridium botulinum spores. J. Microbiol. Methods 60, 403–411 (2005).

Kadota, H., & Ishida, Y. (1972). Production of Volatile Sulfur Compounds by Microorganisms. Annual Review of Microbiology, 26(1), 127-138. doi:10.1146/annurev.mi.26.100172.001015

Kadota, H. and Y. Ishida. 1968 b: Effect of salts on enzymatical production of dimethyl sulfide from Gyrodinium cohnii. Bull. Japan Soc. Sci. Fish., 34, in press.

Kakizono, T., Kobayashi, M., & Nagai, S. (1992). Effect of carbon/nitrogen ratio on encystment accompanied with astaxanthin formation in a green alga, Haematococcus pluvialis. Journal of Fermentation and Bioengineering, 74(6), 403-405. doi:10.1016/0922-338x(92)90041-r

Kang, C. D., Lee, J. S., Park, T. H., and Sim, S. J. (2005). Comparison of heterotrophic and photoautotrophic induction on astaxanthin production by Haematococcus pluvialis. Appl. Microbiol. Biotechnol. 68, 237–241. doi: 10.1007/s00253-005-1889-2

Katayama, T., & Tomiyama, T. (1951). Chemical Studies on Volatile Constituents of Sea Weed. Nippon Suisan Gakkaishi, 17(5), 122-127. doi:10.2331/suisan.17.122

Kim, B.-H., Ramanan, R., Cho, D.-H., Oh, H.-M., and Kim, H.-S. (2014). Role of Rhizobium, a plant growth promoting bacterium, in enhancing algal biomass through mutualistic interaction. Biomass Bioenerg. 69, 95–105. doi: 10.1016/j.biombioe.2014.07.015

Kim, J. H., Affan, M. A., Jang, J., Kang, M.-H., Ko, A.-R., Jeon, S.-M., … Kang, D.-H. (2015). Morphological, Molecular, and Biochemical Characterization of Astaxanthin-Producing Green Microalga Haematococcus sp. KORDI03 (Haematococcaceae, Chlorophyta) Isolated from Korea. Journal of Microbiology and Biotechnology, 25(2), 238–246. doi: 10.4014/jmb.1410.10032

Kimura, K., & Tomaru, Y. (2013). Isolation and Characterization of a Single-Stranded DNA Virus Infecting the Marine Diatom Chaetoceros sp. Strain SS628-11 Isolated from Western JAPAN. PLoS ONE, 8(12). doi:10.1371/journal.pone.0082013

Klapes, N. A. & Vesley, D. Vapor-phase hydrogen peroxide as a surface decontaminant and sterilant. Appl. Environ. Microbiol. 56, 503–506 (1990).

Klochkova, T. A., Kwak, M. S., Han, J. W., Motomura, T., Nagasato, C., and Kim, G. H. (2013). Cold-tolerant strain of Haematococcus pluvialis (Haematococcaceae, Chlorophyta) from Blomstrandhalvoya (Svalbard). Algae 28, 185–192. doi: 10.4490/algae.2013.28.2.185

Kobayashi, M., Kakizono, T., & Nagai, S. (1991). Astaxanthin production by a green alga, Haematococcus pluvialis accompanied with morphological changes in acetate media. Journal of Fermentation and Bioengineering, 71(5), 335–339. doi: 10.1016/0922-338x(91)90346-i

Kobayashi, M., Kakizono, T., and Nagai, S. (1993). Enhanced carotenoid biosynthesis by oxidative stress in acetateinduced cyst cells of a green unicellular alga, *Haematococcus pluvialis*. *Appl. Environ. Microbiol.* 59, 867–873.

Kobayashi, M., Kakizono, T., Yamaguchi, K., Nishio, N., & Nagai, S. (1992). Growth and astaxanthin formation of Haematococcus pluvialis in heterotrophic and mixotrophic conditions. *Journal of Fermentation and Bioengineering, 74*(1), 17-20. doi:10.1016/0922-338x(92)90261-r

Kobayashi, M., Kakizono, T., Nishio, N., Nagai, S., Kurimura, Y., & Tsuji, Y. (1997). Antioxidant role of astaxanthin in the green alga Haematococcus pluvialis. Applied Microbiology and Biotechnology, 48(3), 351-356. doi:10.1007/s002530051061

Koeuth T, Versalovic J, Lupski JR. Differential subsequence conservation of interspersed repetitive Streptococcus pneumoniae BOX elements in diverse bacteria. Genome Research. 1995;5(4):408-418.

Kroken, S., & Taylor, J. W. (2000). Phylogenetic Species, Reproductive Mode, and Specificity of the Green AlgaTrebouxiaForming Lichens with the Fungal GenusLetharia. The Bryologist, 103(4), 645-660. doi:10.1639/0007-2745(2000)103[0645:psrmas]2.0.co;2

Krug, L., Morauf, C., Donat, C., Müller, H., Cernava, T., & Berg, G. (2020). Plant Growth-Promoting Methylobacteria Selectively Increase the Biomass of Biotechnologically Relevant Microalgae. Frontiers in Microbiology, 11. doi:10.3389/fmicb.2020.00427

Lemoine, Y., & Schoefs, B. (2010). Secondary ketocarotenoid astaxanthin biosynthesis in algae: A multifunctional response to stress. Photosynthesis Research, 106(1-2), 155-177. doi:10.1007/s11120-010-9583-3

Letcher, P. M. *et al*. Characterization of Amoeboaphelidium protococcarum, an Algal Parasite New to the Cryptomycota Isolated from an Outdoor Algal Pond Used for the Production of Biofuel. *PLoS ONE* 8, e56232 (2013).

Li J., Zhu D., Niu J., Shen S. & Wang G. 2011. An economic assessment of astaxanthin production by large scale cultivation of Haematococcus pluvialis. Biotechnology Advances 29: 568–574

Li, Y., Sommerfeld, M., Chen, F., and Hu, Q. (2010). Effect of photon flux densities on regulation of carotenogenesis and cell viability of Haematococcus pluvialis (Chlorophyceae). J. Appl. Phycol. 22, 253–263. doi: 10.1007/s10811-009-9453-6

Liang, Y., Sarkany, N., & Cui, Y. (2009). Biomass and lipid productivities of Chlorella vulgaris under autotrophic, heterotrophic and mixotrophic growth conditions. *Biotechnology Letters, 31*(7), 1043-1049. doi:10.1007/s10529-009-9975-7

Lorenz, R., & Cysewski, G. R. (2000). Commercial potential for Haematococcus microalgae as a natural source of astaxanthin. Trends in Biotechnology, 18(4), 160-167. doi:10.1016/s0167-7799(00)01433-5

Lupski, J. R., & Weinstock, G. M. (1992). Short, interspersed repetitive DNA sequences in prokaryotic genomes. Journal of Bacteriology, 174(14), 4525-4529. doi:10.1128/jb.174.14.4525-4529.1992

Lyra, C., Suomalainen, S., Gugger, M., Vezie, C., Sundman, P., Paulin, L., & Sivonen, K. (2001). Molecular characterization of planktic cyanobacteria of Anabaena, Aphanizomenon, Microcystis and Planktothrix genera. International Journal of Systematic and Evolutionary Microbiology, 51(2), 513-526. doi:10.1099/00207713-51-2-513

Ma, M. *et al*. Effective control of Poterioochromonas malhamensis in pilot-scale culture of Chlorella sorokiniana GT-1 by maintaining CO2-mediated low culture pH. *Algal Res.* 26, 436–444 (2017).

Martin, B., Humbert, O., Camara, M., Guenzi, E., Walker, J., Mitchell, T., Andrew, P., Prudhomme, M., Alloing, G., Hakenbeck, R., Morrison, D. A., Boulnois, G. J., and Claverys, J. P. (1992) A highly conserved repeated DNA element located in the chromosome of Streptococcus pneumoniae. Nucleic Acids Res. 20, 3479–3483

Meintanis, C., Chalkou, K., Kormas, K. A., Lymperopoulou, D., Katsifas, E., Hatzinikolaou, D., & Karagouni, A. (2008). Application of rpoB sequence similarity analysis, REP-PCR and BOX-PCR for the differentiation of species within the genus Geobacillus. Letters in Applied Microbiology, 46(3), 395-401. doi:10.1111/j.1472-765x.2008.02328.x

Mitchell, T. G., Freedman, E. Z., White, T. J., & Taylor, J. W. (1994). Unique oligonucleotide primers in PCR for identification of Cryptococcus neoformans. Journal of Clinical Microbiology, 32(1), 253-255. doi:10.1128/jcm.32.1.253-255.1994

Montemezzani, V., Duggan, I. C., Hogg, I. D., & Craggs, R. J. (2015). A review of potential methods for zooplankton control in wastewater treatment High Rate Algal Ponds and algal production raceways. *Algal Research, 11*, 211-226. doi:10.1016/j.algal.2015.06.024

Moreno-Garrido, I., & Cañavate, J. (2001). Assessing chemical compounds for controlling predator ciliates in outdoor mass cultures of the green algae Dunaliella salina. *Aquacultural Engineering, 24*(2), 107-114. doi:10.1016/s0144-8609(00)00067-4

Mostafa N. (2012). Comparative biodiversity and effect of different media on growth and astaxanthin content of nine geographical strains of Haematococcus pluvialis. African Journal of Biotechnology 11: 15049–15059.

Mostafa N., Omar H., Tan S.G. & Napis S. (2011). Studies on the genetic variation of the green unicellular alga Haematococcus pluvialis (Chlorophyceae) obtained from different geographical locations using ISSR and RAPD molecular marker. Molecules 16: 2599–2608.

Murray, K. E. & Whitfeld, F. B. Te occurrence of 3-alkyl-2-methoxypyrazines in raw vegetables. J. Sci. Food Agric. 26, 973–986 (1975).

Obata, Y., II. Igarashi and K. Matano. 1951: Studies on the flavor of seaweeds 1. On the component of the flavor of some green algae. Bull. Japan Soc. Sci. Fish., 17, 60-62.

Okuda, A., & Yamaguchi, M. (1960). Nitrogen-fixing microorganisms in paddy soils: VI. Soil Science and Plant Nutrition, 6(2), 76-85. doi:10.1080/00380768.1960.10430930

Olaizola, M.; Huntley, M.E. Recent advances in commercial production of astaxanthin from microalgae, in Fingerman, M.; Nagabhushanam, R. (eds.), Recent Advances in Marine Biotechnology. Volume 9. Biomaterials and Bioprocessing. New Hampshire: Science Publishers, 2003, 143-164

Olguín, E. J., Giuliano, G., Porro, D., Tuberosa, R., and Salamin, F. (2012). Biotechnology for a more sustainable world. Biotechnol. Adv. 30, 931–932. doi: 10.1016/j.biotechadv.2012.06.001

Orosa, M., Franqueira, D., Cid, A., & Abalde, J. (2001). Carotenoid accumulation in Haematococcus pluvialis in mixotrophic growth .Biotechnology Letters, 23(5), 373-378. doi:10.1023/a:1005624005229

Osek, J., & Gallien, P. (2012). Molecular analysis of Escherichia coli O157 strains isolated from cattle and pigs by the use of PCR and pulsed-field gel electrophoresis methods. Veterinární Medicína, 47(No. 6), 149-158. doi:10.17221/5819-vetmed

Ownley, B. H., Griffin, M. R., Klingeman, W. E., Gwinn, K. D., Moulton, J. K., & Pereira, R. M. (2008). Beauveria bassiana: Endophytic colonization and plant disease control. Journal of Invertebrate Pathology, 98(3), 267-270. doi:10.1016/j.jip.2008.01.010

Pan, J., Wang, H., Chen, C., & Chang, J. (2012). Extraction of astaxanthin from Haematococcus pluvialis by supercritical carbon dioxide fluid with ethanol modifier. Engineering in Life Sciences, 12(6), 638-647. doi:10.1002/elsc.201100157

Panis, G., & Carreon, J. R. (2016). Commercial astaxanthin production derived by green alga Haematococcus pluvialis : A microalgae process model and a techno-economic assessment all through production line. Algal Research, 18, 175-190. doi:10.1016/j.algal.2016.06.007

Park, J. C., Choi, S. P., Hong, M. E., and Sim, S. J. (2014). Enhanced astaxanthin production from microalga, Haematococcus pluvialis by two-stage perfusion culture with stepwise light irradiation. Bioprocess Biosyst. Eng. 37, 2039–2047. doi: 10.1007/s00449-014-1180-y

Peng, Y., Jin, J., Wu, C., Yang, J., & Li, X. (2007). Orthogonal array design in optimizing ERIC-PCR system for fingerprinting rat's intestinal microflora. *Journal of Applied Microbiology, 103*(6), 2095-2101. doi:10.1111/j.1365-2672.2007.03440.x

Piccini, C., Aubriot, L., Fabre, A., Amaral, V., González-Piana, M., Giani, A., . . . Bonilla, S. (2011). Genetic and eco-physiological differences of South American Cylindrospermopsis raciborskii isolates support the hypothesis of multiple ecotypes. *Harmful Algae, 10*(6), 644-653. doi:10.1016/j.hal.2011.04.016

Proudy, I., Bouglé, D., Coton, E., Coton, M., Leclercq, R., & Vergnaud, M. (2007). Genotypic characterization of Enterobacter sakazakii isolates by PFGE, BOX-PCR and sequencing of the fliC gene. Journal of Applied Microbiology, 0(0). doi:10.1111/j.1365-2672.2007.03526.x

Ranga Rao A., Sindhuja H.N., Dharmesh S.M., Sankar K.U., Sarada R., Ravishankar G.A. (2013). Effective inhibition of skin cancer, tyrosinase, and antioxidative properties by astaxanthin and astaxanthin esters from the green alga Haematococcus pluvialis. J. Agric. Food Chem. 2013;61:3842–3851.

Rasmussen, R. A. (1974). Emission of biogenic hydrogen sulfide. Tellus, 26(1-2), 254-260. doi:10.1111/j.2153-3490.1974.tb01974.x

Rippka, R., Deruelles, J., Waterbury, M., Herdman, M., and Stanier, R. (1979). Generic assignments, strain histories and properties of pure culture of cyanobacteria. J. Gen. Microbiol. 111, 1–61. doi: 10.1099/00221287-111-1-1

Ruiz-Barba, J. L., Maldonado, A., & Jiménez-Díaz, R. (2005). Small-scale total DNA extraction from bacteria and yeast for PCR applications. Analytical Biochemistry, 347(2), 333-335. doi:10.1016/j.ab.2005.09.028

Saha, S. K., McHugh, E., Hayes, J., Moane, S., Walsh, D., and Murray, P. (2013). Effect of various stressregulatory factors on biomass and lipid production in microalga Haematococcus pluvialis. Bioresour. Technol. 128, 118–124. doi: 10.1016/j.biortech.2012.10.049

Salih, F. M., Haase, R. A., Companies, C., & Land, S. (2012). Potentials of microalgal biofuel production. Petroleum Technology and Alternative Fuels, 3(January), 1–4. doi:10.5897/JPTAF11.029

Saluja, S. K., & Weiser, J. N. (1995). The genetic basis of colony opacity in Streptococcus pneumoniae: Evidence for the effect of box elements on the frequency of phenotypic variation. Molecular Microbiology, 16(2), 215-227. doi:10.1111/j.136-2958.1995.tb02294.x

Sarada, R., Tripathi, U., and Ravishankar, G. A. (2002b). Influence of stress on astaxanthin production in Haematococcus pluvialis grown under different culture conditions. Process Biochem. 37, 623–627. doi: 10.1016/S0032-9592(01)00246-1

Segal, W., & Starkey, R. L. (1969). Microbial Decomposition of Methionine and Identity of the Resulting Sulfur Products1. Journal of Bacteriology, 98(3), 908-913. doi:10.1128/jb.98.3.908-913.1969

Schöck, M., Liebminger, S., Berg, G. & Cernava, T. First evaluation of alkylpyrazine application as a novel method to decrease microbial contaminations in processed meat products. *AMB Express* 8, 54 (2018).

Sharon-Gojman, R., Maimon, E., Leu, S., Zarka, A., and Boussiba, S. (2015). Advanced methods for genetic engineering of Haematococcus pluvialis (Chlorophyceae, Volvocales). Algal Res. 10, 8–15. doi: 10.1016/j.algal.2015.03.022

Sheehan, J., Dunahay, T., Benemann, J., & Roessler, P. (1998). Look Back at the U.S. Department of Energy's Aquatic Species Program: Biodiesel from Algae; Close-Out Report. doi:10.2172/15003040

Shields, R., & Lupatsch, I. (2012). Algae for Aquaculture and Animal Feeds. TATuP - Zeitschrift Für Technikfolgenabschätzung in Theorie Und Praxis, 21(1), 23-37. doi:10.14512/tatup.21.1.23

Shi, X., Jiang, Y., & Chen, F. (2002). High-Yield Production of Lutein by the Green Microalga Chlorella protothecoides in Heterotrophic Fed-Batch Culture. *Biotechnology Progress, 18*(4), 723-727. doi:10.1021/bp0101987

Shi, X., Liu, H., Zhang, X., & Chen, F. (1999). Production of biomass and lutein by Chlorella protothecoides at various glucose concentrations in heterotrophic cultures. *Process Biochemistry, 34*(4), 341-347. doi:10.1016/s0032-9592(98)00101-0

Shah, M. M. R., Liang, Y., Cheng, J. J., & Daroch, M. (2016). Astaxanthin-Producing Green Microalga Haematococcus pluvialis: From Single Cell to High Value Commercial Products. Frontiers in Plant Science, 7. doi: 10.3389/fpls.2016.00531

Sharp, P. M., & Leach, D. R. (1996). Palindrome-induced deletion in enterobacterial repetitive sequences. Molecular Microbiology, 22(5), 1055-1056. doi:10.1046/j.1365-2958.1996.01546.x

Shi, X., Liu, H., Zhang, X., & Chen, F. (1999). Production of biomass and lutein by Chlorella protothecoides at various glucose concentrations in heterotrophic cultures. *Process Biochemistry, 34*(4), 341-347. doi:10.1016/s0032-9592(98)00101-0

Shimidzu, N., Goto, M., & Miki, W. (1996). Carotenoids as Singlet Oxygen Quenchers in Marine Organisms. Fisheries Science, 62(1), 134-137. doi:10.2331/fishsci.62.134

Sirakov I, Velichkova K, Stoyanova S, Staykov Y. (2015). The importance of microalgae for aquaculture industry. Review. Intl J Fisher Aquat Stud 2: 31– 7.

Solovchenko, A. E. (2015). Recent breakthroughs in the biology of astaxanthin accumulation by microalgal cell. Photosynth. Res. 125, 437–449. doi: 10.1007/s11120-015-0156-3

Sommer, T. R., Potts, W. T., and Morrissy, N. M. (1991). Utilization of microalgal astaxanthin by rainbow trout (Oncorhynchus mykiss). Aquaculture 94 (1), 79–88. . doi:10.1016/0044-8486(91)90130-y

Strobel, G. (2010). Muscodor species- endophytes with biological promise. Phytochemistry Reviews, 10(2), 165-172. doi:10.1007/s11101-010-9163-3

Suseela, M. R., and Toppo, K. (2006). Haematococcus pluvialis—a green alga, richest natural source of astaxanthin. Curr. Sci. 90, 1602–1603

Torzillo, G., Goksan, T., Faraloni, C., Kopecky, J., & Masojídek, J. (2003). Interplay between photochemical activities and pigment composition in an outdoor culture of Haematococcus pluvialis during the shift from the green to red stage. Journal of Applied Phycology, 15(2/3), 127-136. doi:10.1023/a:1023854904163

Tripathi, U., Sarada, R., Rao, S., & Ravishankar, G. (1999). Production of astaxanthin in Haematococcus pluvialis cultured in various media. Bioresource Technology, 68(2), 197–199. doi: 10.1016/s0960-8524(98)00143-6

Uemura, N., Makimura, K., Onozaki, M., Otsuka, Y., Shibuya, Y., Yazaki, H., . . . Kudoh, S. (2008). Development of a loop-mediated isothermal amplification method for diagnosing Pneumocystis pneumonia. Journal of Medical Microbiology, 57(1), 50-57. doi:10.1099/jmm.0.47216-0

Uwai, S., Nagasato, C., Motomura, T., & Kogame, K. (2005). Life history and molecular phylogenetic relationships of Asterocladon interjectum sp. nov. (Phaeophyceae). European Journal of Phycology, 40(2), 179–194. doi: 10.1080/09670260500128285

Valério, E., Chambel, L., Paulino, S., Faria, N., Pereira, P., & Tenreiro, R. (2009). Molecular identification, typing and traceability of cyanobacteria from freshwater reservoirs. *Microbiology, 155*(2), 642-656. doi:10.1099/mic.0.022848-0

Wan, M., Hou, D., Li, Y., Fan, J., Huang, J., Liang, S., et al. (2014b). The effective photoinduction of Haematococcus pluvialis for accumulating astaxanthin with attached cultivation. Bioresour. Technol. 163, 26–32. doi: 10.1016/j.biortech.2014.04.017

Wang, B., Zarka, A., Trebst, A., and Boussiba, S. (2003). Astaxanthin accumulation in Haematococcus pluvialis (Chlorophyceae) as an active photoprotective process under high irradiance. J. Phycol. 39, 1116–1124. doi: 10.1111/j.0022-3646.2003.03-043.x

Wang, J. F., Han, D. X., Sommerfeld, M. R., Lu, C. M., and Hu, Q. (2012). Effect of initial biomass density on growth and astaxanthin production of Haematococcus pluvialis in an outdoor photobioreactor. J. Appl. Phycol. 25(1), 253–260. doi: 10.1007/s10811-012-9859-4

Wang, L. *et al*. Contaminating microzooplankton in outdoor microalgal mass culture systems: An ecological viewpoint. *Algal Res.* 20, 258–266 (2016).

Wang Y., Peng J. Growth associated biosynthesis of astaxanthin in heterotrophic Chlorella zofingiensis (Chlorophyta) World J. Microbiol. Biotechnol. 2008;24:1915–1922. doi: 10.1007/s11274-008-9692-8.

Wayama, M., Ota, S., Matsuura, H., Nango, N., Hirata, A., & Kawano, S. (2013). Three-dimensional ultrastructural study of oil and astaxanthin accumulation duringencystment in the green alga Haematococcus pluvialis. PloS one, 8(1), e53618.

White, T., Bruns, T., Lee, S., & Taylor, J. (1990). Amplification and Direct Sequencing of Fungal Ribosomal Rna Genes for Phylogenetics. PCR Protocols, 315–322. doi: 10.1016/b978-0-12-372180-8.50042-1

Wolfe GV, Sherr EB, Sherr BF. Release and consumption of DMSP from Emiliania huxleyi during grazing by Oxyrrhis marina. Mar. Ecol. Prog. Ser. 1994;111:111–119. doi: 10.3354/meps111111.

Wolfe GV, Steinke M, Kirst GO. Grazing-activated chemical defence in a unicellular marine alga. Nature. 1997;387:894–897. doi: 10.1038/43168.

Wilson, L. A. (2006). Enterobacterial Repetitive Intergenic Consensus (ERIC) Sequences in Escherichia coli: Evolution and Implications for ERIC-PCR. Molecular Biology and Evolution, 23(6), 1156-1168. doi:10.1093/molbev/msj125

Wu, Y. H., Yang, J., Hu, H. Y., and Yu, Y. (2013). Lipid-rich microalgal biomass production and nutrient removal by Haematococcus pluvialis in domestic secondary effluent. Ecol. Eng. 60, 155–159. doi: 10.1016/j.ecoleng.2013.07.066

Xiong, W., Li, X., Xiang, J., & Wu, Q. (2008). High-density fermentation of microalga Chlorella protothecoides in bioreactor for microbio-diesel production. *Applied Microbiology and Biotechnology, 78*(1), 29-36. doi:10.1007/s00253-007-1285-1

Xu, H., Miao, X., & Wu, Q. (2006). High quality biodiesel production from a microalga Chlorella protothecoides by heterotrophic growth in fermenters. *Journal of Biotechnology, 126*(4), 499-507. doi:10.1016/j.jbiotec.2006.05.002

Yokoyama A., Adachi K., Shizuri Y. New carotenoid glucosides, astaxanthin glucoside and adonimxanthin glucoside, isolated from the astaxanthin producing marine bacterium, Agrobacterium aurantiacum. J. Nat. Prod. 1995;58:1929–1933

Yoo, J. J., Choi, S. P., Kim, B. W., and Sim, S. J. (2012). Optimal design of scalable photobioreactor for phototropic culturing of Haematococcus pluvialis. Bioprocess Biosyst. Eng. 35, 309–315. doi: 10.1007/s00449-011-0616-x

Young AJ (1991) The photoprotective role of carotenoids in higher plants. Physiol Plant 83: 702±708

Yu, Z., Song, M., Pei, H., Jiang, L., Hou, Q., Nie, C., et al. (2017). The effects of combined agricultural phytohormones on the growth, carbon partitioning and cell morphology of two screened algae. Bioresour. Technol. 239, 87–96. doi: 10.1016/j.biortech.2017.04.120

Zhang B.Y., Geng Y.H., Li Z.K., Hu H.J. & Li Y.G. (2009). Production of astaxanthin from Haematococcus in open pond by two-stage growth one-step process. Aquaculture 295: 275–281.

Zhang, X. W., Gong, X. D., and Chen, F. (1999). Kinetic models for astaxanthin production by high cell density mixotrophic culture of the microalga Haematococcus pluvialis. J. Ind. Microbiol. Biotechnol. 23, 691–696. doi: 10.1038/sj.jim.2900685

Zhang, W., Wang, J., Wang, J., and Liu, T. (2014). Bioresource Technology. Attached cultivation of Haematococcus pluvialis for astaxanthin production. Bioresour. Technol. 158, 329–335. doi: 10.1016/j.biortech.2014.02.044

Zhang, Z., Wang, B., Hu, Q., Sommerfeld, M., Li, Y., & Han, D. (2016). A new paradigm for producing astaxanthin from the unicellular green alga Haematococcus pluvialis. Biotechnology and Bioengineering, 113(10), 2088–2099. doi: 10.1002/bit.25976

Zinder, S.H., W.N. Doemel and T.D. Brock (1977) Production of volatile sulfur compounds during the decomposition of algal mats. App. Environ. Microbiol., 34:859-860.

# V. Abbreviations

| | |
|---|---|
| BBM | Bold Basal Medium |
| BDI | BioLife Science GmbH |
| bp | Base pair |
| CFU | colony forming unit |
| $dH_2O$ | distilled water |
| etc. | et cetera |
| h | hours |
| Kb | Kilo base |
| L | liter |
| mA | milliampere |
| µ | micro |
| min | minute |
| M | molar |
| NaCl | Sodium Chloride |
| % | percentage |
| rpm | Rounds per minute |
| V | volts |

# VI. List of Figures

# VII. List of Tables